Self-Assembly of Discrete Cyclic Nanostructures Mediated by Transition Metals

Stefan Leininger, Bogdan Olenyuk, and Peter J. Stang*

Department of Chemistry, 315 South 1400 East, The University of Utah, Salt Lake City, Utah 84112

Received April 12, 1999

Contents

I. Introduction

Rapid advances and widespread interest in the study of macromolecules of nanoscopic dimensions is a recent phenomenon. Nanostructure science and supramolecular chemistry are two fast evolving fields that are concerned with manipulation of materials that have important structural features of nanometer size (1 nm to 1 μm). Supramolecular chemistry focuses on a wide range of discrete molecules or molecular assemblies and uses chemical transformations to achieve its goals.[1−4] The challenges presented by current technologies and future applications opened a new field of molecular nanotechnology, called molecular architecture, that utilizes programmed self-assembly combined with sequential methods of covalent chemical synthesis to achieve ordered structures.[5−8]

The preparation of various chemical compounds via the stepwise formation of covalent bonds between appropriate precursors presents the most widely used synthetic method. Although this methodology is very useful for the synthesis of organic molecules, it possesses several inherent limitations. These include the time required for the linear, stepwise synthesis of complex macromolecules and molecular assemblies composed of hundreds or even thousands of subunits as well as a decrease of the overall yield in multistep reactions. Recent advances in the solid-phase synthesis of polypeptides and polynucleotides have partially alleviated this problem, but overall difficulties in the preparation and purification of the larger molecules still pose some problems. As covalent bonds are generally kinetically inert, improperly connected bonds are hard to fix. Therefore, to reach the nanoscopic dimensions upward from the molecular level, an extraordinarily convergent methodology is required.

The self-assembly approach to the design of metal-based supramolecules offers an alternative to the classical organic route. Because it proceeds via the simultaneous assembly of predetermined building blocks, the resulting generation of well-defined, discrete supramolecular architectures under thermodynamic equilibration is already highly convergent and thus requires fewer steps than the corresponding covalent synthesis. The kinetically labile coordinative bonds between the constituents contribute to relatively defect-free, self-healing assemblies of high structural integrity, as a result of the equilibrium between constituents and final product. Nature has been exploiting the same principles of noncovalent interactions for the construction of various cell components. For instance, microtubules, ribosomes, mitochondria, and chromosomes use mostly hydrogen bonding in conjunction with covalently formed peptide bonds to form specific structures. Viruses, such as the rhinovirus, possess a spherical capsid around their nucleic acid.[9] The closed-shell virions are built from smaller proteins via noncovalent interactions, resulting in a structure with icosahedral symmetry. The skeletons of radiolaria and capsid shells of viruses are nature's expression of the most economical structural solution to a given set of growth conditions.[10,11]

10.1021/cr9601324 CCC: $35.00
Published on Web 02/04/2000

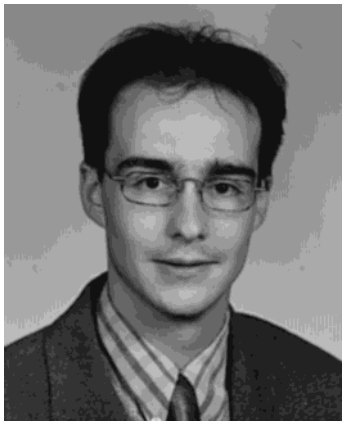

Stefan Leininger was born in Pirmasens, Germany, in 1969. He studied at the University of Kaiserslautern and received his Diploma degree in Chemistry in 1993. Subsequently, he worked as a DFG postgraduate fellow with Professor P. Binger in organic chemistry and received his Ph.D. degree in 1996. For his thesis on metal-mediated cyclooligomerization of phosphaalkynes, he earned a special award from the Fonds der Chemischen Industrie. After postdoctoral research with Professor M. Regitz at the University of Kaiserslautern in 1996, he joined the group of Professor P. J. Stang at the University of Utah as an Alexander von Humboldt Feodor-Lynen Fellow in November 1996. His research interests span organophosphorus chemistry, metallodendrimers, acetylene chemistry, and molecular self-assembly of discrete supramolecules. He is currently a senior research chemist at Degussa-Hüls.

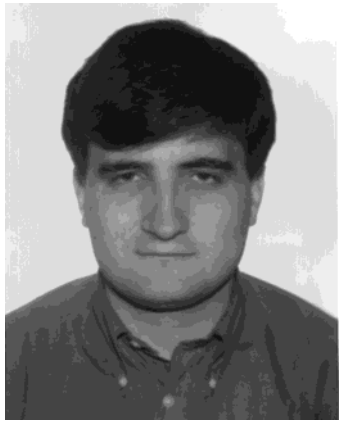

Bogdan Olenyuk was born in Western Ukraine in 1970 and earned his Honors Diploma in Chemistry from the University of Kiev in 1992. He earned his Ph.D. degree in Chemistry under the direction of Professor Stang at the University of Utah in 1998. While at Utah he was a University Research Fellow and then a University Dissertation Fellow and was awarded the Cheves T. Walling Graduate Research Award for his independent and original research on the design and self-assembly of highly symmetrical polygons and polyhedra via coordination. He is presently an NIH Postdoctoral Fellow with Professor P. B. Dervan at Caltech. His interests involve aspects of organic synthesis, transition metal and coordination chemistry, supramolecular assemblies with controlled stereochemistry, and most recently sequence-specific recognition of DNA and regulation of gene expression with small synthetic molecules. He is also interested in molecular modeling, computational chemistry, and computer graphics.

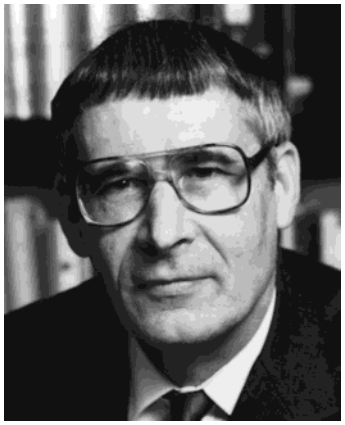

Peter J. Stang was born in 1941 in Nürnberg, Germany, raised in Hungary until 1956, and educated in the United States. He earned his B.S. degree in Chemistry from DePaul University in Chicago in 1963 and Ph.D. degree from the University of California at Berkeley in 1966. After NIH postdoctoral work at Princeton, he joined the faculty at the University of Utah in 1969 where, since 1992, he holds the rank of Distinguished Professor of Chemistry and has served as Department Chair from 1989 to 1995. His research interests over the years involved reactive intermediates such as vinyl cations and unsaturated carbenes, organometallic chemistry, strained ring systems, and, most recently, polyvalent iodine and alkynyl ester chemistry. His current efforts focus on using coordination and chelation to construct supramolecular species via self-assembly. He is the author or coauthor of over 320 scientific publications, including two dozen reviews and six monographs. From 1982 until 1999 he was an Associate Editor of the *Journal of the American Chemical Society* and became Editor-in-Chief of the *Journal of Organic Chemistry* on January 1, 2000. Professor Stang has been the recipient of the A. von Humboldt Senior Scientist Award (1977); JSPS Fellow, Japan (1985, 1998); Lady Davis Fellow, Haifa, Israel (1986, 1997); Fulbright Hays Senior Scholar, Zagreb, Croatia (1988). In 1992 he was awarded honorary doctorates from the Russian Academy of Science and Lomonosov Moscow State University. He was the 1998 recipient of the ACS James Flack Norris Award in Physical-Organic Chemistry. Besides chemistry, he enjoys travel, classical music, gourmet food, and wines.

For chemists, the coordination-driven motif offers an alternative to the biological motif allowing for unique design features in the assembly of discrete supramolecular species. The most important of these is the greater directionality offered by metal−ligand coordinative bonding compared to weak electrostatic and $\pi-\pi$-stacking interactions or even hydrogen bonding. In addition, they offer great versatility due to diverse transition-metal complexes and multidentate ligands available as building blocks and bond energies of 10−30 kcal/mol per interaction that are between the range of the strong covalent bonding in carbon-based macrocycles and the weak interactions of biological systems. The precise control over the shape of the assemblies, coupled with a large variety of available building blocks, allows the regulation of their sizes to within a few angstroms. Control of the polarity and charge state of the desired macrocycles is typically achieved via formation of charged, neutral, and mixed macrocycles; the presence of polar or lipophilic groups provides the ability to create water or organic-soluble macromolecular hosts with hydrophilic or hydrophobic cavities. The use of optically active components allows relatively easy, simple access to chiral supramolecules with controlled stereochemistry.

There have been several attempts in the literature to define the term "self-assembly": Whitesides defined it as "the spontaneous assembly of molecules into structured, stable, non-covalently joined aggregates",[12] while Hamilton defines it as "the noncovalent interaction of two or more molecular subunits to form an aggregate whose novel structure and properties are determined by the nature and positioning of the components".[13] On the basis of these definitions we assigned the following commonalties for metal-mediated supramolecular self-assembly: (a) self-assembling units are held together by coordina-

tive interactions; (b) the assembling of subunits into larger aggregates is selective—the subunits bind cooperatively to form the most stable aggregate; (c) the aggregates can be recognized by their properties that differ from those of the individual components; (d) the aggregates are discrete rather than infinite. In addition, self-assembled supramolecules are normally favored thermodynamically over oligomeric or polymeric systems, profiting from enthalphic as well as entropic effects.

In this review we focused our attention on the discussion of discrete metal-based structures, including only selected discrete self-assembled helicates and polyoxometalates, as well as on the problems related to the preparation, structure, properties, and applications of discrete metal-mediated self-assembled nanostructures. In addition, we attempted to classify the recently reported approaches and motifs into two general design principles while at the same time grouping the compounds based on their shapes or symmetries.

The review is organized into six major parts: (I) Introduction; (II) Design Principles; (III) Two-Dimensional Molecular Polygons; (IV) Three-Dimensional Nanoscopic Cages and Polyhedra; (V) Challenges in the Characterization of Large Supramolecules; (VI) Potential Applications for Metal-Based Polygons and Polyhedra; (VII) Summary and Outlook. Literature coverage is through mid-1999. Reviews, besides our own,[14,15] that have appeared recently in this rapidly growing topical field are those by Fujita and Ogura[16] on two- and three-dimensional synthetic receptors, by Stoddart and co-workers[17] on interlocked and intertwined structures and superstructures, by Albrecht[18] on metallosupramolecular chemistry, by Piguet and co-workers[19] on helicates as versatile supramolecular complexes, by Jones[20] on transition metals as the structural component in the construction of molecular containers, by Hamilton and Linton[21] on metal-templated self-assembly of artificial receptors, by Caulder and Raymond[22] on the rational design of high-symmetry coordination clusters, by MacGillivray and Atwood[23] on the design of spherical molecular hosts, and by Lippert and Navarro[24] on molecular architecture with metal ions, nucleobases, and other heterocycles.

II. Design Principles

The structural and functional features of self-assembled supramolecular entities result from the information stored in their components and the components' intrinsic properties that are dictated by the presence of functional groups. A simple and general concept for generating ordered structures is based on the recognition-derived spontaneous assembly of complementary subunits. While biological systems are formed by many weak hydrogen bonds and van der Waals interactions, metal−ligand bonding interactions are much stronger and generally highly directional. As a result of various transition-metal coordination geometries, metal complexes provide for a pool of different acceptor subunits, which can be linked together by donor building blocks to form rigid frameworks. The final shape of the self-assembled entity is not only defined through the metal coordination geometry, but also through the orientation of the interaction sites in a given ligand. The most common potential building units include nitrogen-containing heteroaryls, cyano-substituted aromatic ligands, *o*-catecholamides, hydroxamates, as well as phosphorus-containing ligands.

As a result of these general considerations, two somewhat different and complimentary approaches for the self-assembly of discrete macrocyclic systems have been developed. While both concepts rely on the formation of a thermodynamically favored product, which requires the metal−ligand bonds to be labile and therefore capable of self-repairing of "mistakes" resulting from the initial formation of kinetic products, there are some important differences.

A. "Symmetry Interaction" Model

This sophisticated strategy has been widely used by Saalfrank,[25,26] Lehn,[27,28] and Raymond[22] as an elegant method to assemble a variety of macrocyclic systems containing main group as well as transition-metal complexes. The concept behind this approach takes advantage of multibranched chelating ligands which show an increased preorganization and stronger binding energies as a result of the chelate effect compared to monodentate ligands.[29] Combination of those ligands with highly coordinating "naked" metal ions results in the formation of neutral or negatively charged macrocycles, depending on the nature of the ligands.

Though most of these interesting complexes have been discovered by systematic variations of the metals and ligands, recently there has been progress toward understanding and developing a rational synthetic approach to the design and synthesis of such ensembles. Raymond and Caulder[22] defined terms that more accurately describe the geometric relationships between ligand and metal. The vector which bisects the bidentate chelating group in the direction toward the metal ion is defined as the chelate or coordinate vector (Figure 1). For a given

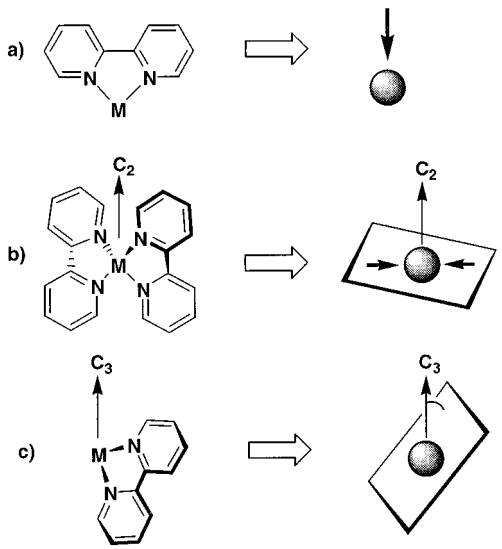

Figure 1. Definitions for the symmetry interaction model. (a) Coordinate vector for a bidentate ligand. (b) Chelate plane defined by the plane orthogonal to the major metal symmetry axis. (c) Approach angle for a bidentate chelator.

metal complex, the plane orthogonal to the major symmetry axis is defined as the chelate plane, which in the case of bidentate chelators holds all chelate vectors. Thus, any symmetrical coordination complex can be described by the orientation of those chelate planes. Furthermore, by carefully pre-arranging the chelate vectors of multibranched ligands, the ability to design more complex macrocycles becomes feasible (Figure 1). In the design of three-dimensional assemblies, a third geometric feature becomes apparent. While the twist angle is commonly used to describe the arrangement of three bidentate chelators around a metal center, defining an approach angle has the advantage of providing more feasible tools that can be readily compared to high-symmetry cluster angles. The approach angle is given as the angle between a plane, which holds the coordinating atoms of the chelating group and the major symmetry axis of the metal center (Figure 1).

To rationally design a M_2L_3 helicate with idealized D_3 symmetry, it is immanent that the C_3 and C_2 symmetry axes are oriented perpendicular to each other. Due to the fact that the two pseudo-octahedral metal centers lie on the same helical axis, the two chelate planes must be parallel (Figure 2). Applying

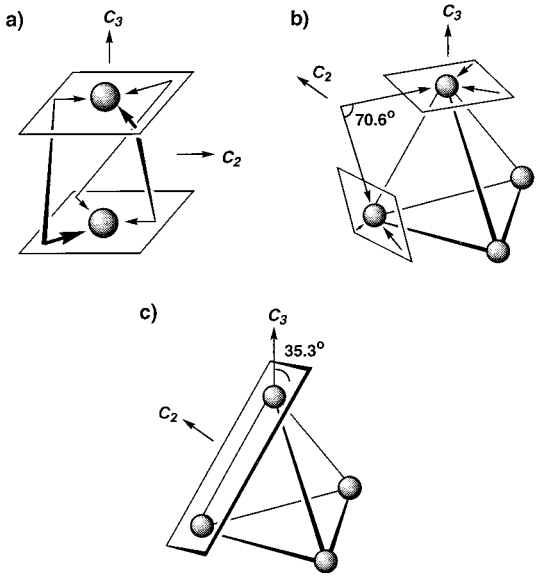

Figure 2. (a) Construction of a D_3-symmetrical triple helicate. (b) Approach to the synthesis of a M_4L_6 tetrahedral cluster. (c) Alternative approach for a M_4L_6 tetrahedral cluster.

the same model to the rational design of a tetrahedral cluster, two different approaches become obvious. In the first strategy, the C_2 axis of the tetrahedron lies in the same plane as the ligand. Since all chelate vectors must lie within the chelate planes, the two chelate vectors within a given ligand must enclose a theoretical angle of 70.6° (Figure 2). In a variation of the above strategy, the 2-fold axis of the tetrahedron is perpendicular to the ligand plane, which implies the use of planar ligands with antiparallel chelate vectors. As a result of the 90° requirement, the angle between the chelate planes becomes obsolete, meaning it does not have any influence on the overall symmetry or geometry of the system. Instead, the approach angle becomes important, requiring a theoretical 35.3° angle for the assembly of an idealized *T*-symmetrical cuboctahedron utilizing perfectly octahedral metal complexes with a 60° twist angle.

B. "Molecular Library" Model

The second design strategy, although first applied by Verkade,[30] was later elaborated by Fujita[16] and systematized by Stang.[14,15] This rational design approach takes advantage of rigid, highly directional multibranched monodentate ligands, which bind to partially coordinatively unsaturated transition-metal complexes via dative bond interactions.

Therefore, construction of almost any type of macrocyclic system that contains a transition metal can be achieved by assessing the appropriate angles between the binding sites of the donor and acceptor subunit. The subunits can be classified into two types based on the value of the binding angle. Linear rodlike subunits (abbreviated as **L**) possess two reactive sites which are opposite (i.e. ~180°), whereas the reactive sites of angular subunits (**A**) enclose angles between 0° and 180°.[14] When these building blocks are combined, the structure of the resulting species will depend solely on the symmetry and the number of binding sites within each subunit. Monocyclic entities can be built by combining subunits with symmetry axes not higher than 2-fold. The construction of polycyclic frameworks requires at least one subunit to possess a symmetry axis higher than 2-fold.[14,15] Thus, the shapes of monocyclic entities will resemble convex polygons and those of polycyclic frameworks will resemble canonical polyhedra.

The assembly of a planar triangle requires the combination of three linear building blocks (abbreviated as L^2_3) and three angular ones (A^2_3) with a 60° turning angle. A molecular square can be assembled in several different ways, such as combining four linear (L^2_4) with four ditopic monodentate angular (A^2_4) building blocks or by combining two different angular subunits. Molecular pentagons can be built by combining five (L^2_5) linear ditopic subunits with five angular ones (A^2_5) that possess a 108° angle between their binding sites as illustrated in Figure 3.

The design of three-dimensional cage compounds and polyhedra generally involves many more building blocks. This results in a more complex system, which consequently requires a more sophisticated approach. As a prerequisite, at least one of the building blocks has to have three binding sites in order to allow for a connection in the third dimension.

The self-assembly of a triangular prism can involve the combination of two tritopic monodentate building blocks with three rigid linear spacers. If the spacers do not have a linear geometry, then the formation of a triple helix can be expected. Likewise, 12 linear subunits (L^2_{12}) combined with eight tritopic (A^3_8) subunits, with all orthogonal coordinating sites, will yield a cubic $A^3_8L^2_{12}$ system. The combination of 12 ditopic angular subunits (A^2_{12}) with eight planar tritopic linkers (L^3_8) will give a $A^2_{12}L^3_8$ system that possesses the shape of an Archimedean dual polyhe-

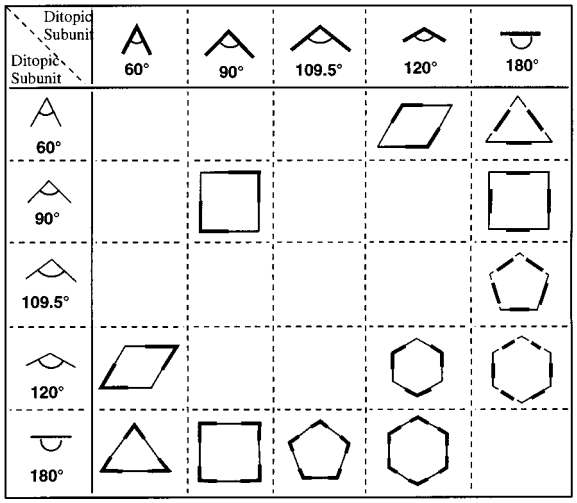

Figure 3. "Molecular Library" of cyclic molecular polygons created via the systematic combination of ditopic building blocks with predetermined angles.

dron known as a cuboctahedron. Likewise, the combination of 20 tritopic angular subunits with 108° directing angles (A^3_{20}) with 30 ditopic linear subunits (L^2_{30}) will form a three-dimensional entity with the shape of a dodecahedron (Figure 4).

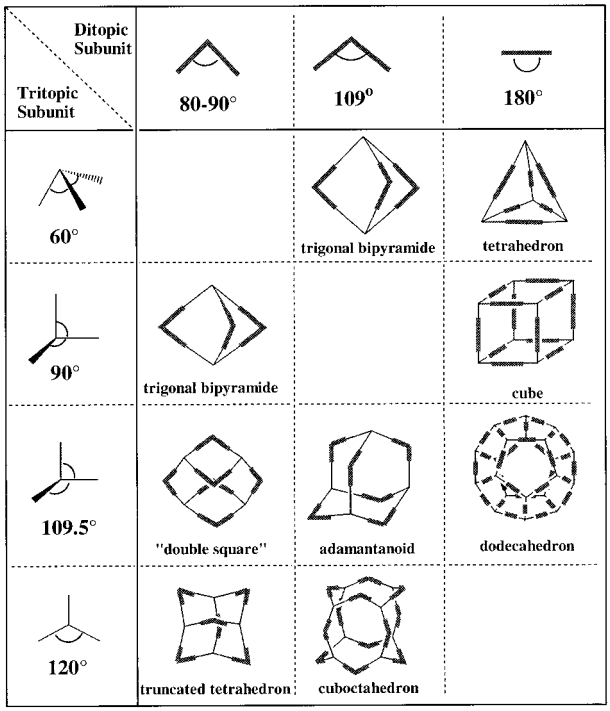

Figure 4. "Molecular Library" for the formation of 3D-assemblies from ditopic and tritopic subunits.

The ultimate strength of this rational approach is its "combinatorial" capability: different combinations of the same angular and linear subunits can be used to construct several different polygons or polyhedra. Figures 3 and 4 illustrate and summarize this ability. For example, the same ditopic linear L^2 subunit can be used to construct a molecular square, pentagon, hexagon, cube, or dodecahedron, whereas the angular 108° subunit can be used in the construction of a pentagon or a cuboctahedron. This methodology allows for the formulation of combinatorial libraries, which consist of different building blocks and allow the prediction of the self-assembly of various polygons and polyhedra.

It is important to note that this methodology accounts only for the angles between the binding sites within each free subunit and extrapolates them into the final self-assembled entity. Therefore, it is assumed that the value of the directing angle within each such subunit does not change significantly upon its incorporation into the self-assembled structure. This assumption is based on the initial requirement of conformational rigidity of the subunits. In reality, however, some distortions of the binding angle of up to several degrees may occur but in most cases can be neglected, as the weak dative bonding to the transition metals is likely to prevent the formation of highly distorted structures.

III. Two-Dimensional Molecular Polygons

A. Dinuclear Structures, Rhomboids, and Helicates

From both chemical and topological considerations, construction of these species must rely on the specific geometry and angles between the binding sites within each individual organic ligand that must be coordinated to the chosen transition metal. One of the first cyclic self-assembled host molecules was reported by Maverick and co-workers.[31] Though not recognized by the authors, this molecular assembly is an early but simple example for the "symmetry interaction" model, described earlier. The work was based on the formation of a cofacial binuclear structure generated from a $Cu(NH_3)_4^{2+}$ complex and a bis-(β-diketone) ligand, which upon mixing in an aqueous solution generated assembly **1** (Figure 5). The ability

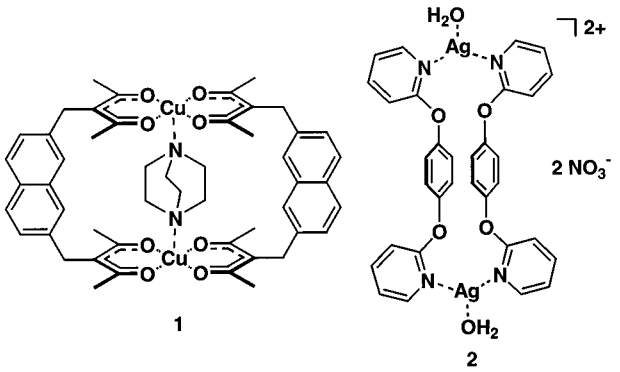

Figure 5.

of **1** to function as a host was tested by measuring its binding constants with pyrazine, pyridine, quinuclidine, and DABCO.[31] For example, diazabicyclo-[2,2,2]octane could be selectively bound inside the macrocyclic host over the other potential guests with a binding constant of 220 l/mol. The internal coordination of diazabicyclo[2,2,2]octane was established by X-ray studies of the inclusion complex. These investigations were among the early observations of the intermolecular coordination of bifunctional Lewis bases to binuclear transition-metal-based hosts.[31]

Another more recent example of binuclear assemblies with potential receptor abilities is the work

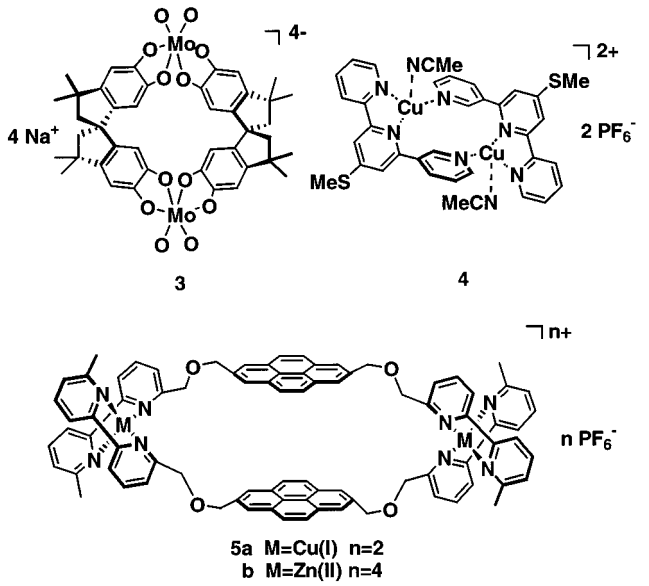

Figure 6.

of Steel and Hartshorn.[32] They used polyheteroaryl-substituted arenes, in combination with silver(I) salts, to prepare binuclear frameworks. When two equivs of 1,4-bis(2-pyridoxy)benzene was allowed to react in acetone with two equivs of silver nitrate, assembly **2** (Figure 5) was formed, as determined by X-ray crystallographic studies. In this assembly, each silver atom is coordinated to two pyridine nitrogen atoms and less strongly to one water oxygen atom. This distorts the geometry of the molecule to become T-shaped with the N−Ag−N′ angle close to 157°. Another interesting feature of this assembly is the close $\pi-\pi$ stacking of the two benzene rings that are coplanar and separated by only 3.33 Å.[32]

Applying a strategy similar to the one used by Maverick, Duhme and co-workers diastereoselectively self-assembled the binuclear complex **3** from the conformationally rigid, racemic 3,3,3′,3′-tetramethyl-1,1′-spirobisindane-5,5′,6,6′-tetrol and $Na_2MoO_4 \cdot 2H_2O$ (Figure 6).[33] The ^1H NMR spectrum of the dinuclear complex **3** gave rise to only one set of sharp signals for the methylene groups, indicating the formation of a highly symmetrical and diastereomerically pure complex. X-ray structure analysis agreed with the NMR data and showed an entirely homochiral macrocyclic anion, which formed microchannels in the solid state due to alignment of the complexes. The planar rhomboid had a Mo−Mo diagonal distance of 10.08 Å and a $C_{spiro}-C_{spiro}$ distance of 8.94 Å. However, as a result of the poor crystal quality, the sodium counterions could not be properly located.[33]

Hannon and co-workers employed an interesting strategy[34] by incorporating chelating ligands into the donor unit, thereby eliminating the need for the additional preparation of a transition-metal complex and allowing the use of transition metals with multiple, open coordination sites. The ligand, 4-thiomethyl-6-(3′-pyridyl)-2,2′-bipyridine, acts as a bidentate chelating ligand for one transition metal and as a monodentate binding site for the other. The preparation of assembly **4** (Figure 6) was achieved by mixing 1 equiv of a copper(I) salt with 1 equiv of the ligand in acetonitrile. Mass spectrometry and single-crystal X-ray studies allowed the unambiguous elucidation of its structure.[34] Interestingly, a topologically similar assembly was also obtained by Hannon and co-workers, using octahedral group IIb metals such as cadmium. Reaction of the same ligand with cadmium(II) acetate furnished a structure similar to **4** in which the cadmium cation occupies a pseudo-octahedral environment, additionally coordinated by a bidentate acetate ligand and a methanol solvent molecule.

Another example of a binuclear structure was prepared by Bilyk and Harding using the coordination of copper(I) or zinc(II) by 2,2′-dipyridine.[35] Since this type of coordination chemistry is well-known, it allowed the authors to use two 2,2′-dipyridyls connected to each side of an aromatic spacer, such as 2,2′-naphthalene and 2,7-pyrene. Treatment of these ligands with Cu(I) salts produced the binuclear assembly **5a** (Figure 6). Fast atom bombardment and electrospray mass spectrometry were used to establish the stoichiometry of these complexes, and variable temperature NMR spectra were used to study their dynamic behavior.

According to the "symmetry interaction" model developed by Raymond and outlined in section II, binuclear triple helicates can be formed by combining transition metals that prefer octahedral coordination, such as iron or group IIIa metals, with three subunits that contain chelating binding sites at each end. Raymond and Caulder[36] successfully employed this motif to characterize highly ordered helical assemblies in solution that form from a mixture of predesigned building blocks. The reaction of 3 equivs of any ligand **6**−**8** with 2 equivs of trivalent $Fe(acac)_3$ (**9**) or $Ga(acac)_3$ (**10**) in methanol and KOH resulted in the formation of three triple-helical assemblies **11a**−**c** in high yields (Scheme 1).[36] When these

Scheme 1

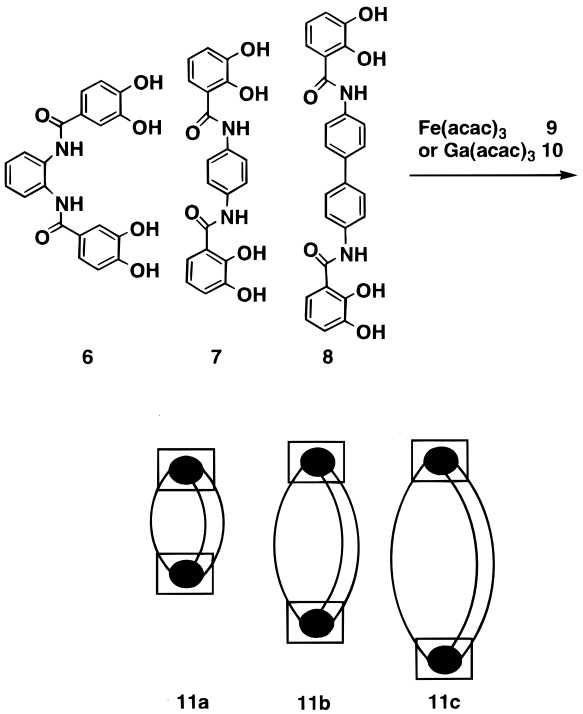

complexes were prepared in the presence of excess ligand, NMR spectra indicated only the formation of the final products and an excess of the free ligand.[36] When mixtures of all three or any two ligands were allowed to react with [Ga(acac)$_3$] (**10**) under these conditions, only complexes containing one type of ligand were formed. Both NMR spectroscopy and electrospray mass spectrometry indicated a mixture of three final helical products in equal amounts with no traces of oligomeric or mixed species. The main reasons for this self-recognition are the high degree of conformational rigidity of each donor subunit combined with different steric requirements due to the different distances between the binding sites in the assembled product.

By introducing additional nonlinear spacers between the two pyridine rings of bipyridine, Fujita and co-workers[37] assembled several water-soluble binuclear macrocycles rather than tetranuclear squares,[38] which had been described earlier by Fujita. When ligand **12** was mixed with an aqueous solution of (en)Pd(NO$_3$)$_2$ (**13**), the formation of assembly **14** was observed (Scheme 2). Since **14** contains the

Scheme 2

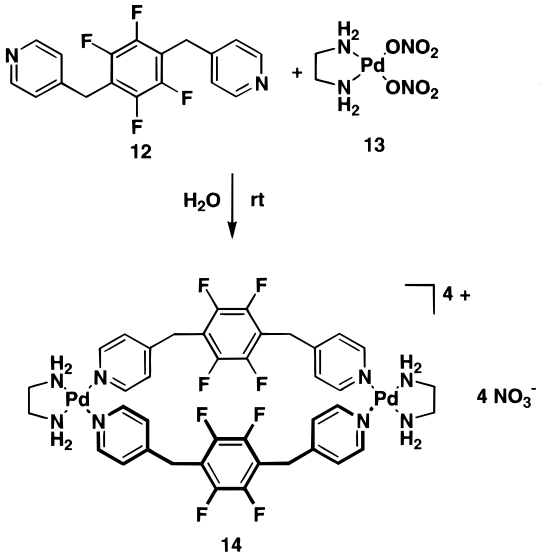

electron-deficient perfluorinated phenylene subunit, the complex was capable of recognizing electron-rich compounds, such as naphthalene, in aqueous medium.[37]

Using a slightly different subunit, 1,4-bis(4-pyridylmethyl)benzene (**15**) (Scheme 3), the corresponding palladium-based bimetallic species **16** was prepared.[39,40] Surprisingly, the authors were able to show that at ambient temperature the dinuclear palladium system **16** was in equilibrium with the catenane **17**, as confirmed by spectroscopic studies. At low concentrations (<2 mM), this equilibrium favored the single-ring assembly, but at high (>50 mM) concentrations, the interpenetrating two-ring system **17** was the dominant species. Formation of the catenane may be understood as the benzene unit of one macrocycle serves as a guest molecule for the other macrocycle, favored by $\pi-\pi$ interactions. Reaction of the homologous platinum precursor **18** with **15** produced an analogous assembly **19** (Scheme 3).

Scheme 3

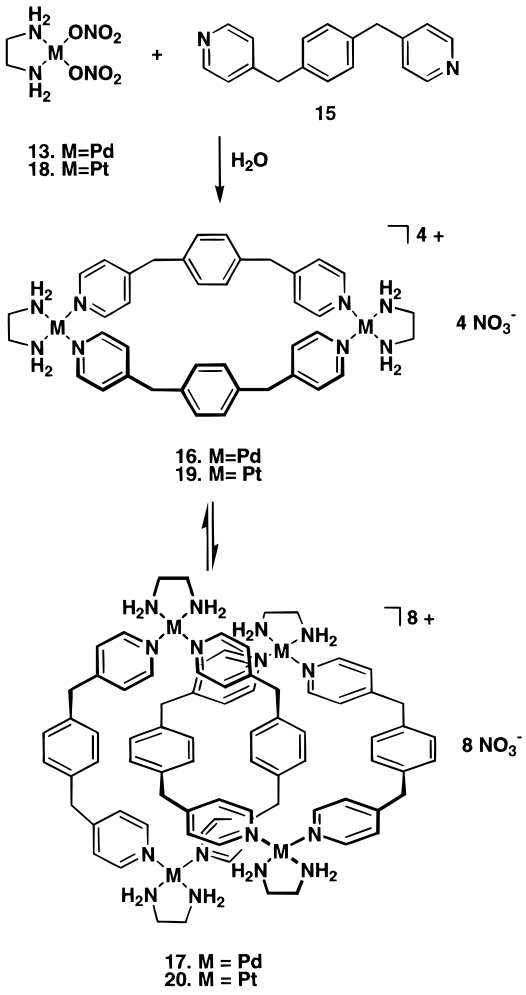

Due to the greater Pt−N bond strength, compound **19** was exclusively formed as the monocyclic structure at room temperature. However, when the reaction mixture was heated in water to 100 °C in the presence of NaNO$_3$, the formation of the catenated dimer **20** was observed due to the increased thermal lability of the Pt−pyridine bond.[39] The irreversible formation of this catenane was confirmed by cooling the solution to room temperature. Isolation and crystallization of catenane **20** allowed the confirmation of its structure by X-ray crystallographic analysis.[39,40]

The self-assembly of molecular rectangles may be accomplished by using organic angular subunits with a modified shape but similar electronic properties.[41] Two types of rectangles were constructed by Fujita and co-workers. One contained two identical angular subunits in combination with (en)Pd(NO$_3$)$_2$ (**13**). The other was composed of the same transition-metal complex combined with two different subunits: one linear and one angular unit. When the unsymmetrical angular building block **21** was mixed with **13**, it quantitatively formed the catenated rectangular assembly **22** (Scheme 4). The yield of **22** (94%) was the highest among those reported for catenane formation, and it consists of only one structure in solution. Catenane **22** is remarkably stable, as its dissociation was not observed even at low concentrations.[41,42] Simultaneous reaction of palladium com-

Scheme 4

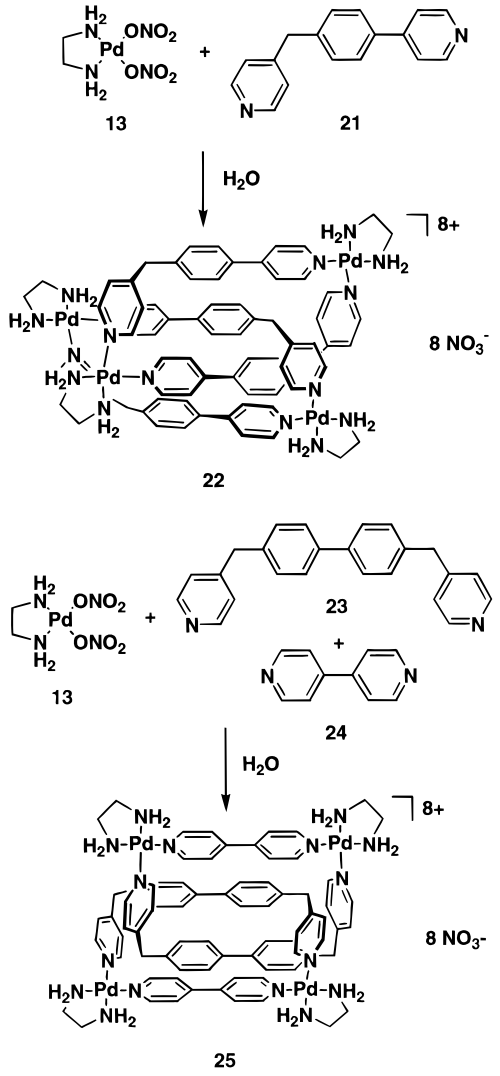

plex **13** with two different heteroaryls, the substituted biphenyl **23** and 4,4′-bipyridyl (**24**), formed catenated assembly **25** (Scheme 4). In the solid state, catenane **22** consists of two crystallographically independent structures whereas catenane **25** exists as a single isomer.[41]

Using the less rigid *exo*-bis-monodentate ligand **26**, Hosseini[43] and co-workers were able to self-assemble similar palladium-based metallamacrocycles. Depending on the size of the diazacyclic core, formation of binuclear complex **27** as well as additional trinuclear complexes were observed (Scheme 5). Due to two possible mutual orientations of the asymmetric cyclic core, two different isomeric complexes, one with ideal C_{2v} and the other with ideal D_{2h} symmetry, might form. However, in the solid state, only the complex with C_{2v} symmetry was found. Similar findings were reported for the self-assembly of binuclear metallamacrocycles using silver cations. In this case the silver atoms were linear, bridged by two pyridine units belonging to separate ligands. Furthermore, the crystal structure analysis revealed the formation of an infinite network formed by double silver−aromatic interaction between consecutive units.[43]

Scheme 5

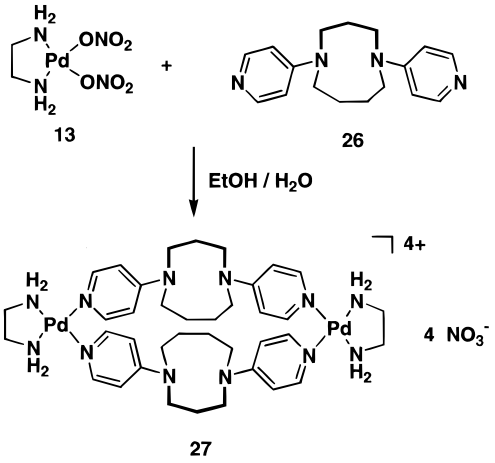

Scheme 6

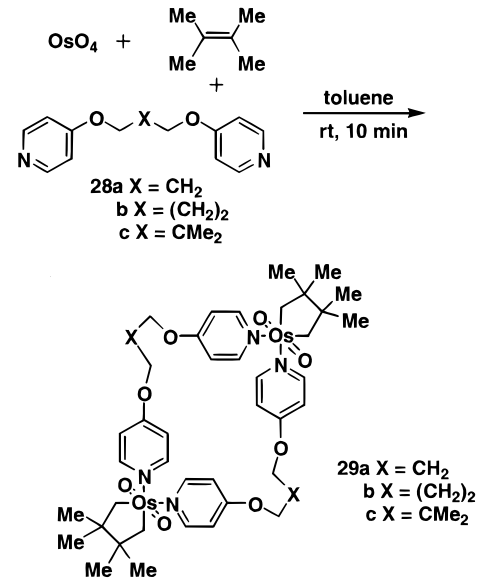

Formation of neutral macrocyclic boxes by spontaneous assembly of osmium tetraoxide, 2,3-dimethyl-2-butene, and the bispyridyl ligands **28a**−**c** was described by Jeong and co-workers (Scheme 6).[44] FAB mass spectra with isotopic distribution patterns and spectroscopic data were consistent with the formation of macrocycles **29a**−**c**. Furthermore, the discrete binuclear structure was confirmed by X-ray diffraction studies of complex **29b** incorporating four molecules of 1-naphthol, revealing N−Os−N angles of 89.5° and 8.59 × 9.69 Å edge to edge distances.

The metal-directed self-assembly of a dinuclear octacationic species was reported by Constable and Schofield.[45] Reaction of the bis-terpyridine linker **30** with an equimolar amount of iron(II) tetrafluoroborate under high dilution conditions in a 1:1 methanol−acetonitrile solution formed structure **31** after treatment with NH_4PF_6 (Scheme 7).[45] Complex **31** was characterized by electrospray mass spectrometry (ESMS), which showed a series of ion peaks corresponding to $[\mathbf{31}(PF_6)_n]^{(8-n)+}$ species. Constable's dinuclear assembly is analogous to Stoddart's covalently linked "blue box",[46] where 4,4′-bipyridine was used as a linking unit.

Scheme 7

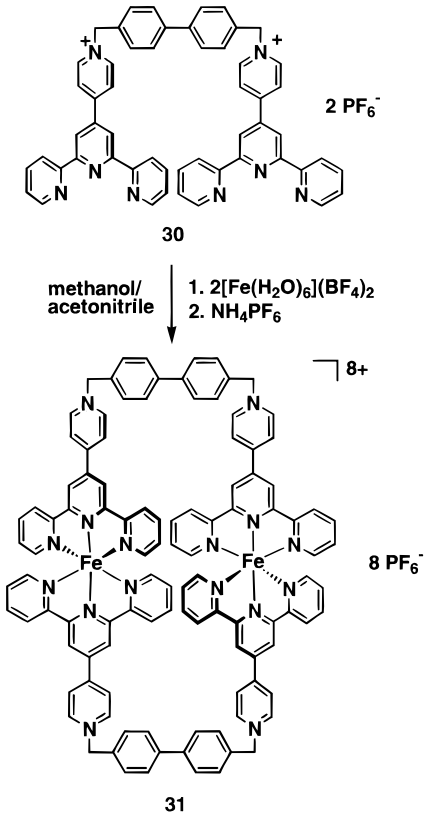

A rare example of a neutral self-assembled dimer was reported by van Koten and co-workers.[47] The tritopic ligand 3,5-bis(dimethylaminomethyl)pyridine (**32**) reacted with dilithium−palladium tetrachloride to form the cyclic dinuclear complex **33** in which the ligand is involved in a bidentate bridging bonding motif (Scheme 8). The ^{1}H NMR spectrum of **33**

Scheme 8

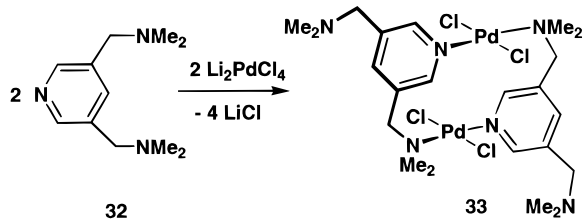

showed two singlets each for the methyl and methylene groups of the coordinated and noncoordinated ligand arms. A fast flip of the 12-membered ring was assumed since only one singlet was observed for the diastereotropic methylene protons. X-ray structure analysis revealed that the 12-membered ring containing the Pd atoms adopted a strained zigzag chairlike conformation with an intramolecular Pd−Pd distance of 4.6 Å, virtually identical to the sum of their contact radii.[48] Some of these features are comparable to those in similar cyclic dinuclear palladium systems described by Constable and co-workers.[49,50]

Evaluating the limits of the self-assembly of cyclic dinuclear compounds, Fujita and co-workers[51] reacted the 90° corner unit (ethylenediamine)Pd(NO_3)$_2$ (**13**) with bidentate pyridine-based ligands having angles

Scheme 9

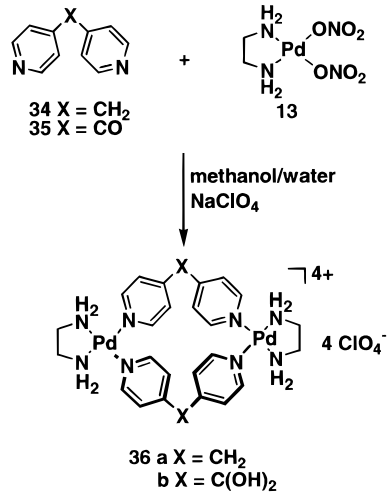

between 109° and 120°. With bis(4-pyridyl)methane (**34**), formation of a rhomboid-like dinuclear complex **36a** was observed in good yields (Scheme 9). Analogous reaction with bis(4-pyridyl)ketone under aqueous conditions led to the exclusive formation of a similar dinuclear macrocycle **36b**. All spectroscopic and analytical data suggested the existence of a hydrate, which was confirmed by X-ray structure analysis. Thus, reduction of an sp^2 angle to an sp^3 angle by hydration of the keto group appears to be essential for the self-assembly of **36b**. Reaction of (ethylenediamine)Pd(NO_3)$_2$ (**13**) with the 120° linker 1,1-bis(4-pyridyl)ethene resulted in the formation of a mixture of different cyclic products as well as polymeric compounds. This study showed that thermodynamic conditions facilitate the formation of macrocycles even if the cycles are strained to some extent, which can be explained in terms of significant entropy effects that favor small cyclic structures over polymeric structures.

To develop fullerene-containing supramolecular assemblies and advanced materials, Diederich and co-workers[52] functionalized fullerene C_{60} to yield dipyridylmethanofullerene **37**. In the reaction of an equimolar amount of **37** and *cis*-[(Et_3P)$_2$Pt(OTf)$_2$] (**38**) the tetraionic cyclophane **39** was obtained quantitatively as the tetrakis−triflate salt (Scheme 10). The ^{31}P NMR spectrum of compound **39** showed one sharp singlet at $\delta = -4.5$ ppm with appropriate Pt satellites for the equivalent phosphorus atoms. All other multinuclear NMR data were consistent with the formation of a highly symmetrical product. X-ray structure analysis confirmed the parallelogram-type structure of **39**, showing a square planar platinum with a significant deviation from the ideal 90° angles. While the N−Pt−N angles were 81.6°, the P−Pt−P angles were opened up to 97.2°. The tetrahedral angle of 113° at the quaternary carbon atom of the dipyridylmethano group was identical to the angle seen for the pure ligand **37** in the solid state.[52]

Larger and more flexible systems have been described by Constable and co-workers.[53] Using alkyl-bridged diamino ligands, 16- and 20-membered cyclic dipalladium systems were formed. Their higher thermodynamic stability with respect to open-chain

Scheme 10

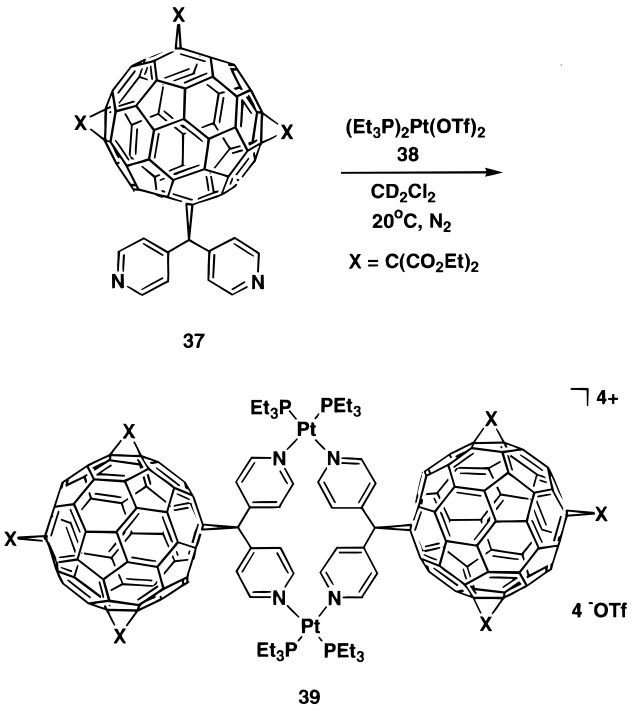

analogues was explained in terms of entropy and conformational effects caused by the bulky dimethylamino groups.

Among the variety of geometries that some main group elements can accommodate, the T-shaped, pseudo-trigonal bipyramidal geometry of the iodonium moiety with its near 90° angles is particularly noteworthy.[54,55] Since hypervalent iodine provides two of the 90° turns, only two transition-metal centers are present in the resulting square. The preparation of the needed bis(heteroaryl)iodonium species can be readily accomplished,[56] resulting in the angular building block **41** where the lone pairs of the nitrogen atoms are located perpendicular to each other. Interaction of equimolar amounts of this bis(heteroaryl)iodonium triflate with the bistriflate complexes of the Pd(II) or Pt(II) bisphosphines **40** and **38** results in the ready formation of the predicted hybrid molecule **42** (Scheme 11).[57,58] These assemblies

Scheme 11

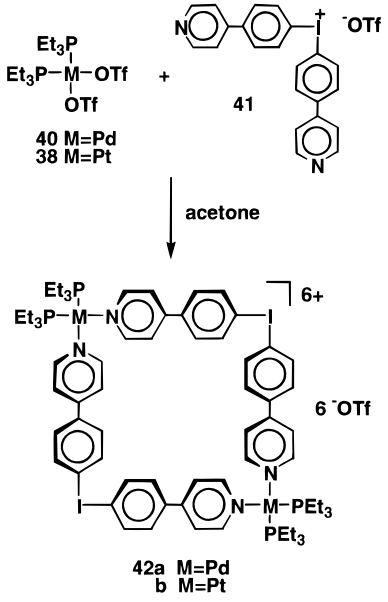

can be isolated as air-stable microcrystalline solids, and due to their relatively high polarity, they are soluble in polar organic solvents such as acetone and methanol and only slightly soluble in dichloromethane. The solid-state structure of rhomboid **42a** was confirmed by a single-crystal X-ray diffraction study.[58] Some important crystallographic data for this dinuclear system as well as its stacking diagram are presented in Figure 7. For the N−Pd(II)−N bite angle a value of 84° was found, whereas the corresponding C−I−C bond angle increased to 98.7°, resulting in an overall planar rhomboidal shape. Furthermore, in the solid state, complex **42a** shows stacking along the *b*-axis resulting in long channel-like cavities.

One way of introducing chirality into self-assembled molecular systems, other than formation of helical systems, is via the use of chiral ligands attached to the metal center. Optically active dinuclear compounds were prepared[59] via the interaction of [Pd(R(+)-BINAP)(H_2O)][OTf]$_2$, **43a**, or [Pt(R(+)-BINAP)(H_2O)][OTf]$_2$, **43b**, and bis(4-(4′-pyridyl)phenyl)iodonium triflate, **41** (Scheme 12). In this case, the diazaligands of the iodonium species possess

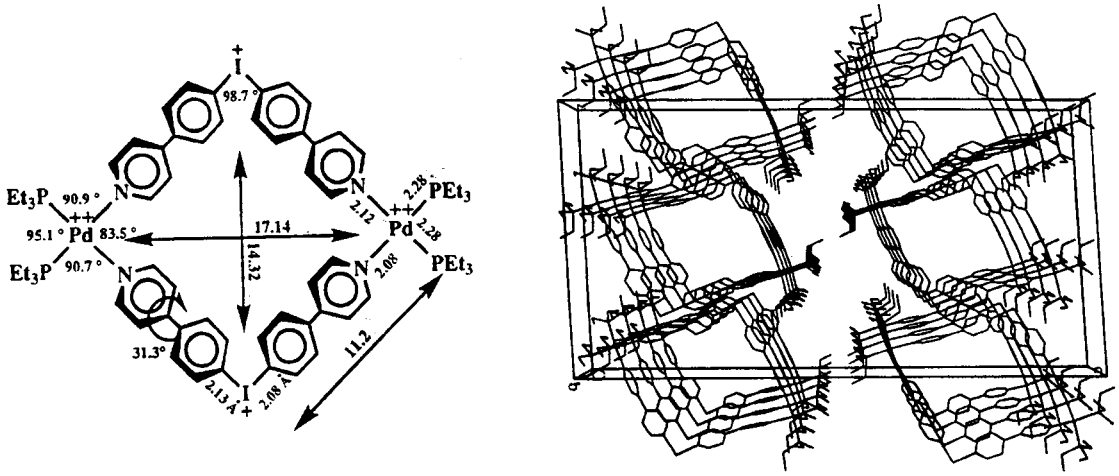

Figure 7. Summary of important geometric features (left) and solid-state stacking diagram (right) of cationic portion of molecular square **42a**.

Scheme 12

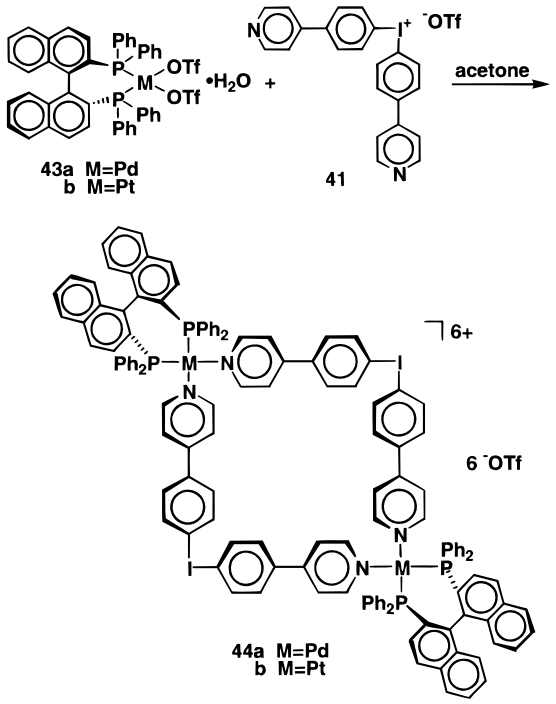

rotation symmetry about their linkages, and hence, molecular squares **44a** and **44b** are chiral due only to the chiral transition-metal auxiliary (BINAP) in the assembly. One interesting feature of these dinuclear species is that they exhibit restricted rotation of the coordinated pyridine moiety around the metal−nitrogen bonds at room temperature. Since both **44a** and **44b** possess D_2 symmetry, with one of the symmetry axes across the plane of the transition metals and rotation of the pyridine ligands restricted, the hydrogen atoms on the pyridine rings are diastereotopic as detected by ^{1}H NMR.

Other interesting examples of chiral hybrid molecular squares were prepared via reaction of bis(3-pyridyl)iodonium triflate (**45**) and chiral Pd(II) and Pt(II) complexes **43a** and **43b** (Scheme 13). An interesting assumption was made during their preparation. Interaction of a chiral square planar Pd(II) or Pt(II) complex with an iodonium precursor where the heterocyclic ring lacks rotation symmetry about its linkages can result in the formation of up to six diastereomers. However, it was anticipated that the use of a chiral auxiliary, such as BINAP, will reduce the complexity of the stereochemical outcome via asymmetric induction upon the self-assembly process. Indeed, when chiral complexes **43a** and **43b** reacted with bis(3-pyridyl)iodonium triflate (**45**) in acetone, the result was the formation of an excess of one preferred diastereomer of **46a** and **46b** as assessed by NMR (Scheme 13). Liquid secondary ion (LSI) mass spectra of **46a** indicate the presence of the $[M - {}^{-}OTf]^{+}$ ion. For square **46b,** however, it was possible to detect the doubly charged $[M - 2^{-}OTf]^{2+}$ ion and to unambiguously establish its charge state. These data as well as the close match of the calculated and measured isotopic patterns of these ions confirmed the predicted molecular weights and helped to establish the structure of both of these chiral macrocycles.

Scheme 13

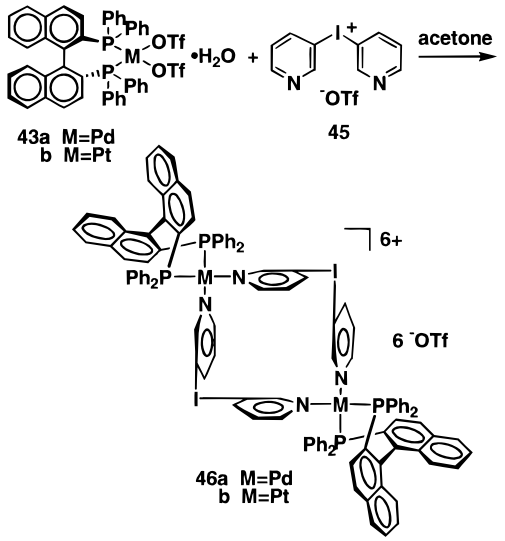

B. Trinuclear Structures and Molecular Triangles

Other interesting examples of self-assembled polygons are the gradually more complex molecular triangles. According to the "molecular library" model, the design of triangles requires three angular and three linear components to be assembled in a cyclic manner. The design of such entities can be accomplished in two different ways: (1) by using 180° connecting linear linking units in combination with 60° angular building blocks or (2) by using distorted angular components with angles higher than 60° in combination with distorted linear linking units with valent angles less than 180°. Although such systems could also be considered as molecular hexagons, the fact that these systems consist of only three metal centers seems to be reason enough to include them in the molecular triangle section. In principle, these assemblies may be constructed by using organic angular components that are specifically designed to have two functional groups enclosing a 60° angle, since there are almost no appropriate metal complexes with 60° angles known. Although the *de novo* construction of a molecular triangle does not seem to be a synthetically complicated task, only a surprisingly small number of compounds have been actually reported in the literature.

An example of the formation of triangles via method one was reported by Loeb and co-workers, where they assembled complementary molecular building blocks with specific angular requirements.[60] Taking advantage of 4,7-phenanthroline (**47**) as a rigid 60° corner that favors bridging metal complexes over forming chelate complexes, reaction with the linear phenyl-bridged bis-palladium complex **48**, formed the self-assembled triangle **49** (Scheme 14). Due to the steric requirements of the phenyl groups, the benzylic protons of the linear linker in **49** were restricted in rotation about the Pd−N bond. Loeb and co-workers were able to provide additional evidence for the cyclic nature of this triangle in solution by variable temperature NMR, showing dynamic behavior of the compound.[60]

Scheme 14

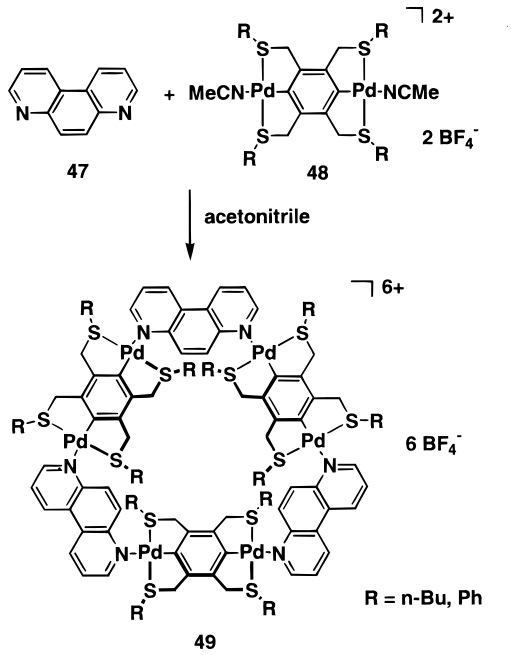

Scheme 15

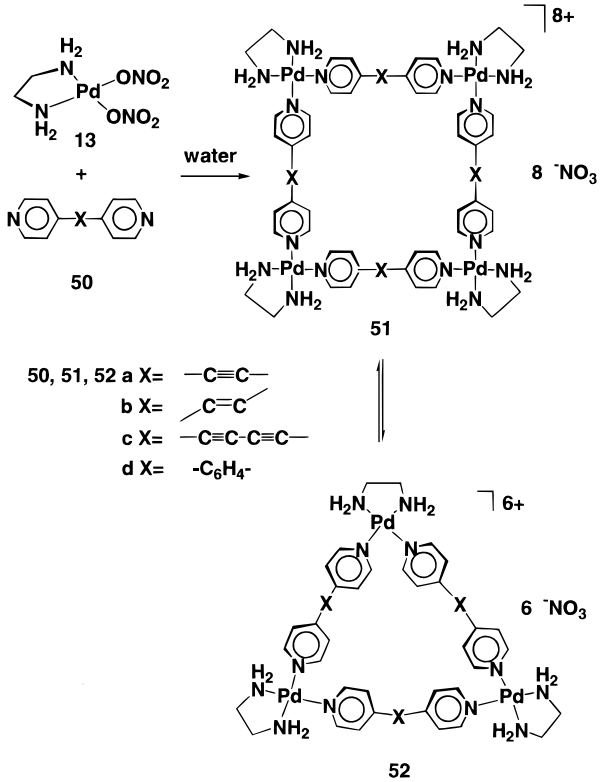

The self-assembly of molecular triangles relying on less rigid building blocks was observed by Fujita and co-workers.[42,61] Specifically, when reacting (en)Pd-$(NO_3)_2$ (**13**) with 1 equiv of several bis-heteroaryls **50** in water, formation of two different self-assembled macrocycles was observed: molecular squares **51** and molecular triangles **52** (Scheme 15). Both products showed a cyclic structure as confirmed by NMR, since no signals for the existence of polymeric compound or uncoordinated end groups could be found. In addition, the two products were in equilibrium with each other, with the major product being the molecular square **51** and the minor product being the molecular triangle **52**. These assignments were supported by the observation of concentration-dependent effects on the equilibrium: at higher concentrations the ratio shifted toward the formation of the less strained molecular square **51**. These equilibria can be rationalized from a thermodynamic standpoint: molecular squares are less strained and hence more stable in terms of enthalpy, while entropic factors favor the triangle since it is assembled from a smaller number of components. The presence of steric effects can also play a vital role in the equilibrium, favoring either the molecular square or the molecular triangle. It was found that if the ethylenediamine groups on Pd were replaced with the more sterically demanding 2,2′-bipyridine, the resulting squares **53** were also in equilibrium with the molecular triangles **54** (Scheme 16), probably due to the steric repulsion between the two adjacent bipyridine ligands.[61]

Scheme 16

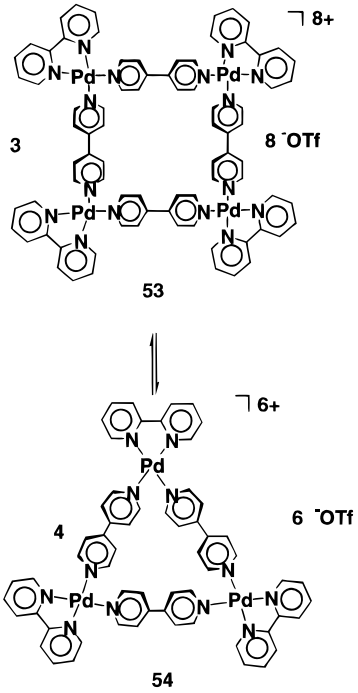

A similar observation of a concentration-dependent equilibrium between a triangle and a square was made by Hong and co-workers.[62] Reaction of the flexible bidentate ligand *trans*-1,2-bis(4-pyridyl)ethylene with either the nitrate or triflate salt of ethylenediaminepalladium resulted in the formation of a mixture of square **55** and triangle **56** (Scheme 17). While the signals for the α-pyridyl protons of **55** and **56** overlapped in the ^{1}H NMR spectra, the *β*-pyridyl and olefinic protons showed up at slightly different frequencies. At higher concentration (∼10 mM) the major component was assigned as the more stable strainless molecular square **55**, while at lower concentration (0.1 mM) the equilibrium shifted in favor of the molecular triangle **56** due to entropic effects. Formation of larger amounts of oligomers was observed at relatively high concentrations (50 mM). Additional information was derived from vapor pressure osmometry, supporting the average molec-

Scheme 17

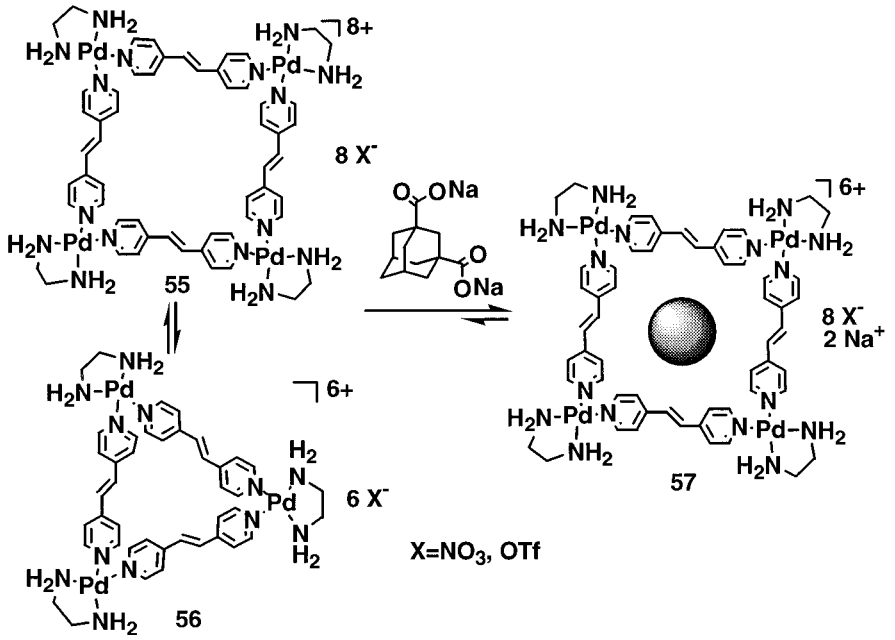

ular masses of the trimer−tetramer mixture depending on the concentration in water. Electrospray mass spectrometry of the triflate complexes showing molecular ion peaks corresponding to the cyclic tetramer **55** and to the cyclic trimer **56** were also observed. Besides the concentration-dependent reorganization behavior, a guest-induced reorganization of complexes **55** and **56** through hydrophobic interaction in water was monitored by NMR. Adding the smaller guest *p*-dimethoxybenzene to an aqueous solution of **55** and **56** resulted in an increased formation of the trimer, whereas addition of the larger guest 18-crown-6 favored the formation of the square over the triangle. Addition of 1,3-adamantanedicarboxylic acid disodium salt completely shifted the equilibrium toward formation of tetrameric host−guest complex **57** within several seconds. Molecular modeling of the inclusion phenomena for the trimer and the tetramer showed good van der Waals contacts inside the guest binding cavity. Therefore, the whole system can be considered as a model of "induced-fit" molecular recognition where the guest induces organization of the recognition site of the receptor itself.[62]

The steric as well as electronic properties of the linking unit have a big impact on the outcome of the self-assembling process. The use of 2,2′-bipyrazine (**58**) instead of the commonly used 4-pyridine derivatives in the reaction with ethylenediamineplatinum dinitrate (**18**) formed the molecular triangle **59**, whereas the corresponding palladium compound formed only a mononuclear chelating bipyrazine complex (Scheme 18).[63] The C_2-symmetrical structure revealed that the two pyrazine rings of each bipyrazine ligand were markedly twisted with respect to each other, and this seems to be crucial for the formation of the triangle. Given that similar twisted angles have been observed for 2,2′-bipyrazine in the gas phase, as well as in solution, it was likely that the formation of the triangle was facilitated by this effect.[63] Subsequent addition of ethylenediaminepalladium dinitrate (**13**) resulted in an immediate

Scheme 18

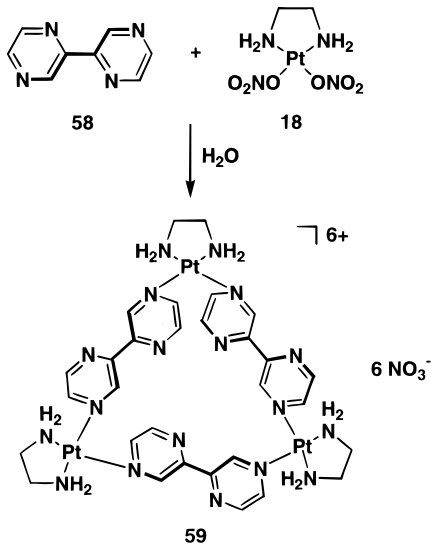

rotation of the pyrazine rings and coordination of the free nitrogen in the 2 and 2′ position to palladium.[64] The newly formed hexanuclear complex **60** (Scheme 19) has 12 positive charges and showed a high counterion affinity. Partial counterion exchange with PF_6^- resulted in the isolation of crystals suitable for X-ray structure analysis. As a direct result of the additional Pd coordination, the formerly triangular-shaped complex **59** changed into a calixarene type of structure **60** in which the six metal atoms formed a twisted trigonal antiprism. In addition, two counterions were found embedded within the cavity of the complex. A nitrate ion was located in the plane of the three platinum atoms, showing weak oxygen−platinum interactions. The second anion, an octahedral PF_6^- ion, was located in the center of the cavity, showing three facial fluorine−platinum as well as three facial fluorine−palladium interactions. Anion exchange experiments monitored by proton NMR spectroscopy showed small association constants for

Scheme 19

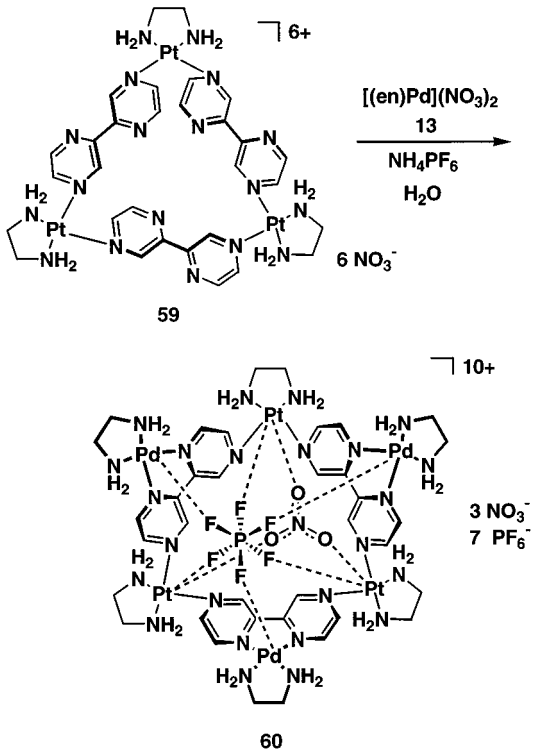

PF_6^-, ClO_4^-, and BF_4^-. Only in the case of sulfate ions was a higher association constant observed, suggesting a different type of interaction.[64]

A more provocative but still theory-consistent approach for the formation of molecular triangles was chosen by Che and co-workers.[65] Connection of three rigid nonlinear 150° linkers with three 90° corner units should result in the formation of a cyclic trimer. Starting from the luminescent cyclometalated complex [Pt(thpy)(Hthpy)Cl] (Hthpy = 2-(2-thienyl)pyridine) (**61**), reaction with the sodium benzimidazolate (**62**) furnished an orange crystalline solid **63** in high yields (Scheme 20). FAB mass spectrometry revealed

Scheme 20

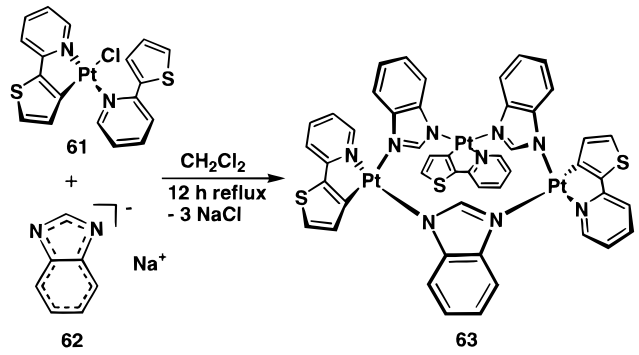

a peak at $m/z = 1417$ that corresponded to a trimeric system. The triangular structure of complex **63** was confirmed by X-ray analysis, which shows three platinum atoms sitting at the corners of a triangle, bridged by three imidazole ligands oriented in a syn−anti−anti arrangement. As a result of minimum ring strain in the system, the N−Pt−N angles were close to 90° (87.8−89.0°), which were larger than the known angles for cyclotrimeric systems formed via interaction of similar corner units with rigid linear linkers such as bipyridine.[61−64] The cone-like-shaped macrocycle **63** resembled calixarenes and showed a 7.4 Å opening at the top which decreases to about 4.7 Å at the center.[65]

As seen above, rigid linkers are suitable for the self-assembly of molecular dimers, triangles, and rectangles. However, there are also examples in which flexible linkers were used to form rigid macrocycles. Baker and co-workers reported that the reaction of 1,2-bis(3,5-dimethylpyrazol-1-yl)ethane (**64**) with palladium dichloride **65** resulted in the formation of a neutral "molecular tricorn" **66** (Scheme 21).[66] In this

Scheme 21

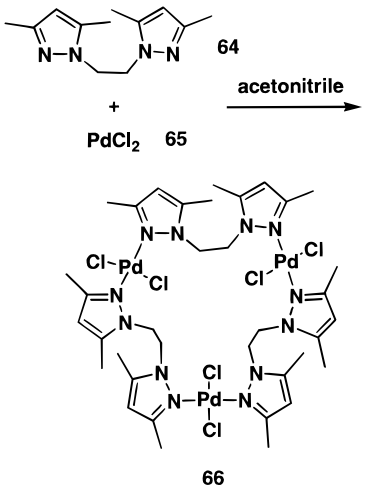

case, the square planar *trans*-palladium dichloride units were linked by a highly twisted ligand molecule. The 1,2-ethanediyl bridges of the ligands were oriented to the inside of the 21-membered trinuclear macrocycle, resulting in intramolecular interaction of the methylene protons with the palladium. This interaction was likely contributing to the stability of the trimeric structure **66**.[66]

Few examples of iron-induced self-assembling systems have been described in the literature, and only a couple of studies describe the different stages of formation of polynuclear self-assembled structures. Trying to better understand the self-assembling processes, Ziessel and co-workers[67] took advantage of electrospray mass spectrometry, which had been successfully applied for the characterization of various polynuclear complexes.[68,69] Reaction of the oligomultidentate ligand **67** with $FeSO_4 \cdot 7H_2O$ in a 1:1 ratio (Scheme 22) instantly produced a deep-violet solution, which showed peaks for the trimeric complex **68** as well as for a tetrameric complex in the ESMS.[67] The same analytical method was then used to monitor formation of intermediates in this reaction. Titration of **67** with the iron salt showed, with increasing amount of Fe(II) relative to **67,** progressive depletion of the intermediate L_2Fe and L_3Fe_2 clusters. At 0.5 equivs of Fe(II) salt, the L_3Fe_2 complex had almost totally disappeared, suggesting that the higher degree of preorganization favors faster complexation of additional Fe(II). Signals for the formation of a tetrameric complex were first observed at almost equimolar concentrations.

Scheme 22

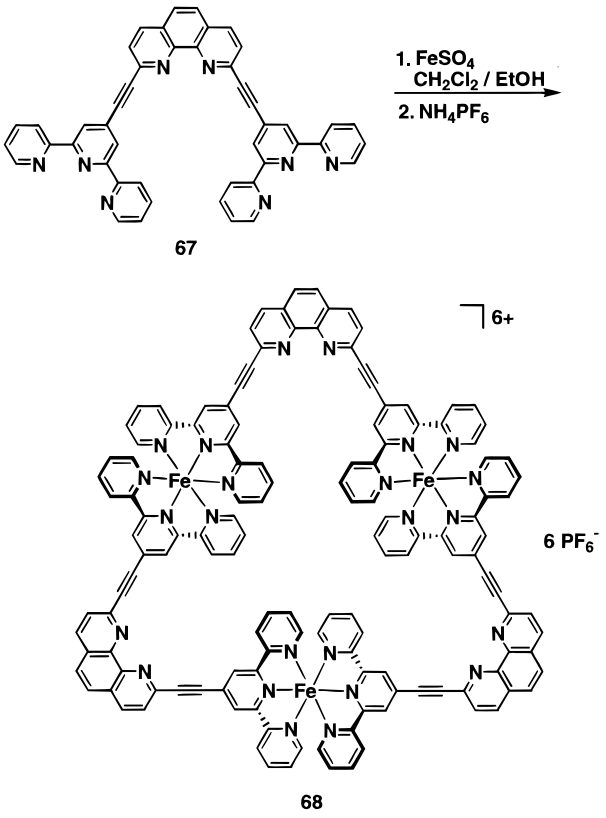

Another example of the stoichiometry-dependent formation of a triangular array has recently been described by Cotton and co-workers.[70] In an attempt to reproduce the successful formation of a molecular square from $[Mo_2(DArF)_2(CH_3CN)_4]^{2+}$ and oxalate dianion, the analogous reaction of $[Rh_2(DArF)_2(CH_3CN)_4]^{2+}$ (**69**) with oxalate dianion **70** in a 1:1 ratio gave instead the triangular molecule $[Rh_2(DArF)_2(CH_3CN)_4]_3$ **(71)** (Scheme 23). Changing the initial stoichiometry to 1:10 resulted in the formation of the expected molecular square **72**. Both compounds

Scheme 23

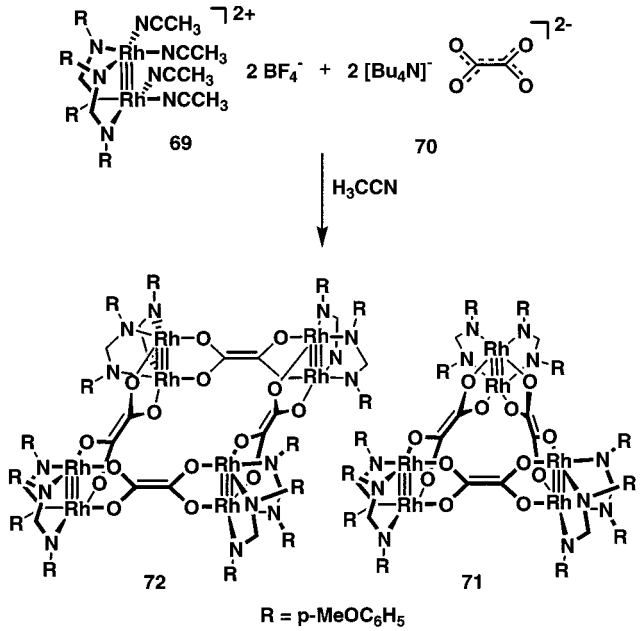

gave identical proton NMR spectra within experimental error, making it impossible to tell whether there was only one species in solution or the NMR spectra were coincidentally the same. X-ray structure analysis and the distinctly different electrochemical behavior unambiguously proved the proposed structures of **71** and **72**. In the solid state, complex **71** showed a stacking pattern, giving rise to tunnel-like cavities which were partially filled with solvent molecules (Figure 8). Though the authors distance

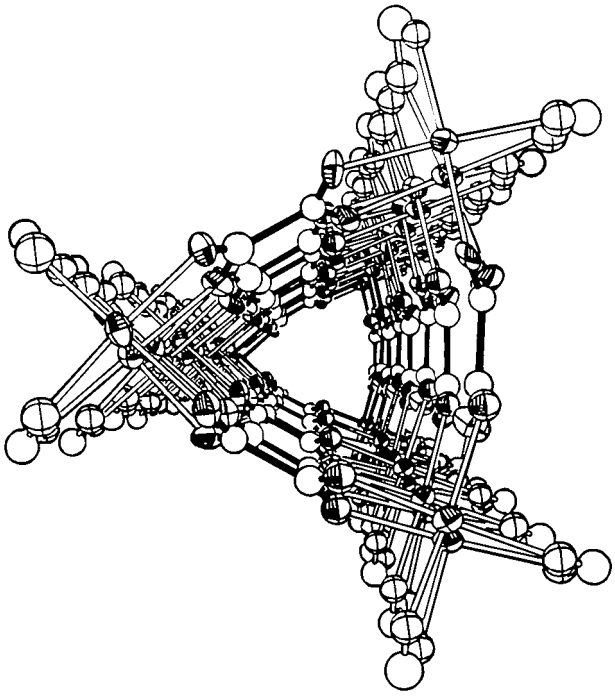

Figure 8. Solid-state stacking diagram of trimeric complex **71**.

themselves from any type of explanation and say forthrightly that they simply do not know why the strained triangular structure is adopted rather than the expected square,[70] it is quite possible that the excess oxalate serves as a template in the formation of the molecular square.

C. Molecular Squares and Tetranuclear Rectangles

Molecular squares remain one of the simplest but nonetheless very interesting members of this diverse family of nanoscopic assemblies. They are macrocyclic species that have per definition 90° turns in the assembly. Therefore, transition-metal complexes with at least two accessible *cis*-coordination sites are predetermined for the formation of molecular squares. As a consequence, almost any transition metal with square planar, trigonal bipyramidal, or octahedral geometry can be used as corner units. If the strain within the ensemble gets too big, the system generally makes up for that by slightly distorting the overall symmetry, forming less strained cyclobutane-like structures. As a result, several different approaches have been exploited in the preparation of these self-assembled tetranuclear species as discussed below.

1. Homonuclear Squares and Rectangles

It is well-known that transition metals have specific, well-defined geometries and coordination numbers based upon their electronic structure. Octahedral complexes such as *cis*-[Cr(CO)$_4$(norbornadiene)] offer two easily accessible coordination sites with bond angles of about 90°. Exploiting this fact, Verkade and co-workers were the first to report the serendipitous formation of a self-assembled molecular square in 1983.[30] Unintentionally, they were also the first to self-assemble a macrocycle via the "molecular library" model. Reaction of the 90° corner units *cis*-[Cr(CO)$_4$(norbornadiene)] (**73a**) or the *cis*-[W(CO)$_4$-(norbornadiene)] (**73b**) with the linear ditopic linker P(OCH$_2$)$_3$P (**74**), gave the mononuclear metal complexes **75**. Taking advantage of the bicyclic geometry of P(OCH$_2$)$_3$P **74** additional complexation of the free bridgehead phosphorus atom with additional *cis*-[Cr(CO)$_4$(norbornadiene)] (**73a**) or *cis*-[W(CO)$_4$(norbornadiene)] (**73b**), respectively, resulted in formation of the neutral molecular squares **76** in good yields (Scheme 24). Both compounds were characterized by means of NMR and IR. Further proof of the tetrametallic structure was given by the observation of the parent ion peak of the tungsten complex in the FAB mass spectrum.

Scheme 24

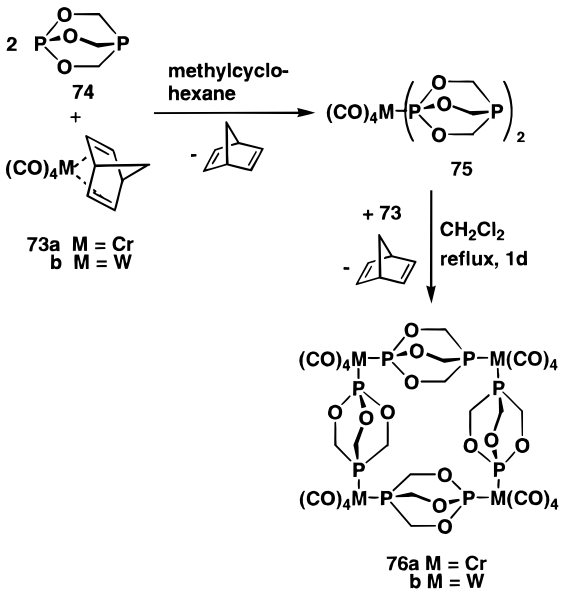

In contrast to early transition-metal complexes, group 10 transition metals are more likely to have square planar coordination geometries. Both palladium and platinum tend to form tetracoordinated complexes with adjacent bond angles of about 90°. By blocking two adjacent coordination sites of Pd(II) and Pt(II) with chelating bisphosphanes or bisamines, formation of chelated complexes with a constrained *cis*-geometry is feasible. If the remaining two coordination sites are occupied by weakly coordinated ligands such as the triflate or nitrate ion, then upon interaction with a linear nitrogen-containing bisheteroaryl, a square planar assembly will be formed.

Unaware of Verkade's earlier results with early transition metals, it was Fujita in 1990 who took advantage of this late transition-metal design strategy to self-assemble a molecular square. When the ethylenediamine complex of Pd(II) dinitrate **13** was reacted with 4,4′-bipyridine (**24**) in water (Scheme 25), Fujita and co-workers observed the quantitative self-assembly of molecular square **77a**.[38] The solution structure of these assemblies was confirmed by NMR spectroscopy and mass-spectrometric investigations, and its solid-state structure was later confirmed by X-ray crystallography.[61] The crystal structure showed an almost perfect square with the pyridine rings slightly twisted. The side-to-side distance in this square was approximately 8 Å. This molecular square showed the unique ability for molecular recognition of neutral aromatic guests such as naphthalene, benzene, etc. Its size can be varied by using larger ligands, incorporating additional spacers, such as acetylene, ethylene, or *p*-phenylene between the heteroaryls of 4,4′-bipyridine. In these cases, however, the reaction products were in equilibrium with other entities, postulated as molecular triangles (see Scheme 15).[61]

Scheme 25

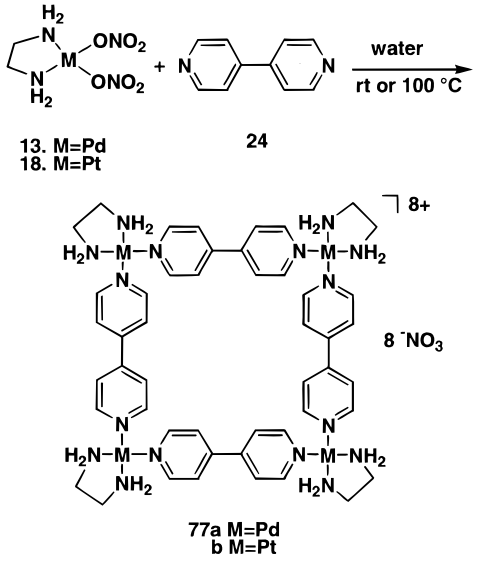

Interestingly, the corresponding Pt(II) analogue (en)Pt(NO$_3$)$_2$ (**18**), when initially mixed with 4,4′-bipyridine (**24**), afforded a mixture of oligomers. This kinetically distributed oligomeric mixture can be converted into the thermodynamically favored square **77b** (Scheme 25) by simply heating the reaction mixture to 100 °C as monitored by time-dependent NMR spectroscopy.[71] This effect is a consequence of the bond strength between Pt(II) and the nitrogen of the 4,4′-dipyridyl that is considerably stronger compared to the Pd(II)−N bond but still much weaker than the average covalent bond found in organic molecules.

In contrast to the work done by Fujita,[37−42] Stang and co-workers in their rational systematic design approach relied heavily on lipophilic phosphine-substituted as well as chelated bisphosphine platinum and palladium complexes.[72,73] Reaction of the chelated complexes **78a** and **78b** with equimolar amounts of 4,4′-bipyridine (**24**) in dichloromethane

Scheme 26

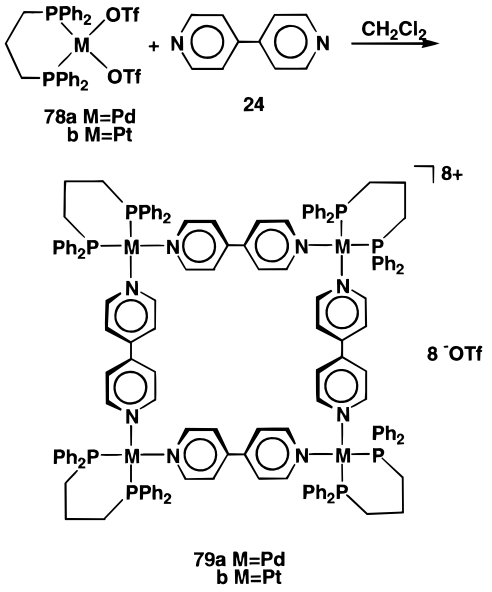

at room temperature resulted in the isolation and identification of the molecular squares **79a** and **79b** (Scheme 26). Characterization of those novel complexes was based on multinuclear NMR, physical properties, and later single-crystal X-ray diffraction studies. The X-ray structure analysis of molecular square **79b** showed a number of interesting geometric features (Figure 9). The geometry about the Pt(II) metal center was square planar with some deviation of the angles from 90°. The edge-to-edge distance in **79b** is 11.2 Å, and the diagonal Pt(II)−Pt(II) distance is nearly 15 Å. Due to the P−phenyl rings stacking with the 4,4′-bipyridyl, the N−Pt(II)−N valent angle decreased to 84°. To accommodate this lesser than 90° angle, the entire molecule was slightly puckered. The deviation from planarity in this molecule was about 4 Å and most likely can only be observed in the solid state, but the shape of the molecule was undoubtedly that of a square. The stacking pattern of this assembly in the solid state is of particular interest (Figure 9).[72] The cationic parts of the square were stacked along the *b*-axis, resulting in long, channel-like cavities with the triflate counterions located between the stacked squares close to the metal corners. Although the quality of the crystal was not perfect, it can be deduced from the data that no counterions are located within the cavity itself of the squares.

When the acyclic bisphosphine complexes **38** and **40** were reacted with 4,4′-bipyridine (**24**), it also resulted in the formation of the desired tetranuclear squares **80a** and **80b** in excellent yields (Scheme 27),

Scheme 27

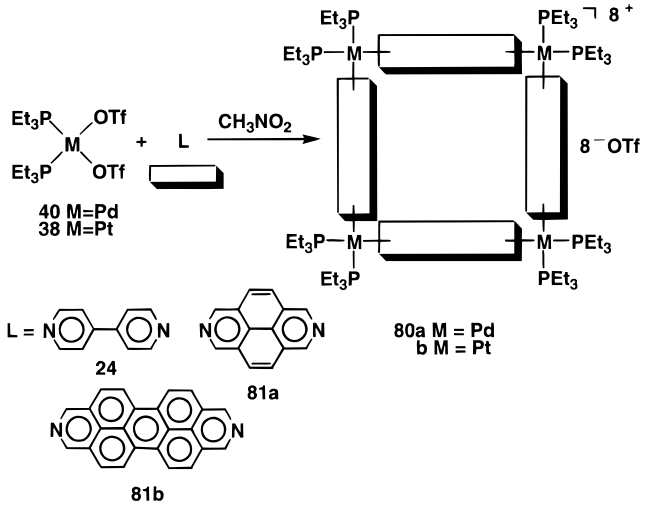

indicating that a variety of nonchelating phosphines may also be employed.[73] Another variation of this motif includes using the planar aromatic linkers 2,7-diazapyrene (**81a**) and 2,9-diazadibenzo[*cd*,*lm*]perylene (**81b**). These corresponding squares possess a deeper cavity than assemblies based on bipyridyl, and they are soluble in nitromethane despite the low solubility of their organic precursors, such as **81b**. Moreover, the polycondensed aromatic linkers form more rigid assemblies compared to bipyridine-linked squares which quite often show twisting of the pyridyl aromatic rings.

When 1,4-dicyanobenzene (**82a**) and 4,4′-dicyanobiphenyl (**82b**) were interacted with transition-metal

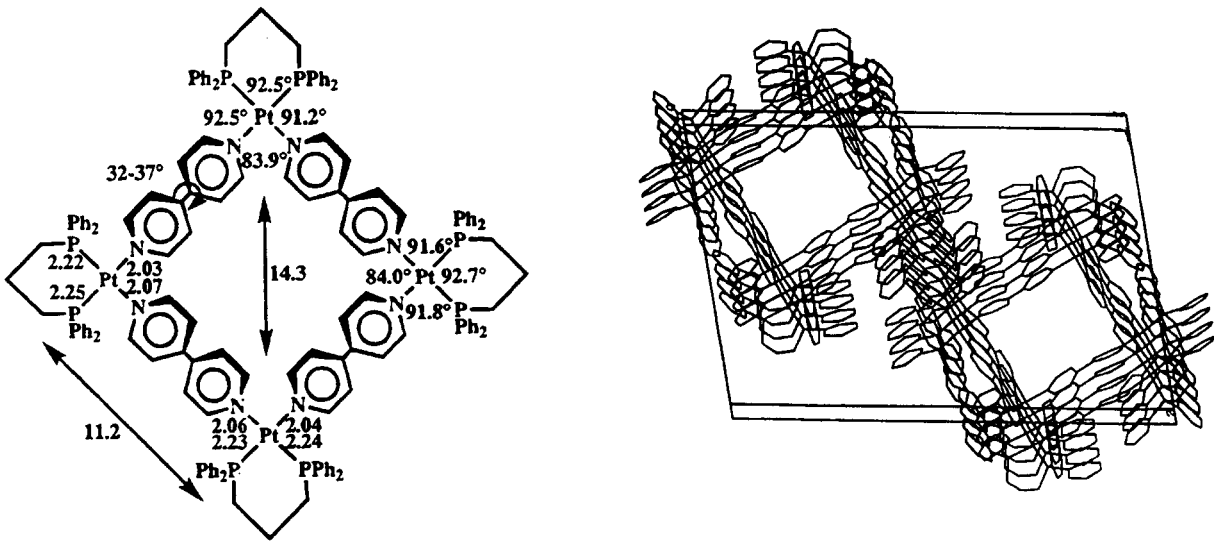

Figure 9. Crystallographic data (left) and solid-state packing diagram (right) of molecular square **79b**.

bisphosphanes **78a** and **78b**, only the Pd(II)-containing analogue **78a** yielded the expected products **83** (Scheme 28). In the case of the Pt(II) analogues, only

Scheme 28

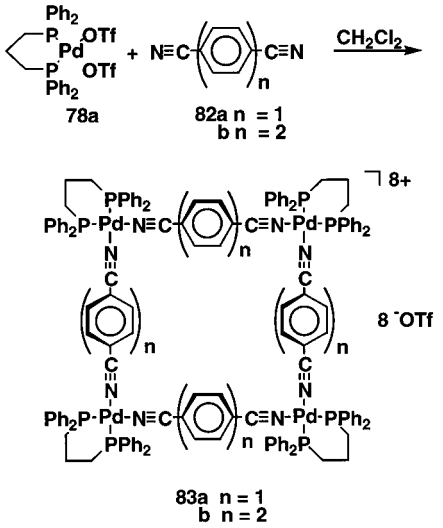

oligomers were produced. This indicates that the formation of these assemblies is governed by at least two other factors besides the valent angle: dative bond strength and the π-stacking interactions between each of the individual components. The delicate relationship between these factors can drastically influence the stability of the resulting assembly. As seen from the X-ray structure analysis based model of the 4,4′-bipyridine-based square **79b**, there is a high degree of π-stacking between the phenyls of the chelated bisphosphine and one of the 4,4′-bipyridine rings.[73] This kind of interaction may ultimately be responsible for the remarkable stability of squares **79a** and **79b**. It was impossible to prepare and isolate only a "corner" or a "side" of these assemblies. Even with a 100-fold excess of 4,4′-bipyridine in solution during the assembly, only the complete squares are formed, with the rest of the free ligand left intact. It is also not possible to obtain an isolable intermediate when the reaction is carried out with a large excess of transition-metal bistriflate. In contrast, when 1 equiv of ligand **82a** or **82b** was combined with two equivs of transition-metal bistriflates, the corresponding bimetallic bistriflate complexes were isolated. In these cases, the intermolecular interaction of the phenyl rings and linker ligand is much weaker due to the unfavorable spatial disposition of the linker mediated by the cyano groups. As a consequence, only the more labile Pd(II)-containing square is formed since it is still capable of internal self-reorganization due to the weaker Pd−N≡C− vs Pt−N≡C− interaction which reduces the possibility of the thermodynamically unfavorable oligomerization.[73] All molecular squares were isolated as robust, air-stable, microcrystalline solids which decompose at their melting points, generally above 200 °C. Most are prone to crystallize with either solvent of crystallization or water, which cannot be driven off even by prolonged heating in a vacuum.[72,73] These assemblies, despite their high molecular weight and charge, are remarkably soluble in organic solvents, such as dichloromethane, acetone, nitromethane, or methanol, but completely insoluble in water.

Chiral self-assembled, cyclic entities may be prepared with the chirality introduced in several different ways: (1) Use of a chiral auxiliary, such as a chiral bisphosphine, coordinated to the transition metal; (2) Employing diaza ligands which lack a rotation symmetry about their linkage axis, which will result in an overall "twist" of the species, thereby introducing elements of helicity in its assembly. In this situation, however, the formation of several (six for a tetranuclear assembly) stereoisomers is possible. (3) Use of optically active atropisomeric diaza−bisheterocycles (substituted 4,4′-bipyridines, bisquinolines) as linear linkers; (4) by employing inherently chiral octahedral metal complexes; (5) Combination of the above methods.

An example for the use of a chiral metal auxiliary in conjunction with elements of helicity was provided by Stang and Olenyuk.[74] When the chiral Pd(II) bistriflate complex **43a** was mixed with the C_{2h}-symmetrical diaza ligands, 2,6-diazaanthracene (DAA), **84a** in acetone, the formation of a single diastereomer of the square **85a** was observed. A single signal in the ^{31}P NMR spectrum is indicative of the exclusive formation of only one highly symmetrical chiral product (Scheme 29). The absolute stereochemistry

Scheme 29

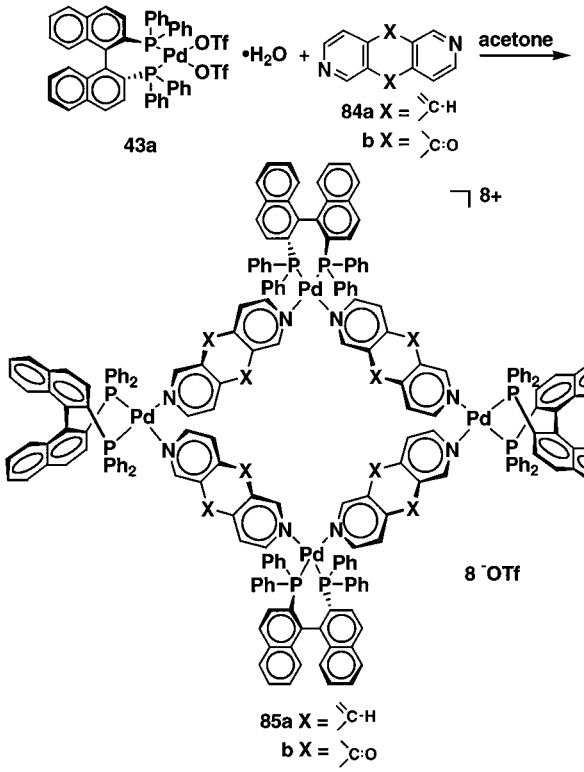

of **85a** as shown was assumed based upon the known X-ray structures of chiral BINAP transition-metal diaryls[75] in combination with transition-metal-parametrized MM2 force field calculations.

In contrast, when 2,6-diazaanthracene-9,10-dione (DAAD), **84b**, was employed as a connector ligand (Scheme 29), the reaction mixture consisted of a

significant excess of one diastereomeric product of **85a** along with minor amounts of other diastereomers, as demonstrated by the ^{31}P NMR spectra.[74] Integration of the individual expanded ^{31}P spectra gave a diastereomeric excess of 81% for **85a**. The macrocyclic nature of this complex was established by multinuclear NMR and confirmed by mass-spectroscopic data. Thus, the ESI mass spectrum of molecular square **85a** showed the presence of the doubly charged $[M - 2^{-}OTf]^{2+}$ and quadruply charged $[M - 4^{-}OTf]^{4+}$ ions. The interesting fact that both these types of assemblies are formed either as a single diastereomer or a significantly enriched diastereomeric mixture is attributable to the significant degree of asymmetry induced by the chiral bisphosphane complexes. A mixture of diastereomers was indeed observed[59] when an achiral transition-metal bisphosphane complex was used instead of BINAP.

The unsubstituted nucleobases uracil and thymine are known to show complex binding patterns due to an increased number of metal binding sites as well as to interconversion of the metal binding sites themselves.[24,76] Treatment of the uracil platinum complex **86** with 1 equiv of silver nitrate lead to the spontaneous self-assembly of the cyclic tetranuclear complex **87** (Scheme 30).[77] Analysis of the solid state

Scheme 30

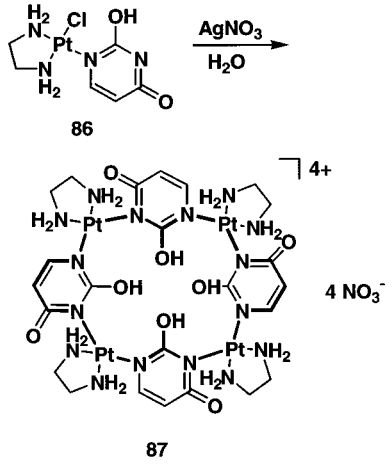

of **87** showed that the uracil ligands are in a rare bisplatinated tautomeric form with the acidic proton bound to one of the uracil oxygen atoms. The exocyclic oxygen of the uracil ligands is arranged in an alternating fashion, with oxygen of opposite square sides pointing into the same direction with respect to the Pt_4 plane. From the interpretation of the X-ray structure, compound **87** was considered to be a metal analogue of a calix[4]arene (Figure 10). Since most calix[4]arenes prefer the cone conformation, Lippert and co-workers investigated the conformer equilibrium of **87**. Interestingly, upon reaction with silver(I) salts, compound **87** spontaneously underwent 1,3-alternate/cone conversion giving rise to an octanuclear cone-shaped species $[(en)Pt(uracil)Ag]_4^{8+}$.[77] Host−guest interaction of similar cone-shaped zinc(II) salt complexes with small organic anions such as sulfonate anions showed guest-specific binding in aqueous solutions as a result of the hydrophobic nature of the cone cavity.[77c]

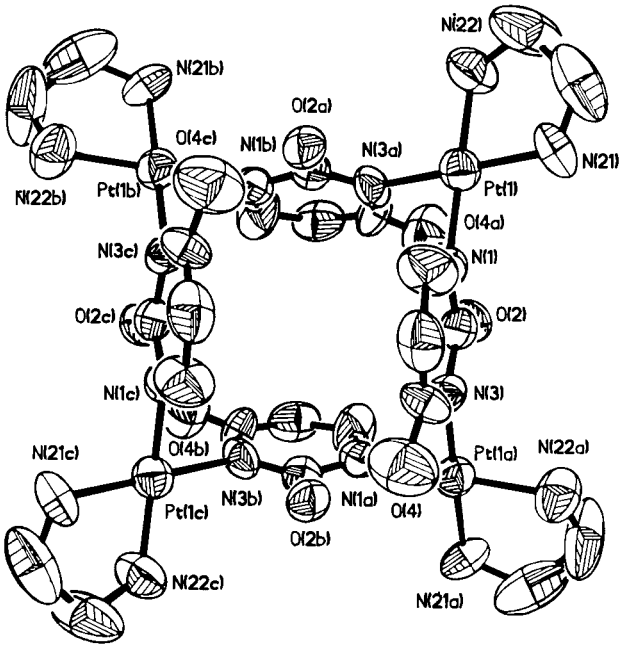

Figure 10. ORTEP plot representation of the tetranuclear complex $[(en)Pt(uracil)]_4(NO_3)_4$, **87**.

A similar approach to the construction of neutral Re-containing chiral squares was carried out by Hupp and co-workers as shown in Scheme 31.[78] Simple

Scheme 31

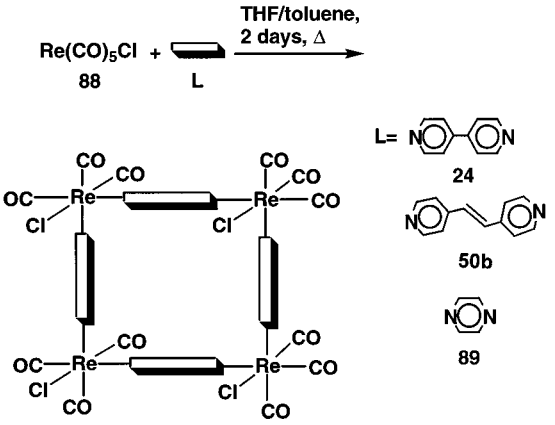

90a L=4,4′-bipyridyl
b L=1,2-di(4-pyridyl)ethene
c L=pyrazine

mixing of $Re(CO)_5Cl$ (**88**) with either 4,4′-bipyridyl (**24**), 1,2-bis-*trans*-(4′pyridyl)ethylene (**50b**), or pyrazine (**89**) in a mixture of THF and toluene resulted in the formation of molecular squares **90a**−**c** in greater than 95% yields.[78] A variety of analytical methods were used to characterize these compounds including X-ray crystal studies of the pyrazine-linked square **90c**. The structural data revealed a near-square-planar shape for macrocycle **90c** with a slight distortion of its geometry (Re−N angles of 85.6°). Unfortunately, due to a disorder of the CO/Cl trans ligand pairs, no reliable information on the configuration of this system was given. Generally, one would expect the formation of a mixture of isomeric products. The proton NMR showed two distinct signals of almost equal intensity for the pyrazine protons,

which was explained as a result of hindered rotation, though the authors could not exclude the formation of equally populated isomers. While the two squares containing 4,4′-bipyridine (**90a**) and pyrazine (**90c**) were found to be luminescent at room temperature, square **90b** did not show any detectable luminescence. Time-resolved luminescence studies of the two photoactive squares revealed that their emissive excited-state lifetimes are much shorter than those measured for the corresponding monomeric corner units. One possible interpretation of this is that the excited states in these squares are quenched by charge transfer to proximal chromophores.[78]

A very interesting method of making molecular squares by interlinking dinuclear molybdenum chelate complexes with oxalate, tetrafluoroparaphthalate, and ferrocene-1,1′-dicarboxylate dianions was applied by Cotton and co-workers.[70] Reaction of $[Mo_2(DArF)_2(CH_3CN)_4][BF_4]_2$ (DArF = *N*,*N*′-bis(*p*-methoxybenzyl)formamidinate anion), **91**, with $(NBu_4)_2(C_2O_4)$, **70**, or the disodium salt of ferrocene-1,1′-dicarboxylate, **92**, resulted in the formation of the corresponding square tetramers **93a** and **93b**, respectively (Scheme 32). Spectroscopic and analytical

Scheme 32

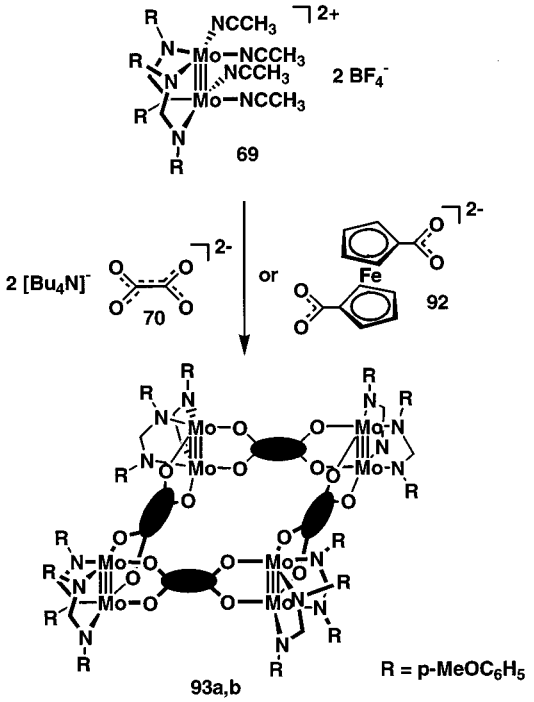

characterization along with X-ray structure analysis established the tetrameric character of both complexes. Furthermore, a large number of solvent molecules were included in the solid state of both complexes as a result of the large empty cavities enclosed by these neutral assemblies. An analogous rhodium complex was also formed in a similar reaction (see Scheme 23) along with an unexpected molecular triangle.[70] While the triangle was solely formed at a metal-to-ligand ratio of 1:1, the square complex formed with a high excess of the chelating ligand.

Attempts to synthesize tetrametallic rectangles by mixing 90° corner units with a 1:1 mixture of linear bridging ligands such as 4,4′-bipyridine and pyrazine resulted exclusively in the formation of the homobridged squares rather than the mixed-bridged rectangles.[14,15,79] An alternative route for the formation of molecular rectangles involves the design of a binuclear complex with two parallel coordination sites, which can be interlinked by 4,4′-bipyridine or pyrazine. Süss-Fink and co-workers recently used this synthetic strategy successfully in a side-by-side assembly of a molecular rectangle (Scheme 33).[80]

Scheme 33

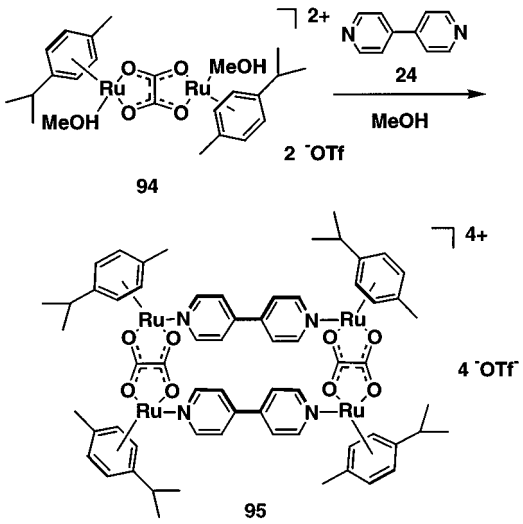

Reaction of the oxalato-bridged binuclear *p*-cymeneruthenium complex, **94**, with 1 equiv of bipyridine, **24**, furnished the tetranuclear molecular rectangle **95** quantitatively. The rectangular shape of complex **95** was confirmed by X-ray structure analysis. It showed a crystallographic C_2 symmetry where the oxalato planes were oriented parallel to each other and the two pyridine rings of the bipyridine were inclined to one another by 19.5°.

Recently, Hupp and co-workers[81] as well as Sullivan and co-workers[82] independently reported other examples of tetrametallic macrocycles with a rectangular shape. Both groups used dimeric Re complexes bridged by either thiolate[81] or alkoxy[82] ligands. Reacting 4,4′-bipyridine, **24**, or pyrazine, **90**, with the dimeric complex $[(CO)_4Re(\mu\text{-}SPr)]_2$, **96**, in refluxing chloroform, Hupp and co-workers[81] were able to isolate the molecular rectangles **97a** and **97b** as crystalline precipitates in good yields (Scheme 34). The X-ray structure analysis of the 4,4′-bipyridine complex **97a** showed a rectangular framework with dimensions of 3.81 and 11.57 Å, as defined by the metal corners. Furthermore, the structure revealed a near planarity of the pyridyl planes of the bridging 4,4′-bipyridines, which was attributed to steric interference of the bipyridine ligands. Unfortunately, calculations demonstrated that the interplanar spacing in these rectangular species were too small to function as receptor sites, even for planar molecules such as benzene. Similar findings and results were reported by Sullivan and co-workers using homologous chalcogenate ligands.[82]

Some success in rectangle synthesis has been achieved by using the above-mentioned two-step

Scheme 34

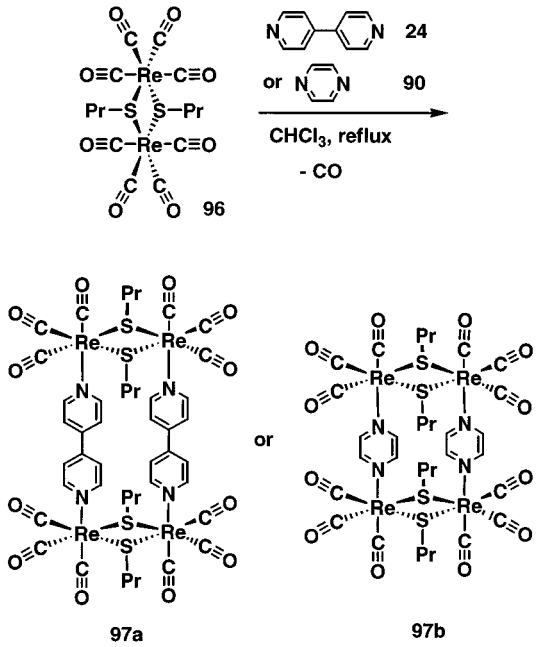

process. Starting with the synthesis of relatively robust dimeric edges, molecular rectangles were assembled upon reaction with linear linkers. Unfortunately, the cavity sizes for those systems were insufficient to allow the molecule to function as a host for small guest molecules.[80−82] Building upon the same strategy, Hupp and co-workers[83] were able to synthesize molecular rectangles by first assembling a stabilized bimetallic rhenium edge using the bridging 2,2′-bipyrimidine and then adding difunctional pyridyl-based linear linkers. Heating 2 equivs of $Re(CO)_5Cl$ with 1 equiv of 2,2′-bipyrimidine in toluene furnished a syn and anti mixture of the bimetallic edge **98** analogous to Vogler's[84] synthesis. Subsequent removal of the chloride ligand with silver triflate and addition of 1 equiv of 4,4′-bipyridine, **24**, in refluxing tetrahydrofuran resulted in precipitation of the product **99** in 50% yield, leaving the noncyclic products, formed by the anti bimetallic edges, in solution (Scheme 35). The X-ray structure analysis of rectangle **99** showed an empty cavity with dimensions

Scheme 35

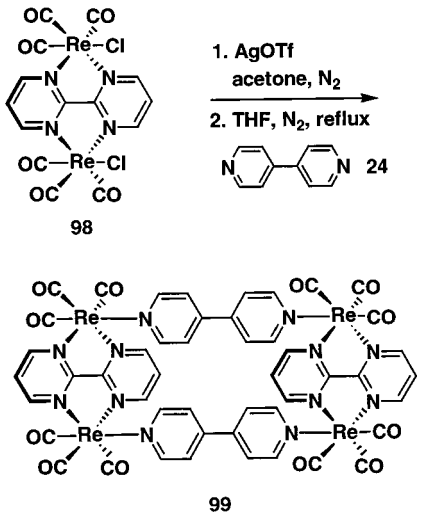

of 5.84 × 11.55 Å. All counterions and solvent molecules were located outside the self-assembled molecule, some being located within the channels formed by offset packing of the rectangles. Preliminary ^1H NMR affinity studies of **99** for the bis-sodium salt of 2,6-naphthalenedisulfonic acid gave an association constant of $2.3 \times 10^3\ M^{-1}$, showing the best fit based on a 1:1 host/guest ratio.

An interesting example of a copper-containing tetranuclear assembly prepared from copper(I) triflate, **100**, and 3,6-bis(2′-pyridyl)pyridazine (dppn), **101**, was given by Youinou et al. (Scheme 36).[85] When

Scheme 36

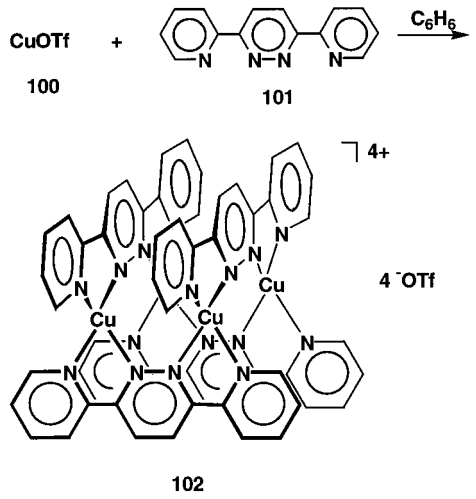

2 equivs of dppn was added to 1 equiv of **100** in benzene, the formation of a brown precipitate resulted,which was isolated in 81% yield. Analytical NMR combined with FAB mass spectrometry and X-ray crystallography confirmed the tetrameric structure of the final product **102** to be $[Cu_4(dppn)_4](OTf)_4$. The four copper atoms are spanned by the four dppn ligands, two lying above the plane of the transition metals and two below. The copper geometry is distorted tetrahedral. Apparently, the ligand is sufficiently flexible to adjust to the steric requirements of the four copper units. The X-ray structure also indicated a high degree of π-stacking between each pair of the dppn ligands, which may play an important role in the formation of this cyclic structure. The internal dimensions of this assembly are equal to the distance between each ligand, 3.47 Å.[85] Additionally, the electrochemical properties of **102** were studied by cyclic voltammetry in DMF. Cyclic assembly **102** is a rare example of a planar arrangement of four copper atoms where each of them possesses tetrahedral geometry.

The formation of a cobalt-containing assembly was also reported.[86] In this study, the authors utilized the chemistry of 2-thiouracil Co(III) complexes. Specifically, they employed the complexation of 1-(2-thiouracil-4-methylene)-3,6-diazahexane which, upon dissociation of the NH proton in the uracil ring, becomes a potential bidentate complexing ligand with free N and S donors that can coordinate to an octahedral metal center via the formation of a four-membered ring. When Co(II) bistriflate, **103**, was mixed with diethylenetriamine, **104**, and 1 equiv of 2-thiouracil-

Scheme 37

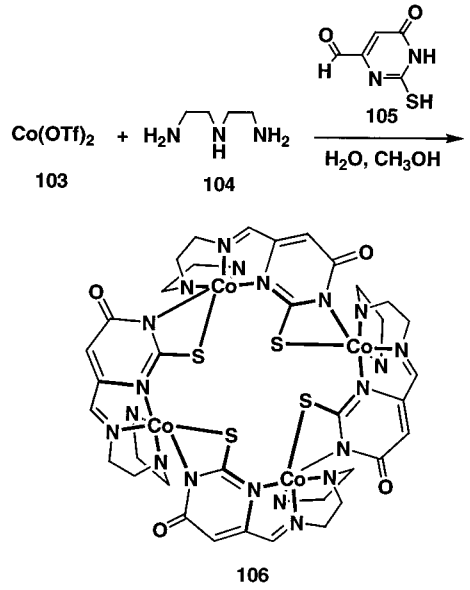

4-aldehyde, **105**, in aqueous methanol solution, the cobalt(III) complex $[Co_4L_4](OTf)_4$, **106** (Scheme 37), resulted. The X-ray structure of this product confirmed its cyclic form. The Co−Co distances in this square are 7.12 Å across the diagonal and 5.54 Å along the side. This cyclic assembly has a relatively large cavity with the heterocyclic rings arranged almost perpendicularly to the plane of the cobalt ions.[86]

A variation of the above systems was achieved by introduction of a ferrocenyl-substituted phosphine ligand.[87] The diaqua complexes of the ferrocenyl palladium and platinum complexes **107a** and **107b** exhibit a high reactivity toward nitrogen-containing heteroaryls, similar to that of the corresponding bistriflate complexes. When the aqua complexes **107a** and **107b** were treated with 2,7-diazapyrene, **81a**, they produced the desired heterobimetallic assemblies **108a** and **108b** in excellent isolated yields (Scheme 38). These molecular squares are an interesting combination of several redox-active ferrocenyl centers with highly conjugated aromatic linker units.[87] They are intensely colored both in solution and in the solid state and have interesting UV−Vis absorbance spectra. Their unique structure may suggest the presence of interesting electrochemical properties, which are still under investigation.

Crown ethers[88−93] and calixarenes[94,95] are two classical covalent macrocycles that played an important role in the development of host−guest chemistry and the study of inclusion phenomena and continue to be subjects of intensive research.[96−98] Metallacrown ethers[99−103] and metallacalixarenes[104−110] are interesting transition-metal analogues to crown ethers and calixarenes that preserve their guest-binding functionality. Since crown ethers are excellent hosts for hard metal cations and calixarenes have a high affinity for neutral guests, they are expected to extend the functionality of molecular squares when combined into a single supramolecular assembly.

Interaction of the metallacrown bistriflate **109**[111] with 2,7-diazapyrene, **81a**, resulted in the formation

Scheme 38

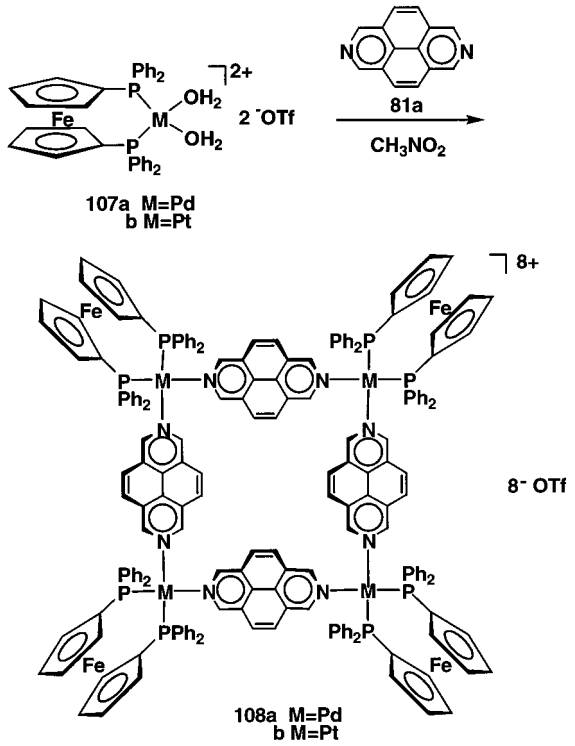

of the macrocyclic product **110** in good isolated yields (Scheme 39).[111] Likewise, reaction of the previously prepared metallacalix[4]arene triflate complex **111** with 4,4′-bipyridine, **24**, in dichloromethane at room temperature afforded the unique multicalixarene assembly **112** in excellent yields (Scheme 40).[111] All the physical and spectroscopic data for these assemblies confirmed their expected structure. Additional ESI−FTICR mass spectra[112] proved the presence of at least one H_2O molecule in this assembly. The inclusion of water in these assemblies is particularly interesting, and it was hypothesized that the water is likely to interact with the cationic parts of the assembly via the oxygen lone pairs and is simultaneously hydrogen bonded to the crown ether oxygen atoms. This results in exceptionally stable

Scheme 39

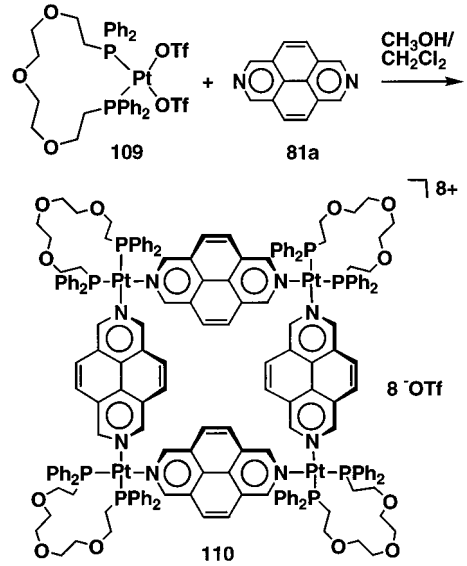

Scheme 40

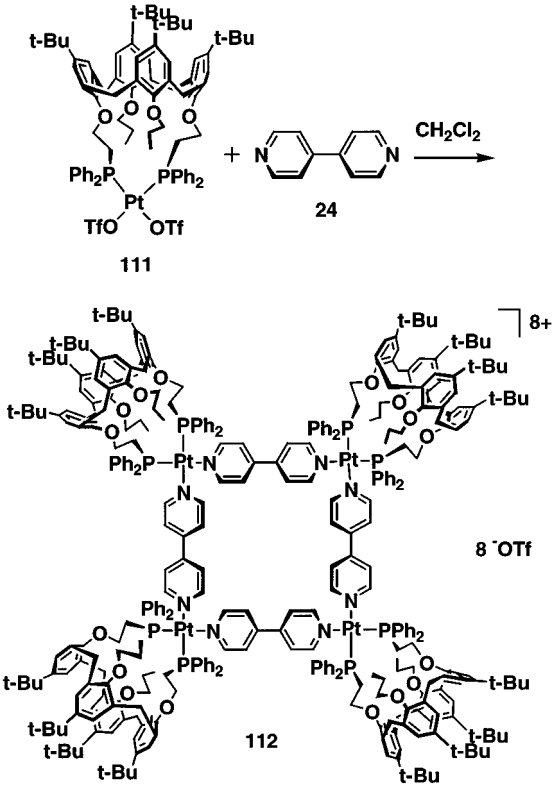

water adducts from which the water cannot be removed even on heating at 100 °C for several days. A similar explanation was suggested for the relatively high water content in metallacrown ethers.[113,114]

2. Heteronuclear Squares and Rectangles

The versatility of the "molecular library" approach can be demonstrated via the preparation of an interesting class of molecular squares incorporating different transition-metal centers. There are examples that contain different transition metals at the alternating corners of the assembly as well as examples with the same transition metal in different charged states. Decreasing the overall symmetry of these systems and at the same time introducing different types of binding sites makes such ensembles more suitable as possible molecular hosts, thus providing for a better host−guest fit. The simplest way to prepare mixed neutral-charged or heterobimetallic molecular squares is to use the Pd(II) and Pt(II) bistriflate complexes **40** and **38** for the charged portion of the assembly along with specially designed subunits which contain covalently bound ethynylpyridine and thus neutral late transition-metal bisphosphane complexes.[115,116] Reaction of equimolar amounts of transition-metal bistriflates **40** or **38** in an appropriate solvent with either **113** or **114** afforded the predicted mixed heterobimetallic squares **115** and **116** in high isolated yields (Scheme 41).[115,116] Although squares **115b** and **116b** formed within minutes, the formation of the Pt(II)-containing assemblies **115a** and **116a** required several hours. These squares were successfully characterized by various physical and spectrometric techniques, including fast atom bombardment mass spectrometry FABMS[117] and an X-ray structure analysis.[116]

Attempts to bind metals such as copper, silver, and gold via π-interaction to the acetylene units[118−120] via the so-called "π-tweezer effect"[121] resulted in the isolation of two silver complexes **117a** and **117b** (Scheme 42).[115] Particularly interesting is the fact that attempts to bind 1 equiv of silver salt failed, resulting in a mixture of several products that quickly formed an insoluble precipitate. Both silver

Scheme 41

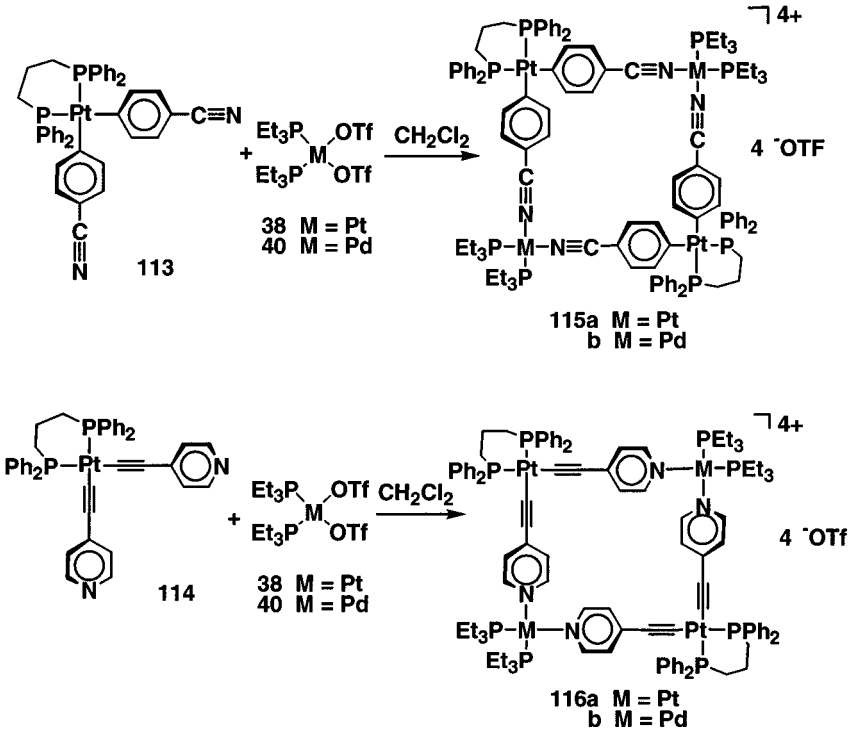

Scheme 42

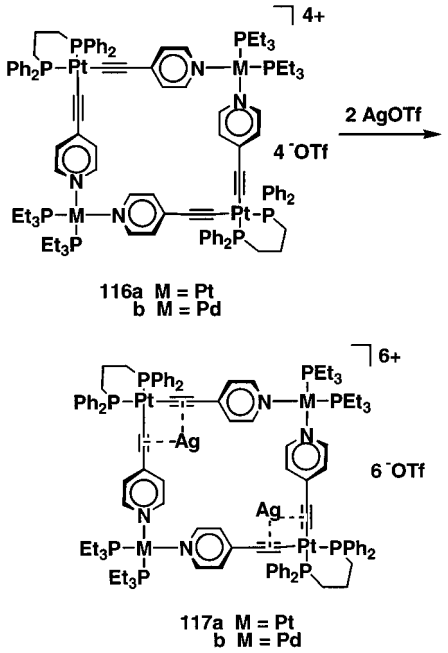

complexes **117a** and **117b** were characterized by multinuclear NMR, IR, and UV spectroscopy, as well as FAB mass spectrometry unambiguously establishing the molecular weight of both of these interesting adducts.

Taking advantage of those newly introduced coordination sites, attempts to bind a guest molecule within the cavity were successful. Reaction of the Lewis acid receptor assembly **117** with an equimolar amount of pyrazine, **89**, phenazine, **118**, or dipyridyl ketone, **35**, respectively, in CH_2Cl_2 at room temperature, results in the formation of host−guest complexes **119a,b** (Scheme 43).[122−125] The Lewis acid/base host−guest complexes were fully characterized by physical and spectroscopic techniques. The geometrical features of molecular square **119a** with phenazine, as determined through X-ray crystallography, provided insight toward molecular receptor design (Figure 11). There are several interesting structural features evident for this complex. The overall geometry of the perimeter for this complex is nearly planar with the guest phenazine oriented nearly orthogonal to the Pt−Pt^{2+}−Pt plane. The π-complexed silver atoms are located in a pseudo-trans arrangement with respect to the Pt−Pt^{2+}−Pt plane, resulting in a C_i-symmetric relationship. The use of chiral phosphine ligands such as BINAP made it possible to monitor the host−guest interaction via circular dichroism.[126] The coordination of silver was readily monitored by a significant change in the intensity and shape of the CD absorption bands, while the stoichiometric addition of respective guests to the Lewis acid/base receptors was followed by a subsequent decrease in the absorption intensities and a variation of the signal shape.[126] These unique geometric features and the high stability of the abovementioned assemblies will undoubtedly make them useful in the development of artificial receptors.

Scheme 43

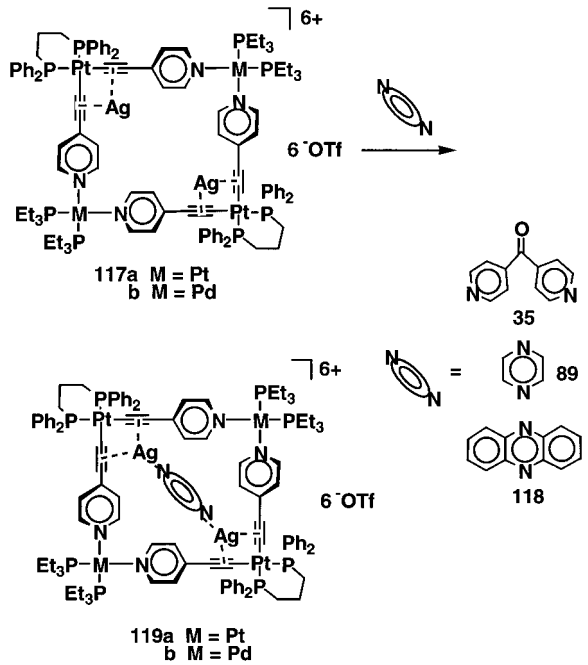

Building modules that contain early transition metals are especially interesting, since the incorporation of these metals may allow one to further vary charge density on each individual subunit of a multinuclear assembly. Some additional benefits of this approach include the possible variations in physical dimensions as well as the shape of the resulting macrocyclic structure. Titanocene complexes are good examples of early transition-metal modules due to the favorable valent angle between the metal and the attached ligands as well as their rich and versatile chemistry. Interaction of the easily accessible titanocene complex **120**[127] with the platinum bisphosphine complex **38** in nitromethane produced the macrocyclic assembly **121** in excellent yield (Scheme 44).[128] The compound was isolated as a stable orange microcrystalline solid and characterized by a variety of spectroscopic methods as well as by LSIMS. These mass-spectroscopic data show the doubly charged ion $[M - 2OTf]^{2+}$ at $m/z = 1002.6$ whose experimental isotope pattern matches very closely the calculated value, thereby confirming the tetranuclear nature of this macrocycle. Unlike all previously discussed assemblies, **121** contained relatively flexible oxygen linkers and was therefore significantly less rigid in conformation.

An interesting example of a luminescent macrocyclic assembly was prepared by utilizing the chromophore complex *fac*-$Re(CO)_3Cl(4,4'$-bipydidyl$)_2$, **122**. When Hupp and co-workers combined the rhenium corner **122** with the dppp Pd(II) bistriflate **78a**, it produced the luminescent molecular square **123** in 83% isolated yield (Scheme 45).[129] The introduction of photoluminescence is especially interesting in these types of assemblies since it might be used as an alternative to NMR spectroscopy in the detection of guest inclusion. This is a particularly attractive feature if these assemblies are to be used as molecular sensors. In addition, luminescence allows the examination of the excited-state reactivity of these

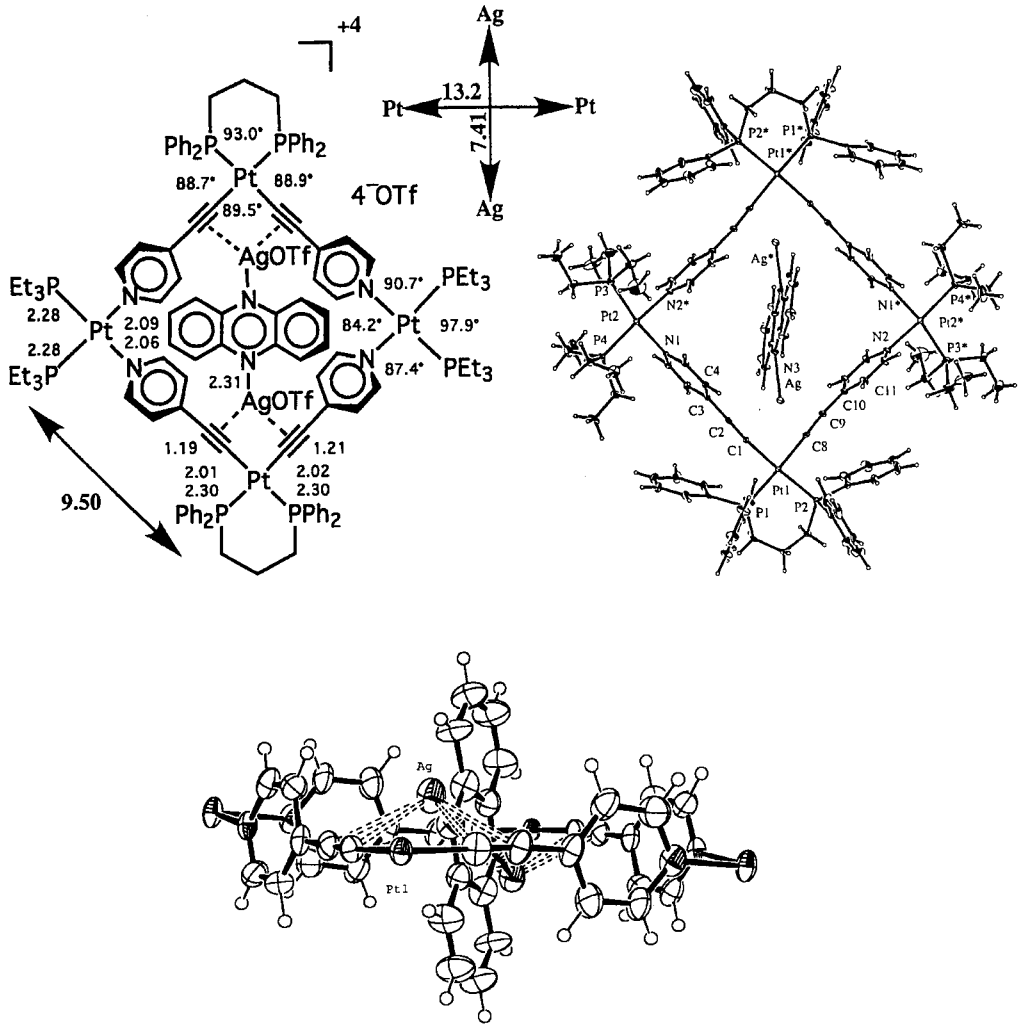

Figure 11. Summary of the significant geometric features (left), top view (center), and ORTEP side view (right) of the cationic portion of host−guest complex **119a** and phenazine.

Scheme 44

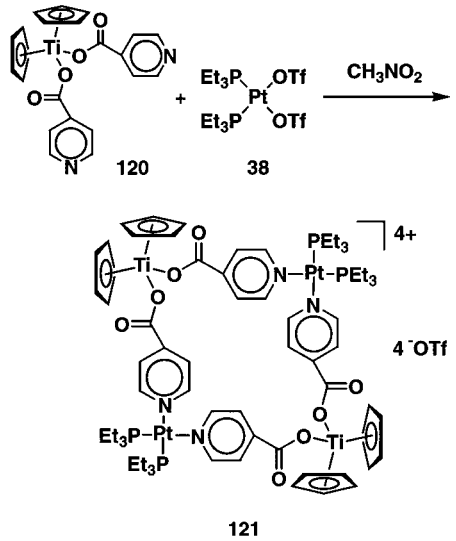

Scheme 45

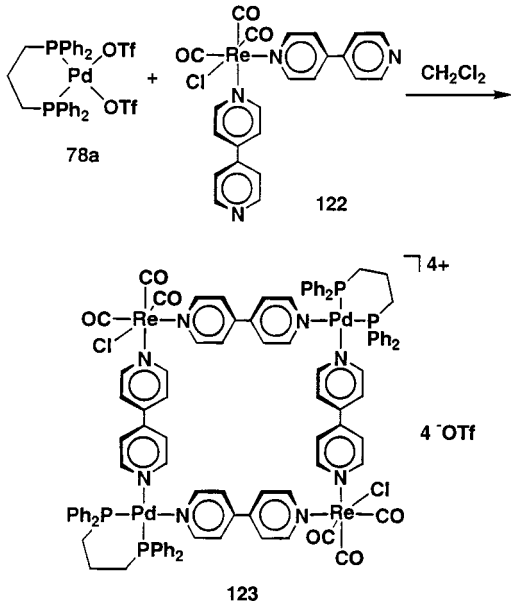

assemblies and the possible manipulation of the reactivity by the encapsulated guests. In the case of square **123**, it was noted that the emission from the square was greatly enhanced by the addition of perchlorate salt, presumably due to perchlorate anion binding within the cavity of the square.[129]

The preparation of nanoscale platinum macrocycles was achieved with surprising simplicity and, by employing the proper conditions, in essentially quantitative yield in all cases. Addition of a CD_2Cl_2

Scheme 46

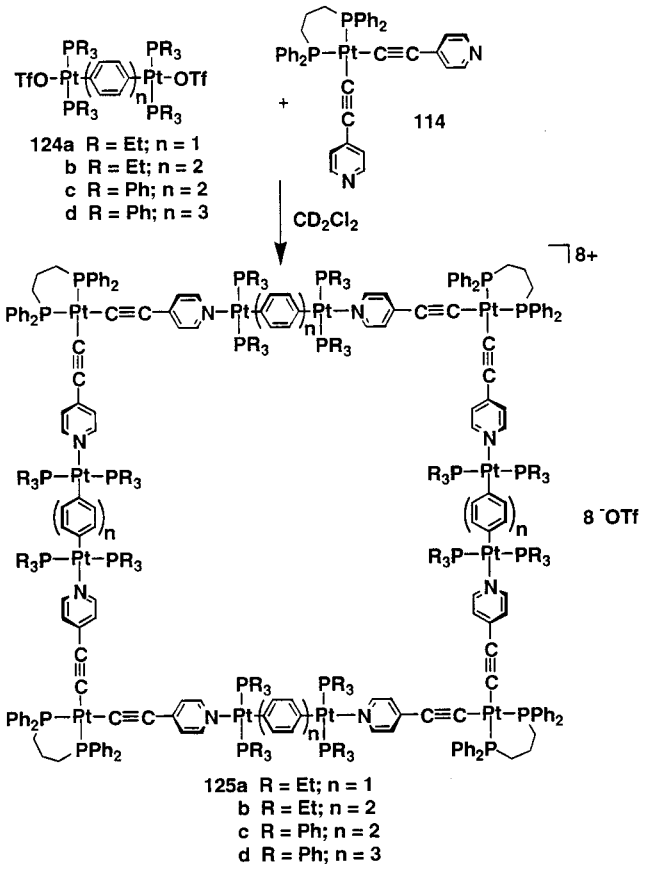

solution of the neutral *cis*-platinum complexes **114** to the solid bistriflate monomers **124a**−**d**[130,131] resulted in the quantitative formation of the squares **125a**−**d** (Scheme 46), respectively, of differing topology and dimensions.[132] Interestingly, it was found that the self-assembly of macrocycle **125c** was concentration dependent. If a 2.0×10^{-2} M CD_2Cl_2 solution of corner **114** was added to a 2.0×10^{-2} M solution of linear linker **124c** in CD_2Cl_2, a mixture of two products formed; however, neither product was oligomeric in nature. One of the products was indeed identified as macrocycle **125c** (70%), whereas the other product was structurally unidentifiable (30%). If the reaction was performed by the addition of a concentrated solution of **114** (4.0×10^{-2} M) to solid **124c**, then macrocycle **125c** was the only product obtained in this reaction.

It has been demonstrated that in certain systems the formation of macrocycle versus polymer is, as might be expected, concentration dependent. For example, Hunter and co-workers[133] showed that at low concentration monomer is prevalent in solution, while at higher concentration tetramer formation is preferred, while at even greater concentration polymer formation is expected. In contrast, the results for **125c** indicate that at higher concentration the simplest macrocycle expected is formed while in a dilute solution the product distribution includes more complex systems.

To get a rough idea of the expected dimension of these new macrocycles, the simplest macrocycle prepared, **125a**, was structurally minimized by employing computer modeling.[134−136] The calculated dimension between each diagonal *cis*-Pt center is ∼36 Å. The new nanoscale macrocycles prepared were characterized by Fourier transform infrared spectroscopy, NMR spectroscopy, elemental analysis, and physical means. Macrocycle **125d** was additionally probed by ESI FT-ICR mass spectrometry.[137]

These macrocyclic assemblies belong to the category of ultrafine particles, because their estimated dimensions are about 3.4 nm along the edge and 4.8 nm across the diagonal for assembly **125c**. Because of their unique structure they may become useful in the construction of nanoscale molecular devices.

3. Porphyrin-Containing Squares

One of the goals of modern supramolecular chemistry is to expand our understanding of complex processes in nature by studying artificial models that mimic the function of the desired natural receptor. The photosynthetic reaction center and the light-harvesting complex of bacteria are two examples of such natural aggregates.[138,139] A first step toward understanding their function is to construct artificial multichromophore aggregates suitable for the investigation of directed energy- and electron-transfer processes.[140,141] In most cases, linked porphyrin arrays are good examples of such aggregates. Over the last couple of years, various molecular devices based on oligoporphyrins have been designed and prepared. These include photoinduced picosecond molecular switches,[142] optoelectronic gates,[143] artificial photosynthetic systems,[144] fluorescence quenching sensors,[145] photonic wires,[146] and anticancer drugs.[147] Different types of porphyrin arrays including linear chains,[147,148] cyclic oligomeres,[149] squares,[150] dendrimers,[151] sheets and tapes,[152] stars,[153] and rosettes[154] have been characterized. Since all molecular squares made to date are conformationally rigid entities, it was expected that the resulting porphyrin-based assemblies should also possess this important feature required for photochemical studies, since the relative distance between individual porphyrin chromophores, their orientation, and overlap have a drastic influence on the photoactivity of the entire assembly.[155−159]

Porphyrin-containing ligands that possess pyridyl groups in a proper spatial orientation may serve as sides of the square, whereas the transition-metal bisphosphanes are corner units of such a tetranuclear assembly. Self-assembly is carried out according to Scheme 47. Porphyrin **126a** was chosen due to its high solubility in common organic solvents. Upon mixing with the Pd(II) bistriflate complex **78a**, the desired tetranuclear assembly **127a** was isolated as a deep-purple solid with a high decomposition point.[160] When the Zn-containing porphyrin **126b** was employed, the heterobimetallic assembly **127b** was isolated. Evidence of their conformational rigidity was obtained from the analysis of multinuclear NMR, especially the proton and carbon spectra. Since the porphyrin units are restricted in rotation around the metal−ligand axis, they are located nearly parallel to the transition-metal coordination planes, as derived from ESFF force field simulations. Such an arrangement subjects the inner protons of the assembly to the cyclic magnetic currents of the entire

Scheme 47

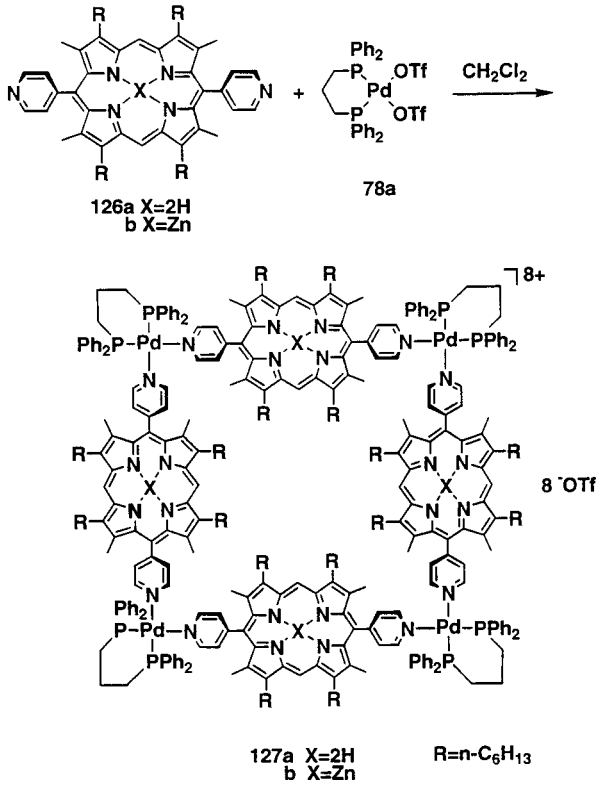

tetranuclear system and as a consequence renders them considerably high-field-shifted compared to their outer counterparts. Indeed, this high-field shift was detected in all porphyrin-containing assemblies.

In a study conducted by Lehn and Drain,[150a] the preparation of ordered square-shaped multiporphyrin assemblies was achieved via the coordination of bispyridyl porphyrins to cis and trans palladium dichloride, which served as either angular or linear binding units. Titration of 5,10-bispyridylporphyrin **128a** or its Zn complex **128b** into 1 equiv of *cis*-$Pd(NCPh)_2Cl_2$, **129**, at micromolar concentrations provided the complexes **130** (Scheme 48) which were characterized by NMR spectroscopy and mass spectrometry combined with UV−vis spectrophotometry and vapor-phase osmometry. Titrations of *trans*-$Pd(NCPh)_2Cl_2$, **131**, in a similar manner, into micromolar solutions of **128** yielded the assemblies **132** in high yield (Scheme 49). Clear isosbestic points in the UV−vis spectra were observed during such titrations. The Sorét band of the resulting species is red shifted by 6−8 nm, and its intensity decreased by about 50% with its simultaneous broadening as compared to the uncomplexed porphyrins. This indicates that the electronic interactions in the square are greater than those in the simple dimers. The relative fluorescence intensity of both **132a** and **132b** sharply decreases by 80%. A fluorescence polarization study also provided additional support for the structure of this assembly.[150a] The NMR spectroscopic data for **132** were also consistent with the formation of cyclic structures, despite oligomer formation at concentrations higher than 800 μmol·dm^{-3}.

The preparation of constitutionally similar but topologically different multiporphyrin squares **134** from 5,10-di(4′-pyridyl)-15,20-diphenyl-porphyrin (*cis*-

Scheme 48

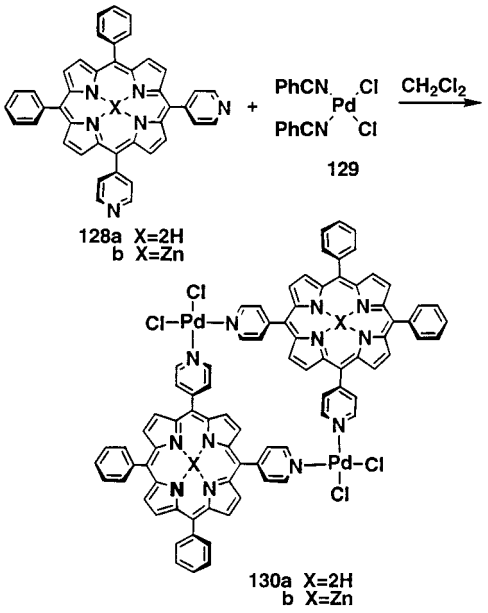

Scheme 49

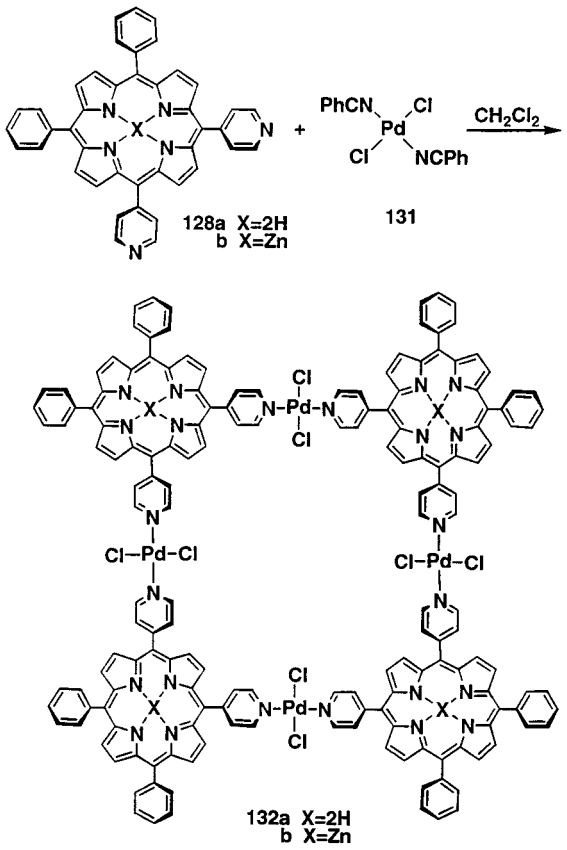

DPyDPP), **133a**, or *cis*-ZnDPyDPP, **133b**, with **129**, was carried out in refluxing toluene as depicted in Scheme 50. Very similar trends were observed as for **132**, except that the isolated material was more robust.[150a] Thus, monitoring the reaction at 55 °C also indicated the isosbestic point in the Sorét region; the reaction was complete within 24−48 h. Both NMR data and fluorescence polarization combined with mass spectrometry confirmed that only one product was present in the reaction mixture.

Scheme 50

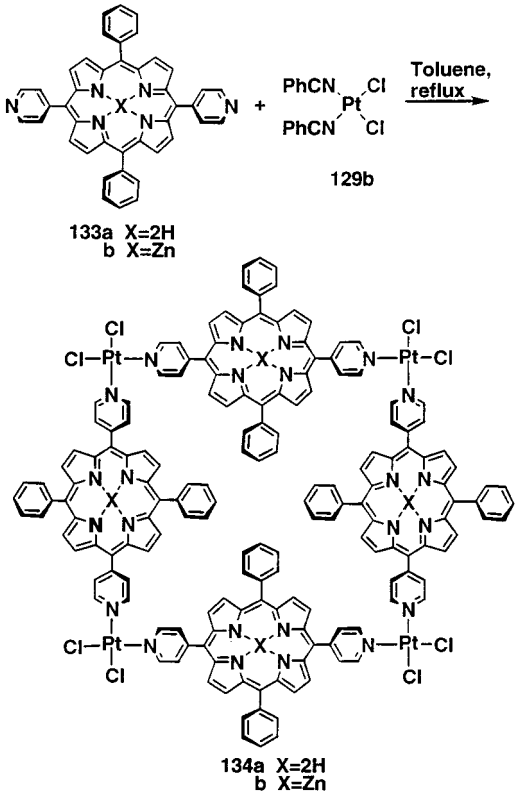

In contrast to the neutral porphyrin squares reported by Lehn, cationic cyclic porphyrin tetramers **135** were obtained by reacting the bistriflate salt **78a** with 5,15-di(4′-pyridyl)-10,20-diphenyl-porphyrin (*trans*-DPyDPP), **133a**, and its zinc-containing analogue **133b** (Scheme 51).[161] The spectroscopic data for complexes **135** were in accord with the results of molecular modeling of the structure of tetramers

Scheme 51

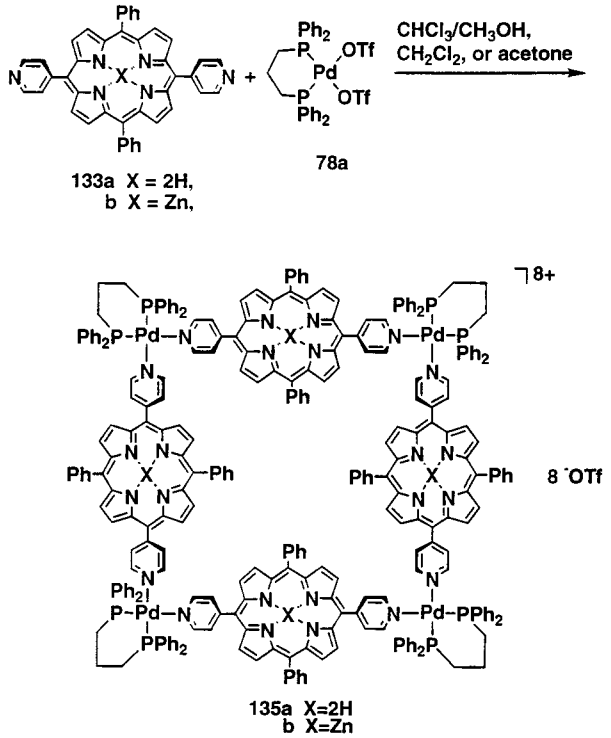

135a and with studies of restricted rotation in pyridine−transition-metal complexes.[162] The $^{31}P\{^{1}H\}$ NMR spectra of each of the tetramers **135a** and **135b** consist of one singlet at ambient conditions. Compared to the $^{31}P\{^{1}H\}$ NMR signals of the bistriflate **78a**, the tetramer signals are shifted upfield by ∼10 ppm, indicative of the coordination of the nitrogen lone pair to the transition metal.[57,72,87,115]

The bistriflate **78a** was also reacted with 5,10-di(4′-pyridyl)-15,20-diphenylporphyrin (*cis*-DPyDPP), **128a**, and *cis*-ZnDPyDPP, **128b**, to yield the smaller macrocycles **136** (Scheme 52). Fast atom bombardment

Scheme 52

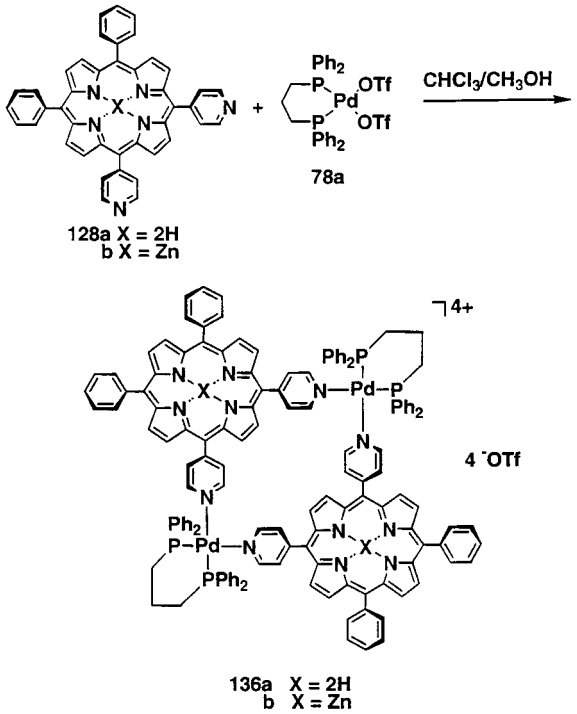

mass spectrometry analysis of **136a** gave M − OTf peaks of m/z = 2716.5 with +1 charge states (i.e., separation of peaks by 1 m/z unit) resulting from a loss of one triflate from a total of four.

Larger macrocycles **137a** and **137b** resulted from the reaction between the angular porphyrin precursors **128a** and **128b** and 1,4-bis-[*trans*-$Pt(PEt_3)_2$-(OTf)]benzene, **124a** (Scheme 53).[161]

Interestingly, all porphyrin-based macrocycles were more soluble than the precursor porphyrins alone. Presumably, the positive charge of the macrocycles and the arrangement of the phosphine ligands is such that they project out of the plane defined by the corners of the macrocycles and prevent intermolecular stacking. This made the crystal packing less thermodynamically favorable and, thus, increased the solubility of the macrocycles. In this respect, the bisphosphine-coordinated Pd(II) and Pt(II) angular modules have solubility advantages over the analogous neutral transition-metal chlorides.[150a] The higher solubility of the charged porphyrin oligomers allowed self-assembly on a preparative scale at higher concentrations without precipitation of the intermediates.

Scheme 53

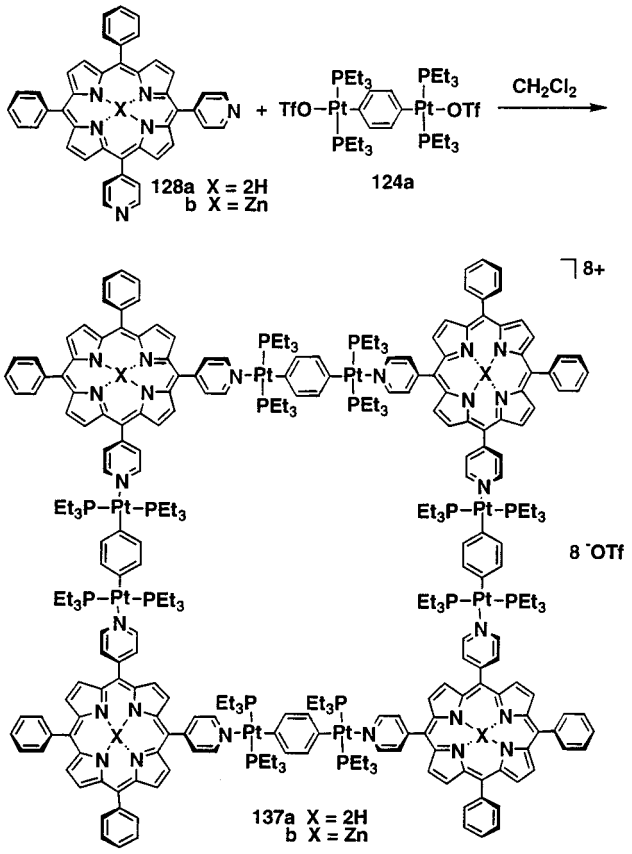

D. Molecular Pentagons and Larger Ring Systems

The self-assembly of iron-containing cyclic helical pentagons was reported by Lehn and co-workers.[163] They employed the trisbipyridyl ligand **138** in combination with two different iron(II) salts forming the circular double helicates that resemble the geometries of a pentagon or hexagon (Scheme 54). When the mixture of an equimolar amount of **138** with $FeCl_2$ was heated to 170 °C in ethylene glycol, a bright red solution of assembly **139** was obtained and isolated in almost quantitative yield. Spectroscopic data confirmed that the product has a cyclic, highly symmetrical pentameric structure. An interesting feature of this cyclic supramolecular assembly is that it contains a tightly bound chloride ion within its central cavity.

The preparation of the cyclic hexameric assembly **140** was carried out in a strikingly similar manner.[164] The only noticeable difference was that the iron salt used was a sulfate rather than a chloride (Scheme 55). Heating a mixture of **138** with $FeSO_4$ in ethylene glycol followed by precipitation with NH_4PF_6 produced the hexanuclear assembly **140** in high isolated yield. Its structure was assigned by NMR spectroscopy, including NOE experiments. Evidence of its hexameric structure was obtained from electrospray mass spectrometry. Since iron−bipyridine complexes typically remain intact at low ionization potentials during the electrospray process, the polynuclear architecture is usually observed as a cation with different number of charges. The mass spectrum of **140** after precipitation with NH_4PF_6 displayed the

Scheme 54

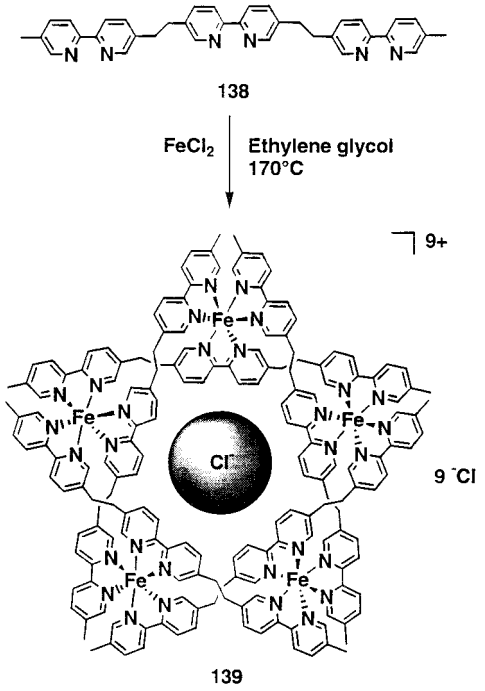

Scheme 55

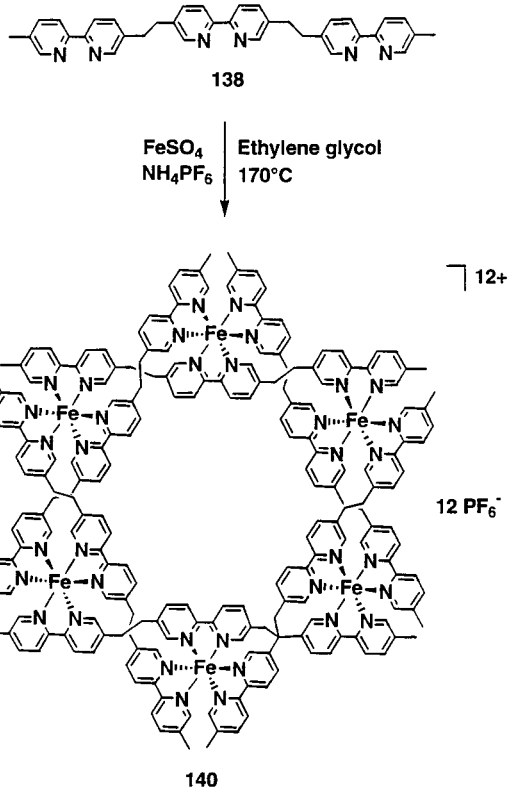

signals of multiple-charged entities ranging from +4 to +9 charge state, all generated from the cyclic hexamer.[164]

These two reactions demonstrate the remarkable influence of the ion templating effect on the formation of polynuclear assemblies. The templating effect of the smaller chloride drives the reaction toward the formation of a smaller metallacycle, whereas the larger sulfate counterion induces the formation of a larger hexagonal assembly.

In an attempt to synthesize novel adamantanoid-like tetranuclear chelate complexes, Saalfrank and co-workers reacted triethanolamine, **141**, with sodium hydride, iron(III) chloride, and fumaric acid dinitrile in tetrahydrofuran.[25] Instead of the expected iron-to-ligand ratio expected for a 3-D assembly (4:6), they found a 1:1 ratio without any fumaric acid dinitrile. X-ray structure analysis revealed the formation of a cyclic iron complex **142** with a [12]metallacrown-6 structure in which a sodium ion is encapsulated in the center (Scheme 56). The six

Scheme 56

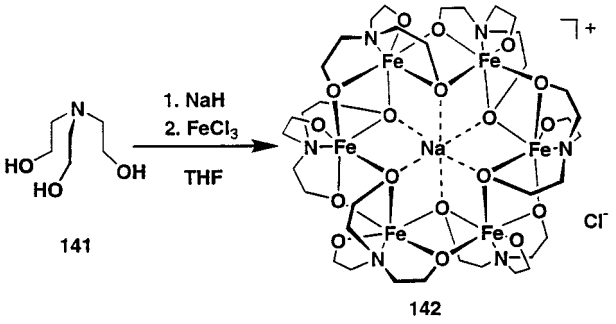

iron atoms of the complex are located at the corner of a regular hexagon with a diameter of 6.43 Å, being bridged by the tetradentate triethanolamine ligand. The encapsulated sodium ion is coordinated by six μ^3-oxygen atoms, three above and three below the hexagonal plane.[25] This perfect fit of the cation suggested a template-mediated formation of this six-membered ring, which was shown to be true by using cesium carbonate instead of sodium hydride. The template effect of the lager cesium ion resulted in the isolation and characterization of a larger, eight-membered ring. Similar to the previous complex, a cesium ion is encapsulated in this regular octagon of a [16]metallacrown-8 structure, embedded in a quadratic antiprism coordination of eight oxygen atoms.

The ability to readily interchange angular building blocks is a major strength of the self-assembly based "molecular library" design strategy. If the nitrogen-containing corner unit has 120° bond angles, then in combination with a complementary linear organometallic linking unit, such as **124c**, it may produce a molecular hexagon. As the covalent angle of an sp^2 hybrid carbon is 120°, the bis(4-pyridyl) ketone **35** was used as the corner unit, which upon interaction with spacer **124c** in dichloromethane at room temperature afforded the desired hexamer **143a** (Scheme 57).[165]

The bimetallic complex **144** that is complementary to **35** was prepared via oxidative addition from 4,4′-diiodobenzophenone followed by conversion to the triflate with silver triflate. Upon mixing of **144** with 4,4′dipyridyl, **24**, in dichloromethane, the desired hexagon **143b** formed (Scheme 57). The two assemblies **143a** and **143b** are isostructural and have identical molecular weights (MW = 12 443.1).[165] Unfortunately, neither conclusive mass spectrometry data nor crystallographic data on these systems were obtained to support the formation of molecular hexagons. As pointed out by Raymond,[22] the discrepancy between the 120° angle needed for the hexagons

Scheme 57

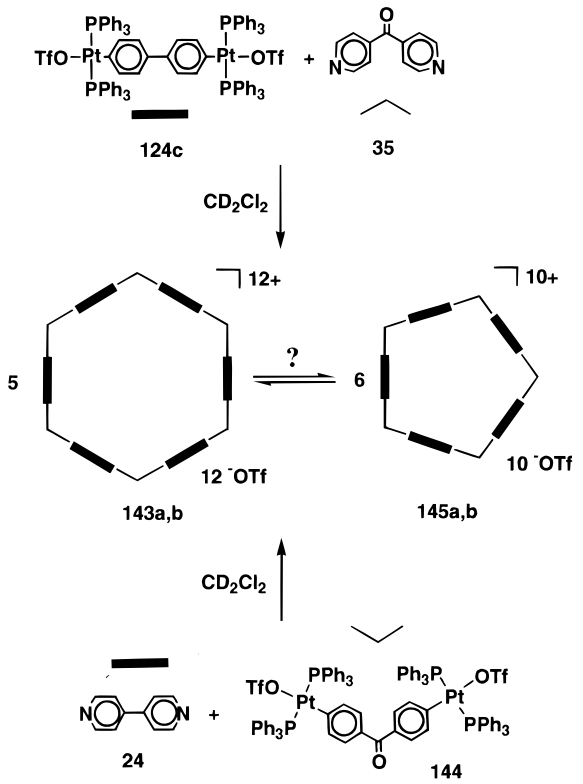

143 and the 108° angle needed for the analogous pentagons **145** can easily be accounted for once one considers the size of the macrocyclic assembly. Since the building blocks are relatively large and therefore quite flexible, small distortions of the ideal bond angles of the subunits can occur and make up for the necessary 12° difference per corner between hexagon and pentagon. Meanwhile, ES-MS data were obtained for similar macrocyclic systems, showing that in solution under highly diluted conditions (2×10^{-5} M) hexameric, pentameric, and perhaps even tetrameric systems are formed. At the same time, NMR data only point to the existence of a single symmetric structure under more concentrated conditions (5×10^{-3} M), suggesting a shift of the possible equilibrium toward a hexagon at higher concentrations.[166]

An interesting aspect of metal-mediated self-assembly reactions is the generation of macrocycles with fascinating structural and spectroscopic properties such as fluorescence and luminescence. Unfortunately, only a handful of luminescent molecular hosts have been described so far.[76,79,167] Using square-planar platinum complexes as building blocks, Che and co-workers were able to isolate and characterize a luminescent hexanuclear platinum macrocycle **146** containing chelating dicarbene and bridging cyanide ligands (Scheme 58).[168] The X-ray structure analysis showed that the hexanuclear complex has a chairlike conformation rather than a planar hexagon type of structure. Alternatively, complex **146** can also be described as an open cube-type structure which is missing a pair of opposite corners. The CN−Pt−CN angles are almost orthogonal (92.4°), while the nitrile and isonitrile groups are almost linear (174°). A strong absorption band at 356 nm indicated a spin-

Scheme 58

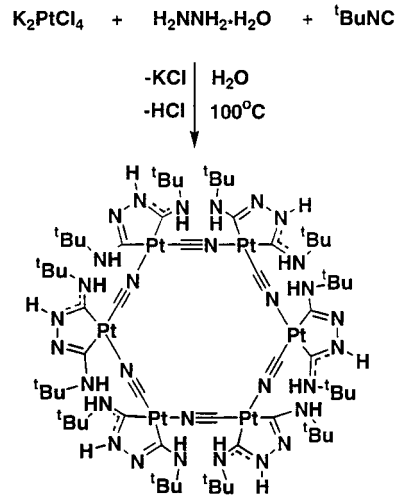

146

allowed charge-transfer (CT) transition that was assigned to a Pt−π*(carbene) transition. Additional observation of a structureless emission band centered at 514 nm with a lifetime of 0.22 μs provided further evidence for this transition.[168]

The complete stereospecific self-assembly of a circular helicate with labile metal centers was reported by von Zelewsky and co-workers.[169] Using nonchiral ligands in the self-assembly of helicates results in the formation of a racemic mixture of chiral helicates.[170] Therefore, the enantioselective synthesis of chiral helicates posed an interesting challenge, which was solved by the use of chiral helicating ligands.[171] Pyridine and bipyridine ligands were used to synthesize configurationally stable coordination complexes in which the stereochemistry at the metal center is predetermined by the configuration of the ligands.[172] Reaction of the α,α′-bis(pinene-2,2′-bipyridyl)-*p*-xylene linker **147** with $AgPF_6$ in a mixture of acetonitrile and chloroform spontaneously formed the 6-fold, circular single-stranded helicate $[Ag_6(\mathbf{147})_6](PF_6)_6$ (**148**) (Scheme 59) as indicated by X-ray structure analysis. NMR and CD spectroscopy in solution along with electrospray mass spectrometry results indicate that the assembled system persists in the dissolved state. In the solid state, compound **148** reveals its circular helical nature, in which one bisbidentate ligand forms a bridge between two adjacent silver centers. As a result, the silver ions are tetrahedrally coordinated by four almost equidistant (2.31 Å) nitrogen atoms from two independent bipyridine ligands. The outside diameter of the hexagon is about 3 nm, whereas the cavity size itself is only 0.84 nm in diameter. The hexagonal disk is about 1.4 nm thick.[169]

A pH-dependent monomer−hexamer interconversion of a copper(II) complex of *N*-(2-phenylimidazol-4-ylmethylidine)-2-aminoethylpyridine, **149**, was reported by Matsumoto and co-workers.[173] The closest documented reactions which describe interconversions of metal complexes between monomers and self-assembled oligomers are alcoholation and oxolation reactions generating iso- and heteropolyanions.[174] However, these systems do not allow for control of

Scheme 59

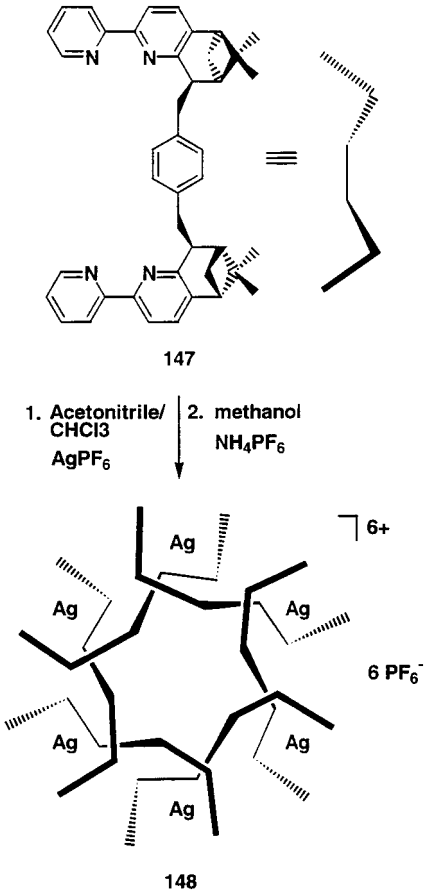

148

the nuclearity or structure of the final oligomeric structure. The mononuclear copper complex **149** used by Matsumoto and co-workers has the characteristics of a self-contained building block, allowing for simple self-assembly. Deprotonation of complex **149** with an equimolar amount of triethylamine resulted in the condensation of complex **150** via dative bond formation between the imidazolate nitrogen atom and the copper ion (Scheme 60). X-ray structure analysis of compound **150** revealed a crown-like arrangement of the linker units forming a cyclic hexanuclear entity. Interestingly, deprotonation of the analogous methyl-substituted copper complex afforded a cyclic tetranuclear complex. Although there were no relevant differences in the Cu−N coordination bond distances and imidazolate bridged Cu−Cu distances, the steric repulsion between the 2-imidazolate substituents prevented the formation of a tetranuclear system in the case of **149**. In the cyclic hexanuclear structure of **150**, the distance between similarly oriented units is increased, reducing steric repulsion of the phenyl substituents.[173]

The unique formation of two interpenetrating hexagons was reported by Mingos and co-workers.[175] Treatment of the gold salt $[Au(NH_3)_2]BF_4$, **151**, with phenylacetylene, **152a**, has been known to yield a monomeric gold complex **153** in excellent yields. When the same reaction was carried out with *tert*-butylacetylene, **152b**, instead of phenylacetylene, an oligomeric compound $[\{Au(C{\equiv}C^tBu)\}_6]_2$, **154**, was isolated (Scheme 61). The X-ray structure analysis of the gold complex **154** revealed a novel catenane

Scheme 60

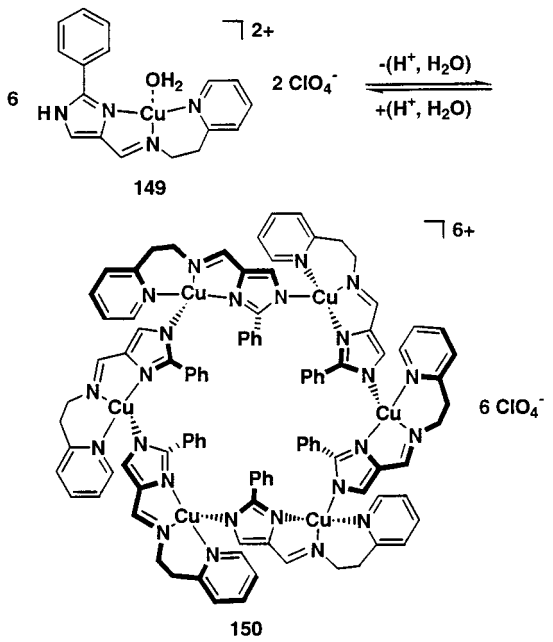

Scheme 61

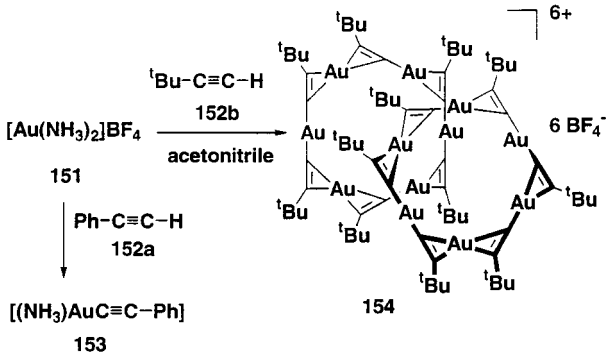

structure based on two interlocked six-membered rings, each containing six gold atoms and six acetylene units. Surprisingly, the ethynyl ligands adopted both η^1 and η^2 coordination modes, resulting in pairs of gold(I) atoms with different ligand arrangements and formal charges for each ring. Besides $\eta^1-\eta^1$ and $\eta^1-\eta^2$ coordinations, a previously unobserved $\eta^2-\eta^2$ coordination mode in gold(I) chemistry resulted in a perpendicular orientation of the ethynyl ligands. The gold(I) atoms within one ring formed an approximately regular planar hexagon with gold−gold distances (between 3.30 and 3.36 Å) significantly longer than those in the bulk metal (2.88 Å) but still in the range where weak "aurophilic" interactions can occur.[175] The mechanism for this rearrangement of the coordination environments of the basic [Au(C≡C^{t}Bu)] fragments in solution to self-assemble into the observed [2]catenane structure is still unexplained.

An unusual ferrocene-based heptagon was reported by Köhler and co-workers.[176] Reaction of the doubly bridged ferrocene precursor with $FeCl_2$ produced, albeit in low yield, cyclic heptamer **155** (Figure 12) as confirmed by X-ray crystallography. Although it is not easy to explain why this particular structure is formed, it is useful to consider the topology of its constituents. The main degree of freedom is the rotation of two cyclopentadienyl rings, so the substituents are pointing away from each other. This effect is largely responsible for preserving the coplanar arrangements of the ferrocenyl rings. The reduction in the number of degrees of freedom in such a metallocene still does not fully explain the formation of the heptagon but it does emphasize this atypical ring closure reaction.

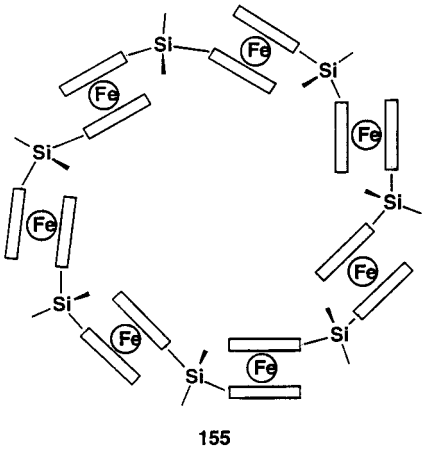

Figure 12.

For some self-assembly reactions, there is only one optimal structure for the supramolecular system defined by a specific metal-to-ligand ratio. For other systems, a wide variety of stoichiometries are possible and therefore various structures can be observed by use of the same linkers.[163,164] Reacting the potassium salt of the bisbidentate ligand bis[3-(2-pyridyl)pyrazol-1-yl]dihydroborate (L^-), **156**, with cobalt(II) acetate, **157**, McCleverty and co-workers were able to isolate a cyclic supramolecular complex **158** containing 8 cobalt ions and 12 bridging ligands (Scheme 62).[177] The electrospray mass spectra of the corresponding PF_6^- salts revealed strong peaks at m/z = 1410 in each case, corresponding to triply charged cations $[Co_8L_{12}(PF_6)]^{3+}$ and $[Ni_8L_{12}(PF_6)]^{3+}$, which were confirmed by 1/3-integral spacing between

Scheme 62

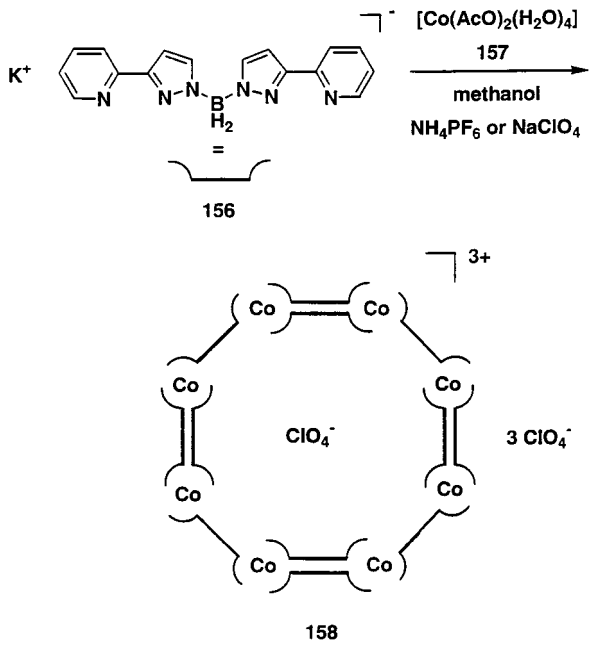

isotopic components. The nonexistence of an anion-free peak, corresponding to $[M_8L_{12}]^{4+}$, suggested the formation of an eight-membered ring, containing one tightly bounded anion in the central cavity. The X-ray structure analysis of the perchlorate salt of the cobalt compound **158** confirmed the results derived from the ESMS spectra, namely, a perchlorate ion in the central cavity of the octagon.[177] Furthermore, each ligand L acted as a bridge between two adjacent metal ions, with an alternating pattern of one and then two bridging ligands, resulting in a helical system in which all eight metal centers had the same chirality. One question still stands: does the central anion act as a template to control the size of the ring, or is the ring a particularly stable structure which forms on its own and eventually traps a guest?

IV. Three-Dimensional Nanoscopic Cages and Polyhedra

If molecular building blocks of various nanostructured materials are to be connected in a three-dimensional fashion, one needs to find rigid three-dimensional molecules which can serve as skeletons, thus providing the core of such nanostructures. Apart from the fact that the overwhelming bulk of molecules are of a flexible chainlike nature, the few rigid and compact cages (cubane,[178] adamantane,[179] dodecahedrane,[180] the norbornanes, and the fullerenes[181]) are very difficult to functionalize in a useful and systematic way as they are extremely inert once synthesized. Even norbornanes, which are usually assembled in one step by Diels−Alder cycloaddition reactions, are not totally free from these limitations. The synthesis of conformationally rigid large cages with multiple functional binding sites by using only the tools of classical synthetic organic chemistry becomes more difficult with the increasing number of carbon atoms in the cage. As any individual molecular building subunit has to be incorporated into the skeleton in a confined, rigid fashion, it usually will have to be attached by at least three bonds. If this building block then provides one additional functional group that will actually appear on its periphery, then in the overall analysis, three functional groups have been consumed for the one that has been delivered. If one looks at the totally assembled structure, one finds that essentially nothing has been gained in terms of providing more potential functionalization sites, which would have been desirable for design and which was the reason one wanted larger cages in the first place. The functional groups needed for holding together the subunits into the skeleton are lost because usually the atoms in such a bond cannot engage in any further function other than the bond-formation itself. Similarly, no additional functionality can be gained by using the sp-hybrid carbons of acetylene, except larger overall dimensions. Hence, the formation of organic, carbon-based nanostructures suffers from the one fundamental limitation of the carbon atom, namely, that its maximum number of valences cannot exceed four. Transition-metal-based nanosystems, on the other hand, are free from such limitations because it is relatively easy to find, for each specific task, a suitable transition metal with a coordination number higher than four. Moreover, due to multiple binding sites, the resulting cages can be of significantly larger size and can still retain their conformational rigidity. Furthermore, due to their symmetrical three-dimensional nature, self-assembled entities usually enclose a rigid and symmetrical cavity, providing an ideal environment for the trapping of larger guest molecules.

So far we have discussed the application of the self-assembly strategy in the formation of molecules resembling various two-dimensional geometric shapes such as squares or hexagons. However, there is also a nearly infinite number of possibilities for formation of structures whose overall symmetry will not resemble figures within two-dimensional space. Closed three-dimensional structures or molecular cages of various shapes have been prepared through self-assembly from simpler components through hydrogen bonding[182] and metal−ion interaction.[2−21] It is particularly noteworthy that the subunits of most self-assembled biomolecules, such as the viral and bacterial capsides, indeed exhibit a three-dimensional spatial orientation.[1−10,183,184]

A. Self-Assembled Prisms and Cylinders

The simplest and therefore smallest three-dimensional assemblies with the fewest number of components are triangular prisms. Their design requires only five building blocks, two angular tritopic subunits, and three linear connecting units. Covalently bonded systems with a triangular prismatic shape like [2.2.2]cryptands[185] and [2.2.2]cyclophanes[186] have been known for a long time. Though both systems enclose a three-dimensional cavity, only atomic cations could be trapped inside due to the small size of their cavity.[185,187] Self-assembled entities on the other hand enclose a much larger space due to the larger building blocks and therefore should be capable of hosting multiatom ions or smaller organic guests molecules. In addition, the use of the self-assembly principle allows for the guest-specific construction of an adequate host, which assembles in a certain way upon recognition of the guest.

Current understanding of the molecular recognition in many biological systems is based on the "induced fit" mechanism, in which substrates induce the organization of the recognition site of a receptor, rather than on the lock and key model.[188,189] Most examples of induced-fit models use flexible artificial hosts which show restricted conformation only if they recognize a specific guest.[190,191] One of the few examples of induced-fit models in which the guest actually induces the organization of the host itself is given by Fujita and co-workers.[188] When 2 equivs of the tritopic ligand 1,3,5-tris(4-pyridylmethyl)-benzene, **159**, was treated with 3 equivs of ethylenediaminepalladium dinitrate, **13**, in the presence of sodium 4-methoxyphenylacetate, **160**, the three-dimensional, cage-like complex **161** with trigonal prismatic shape was solely formed (Scheme 63). Characterization of this complex relied mainly on NMR and electrospray ionization mass spectrometry. From a series of prominent peaks of $[(M + H) - NO_3$

Scheme 63

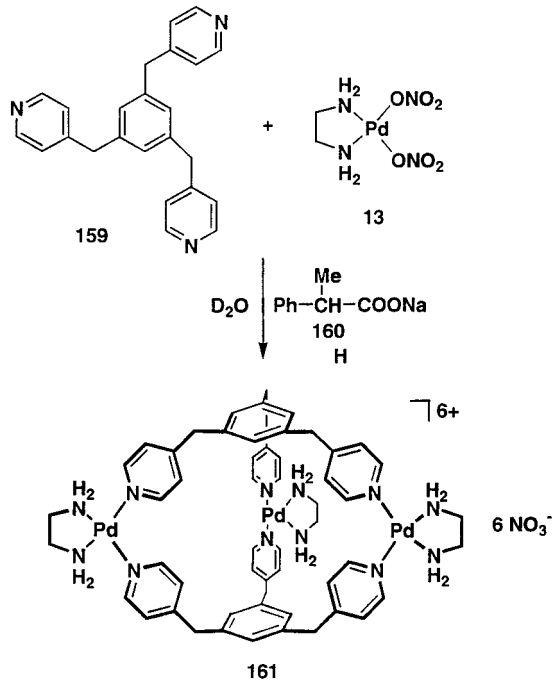

$-(HNO_3)_n]^{2+}$ it was deduced that the cage-like host binds 4-methoxyphenylacetate as a guest in a 1:1 stoichiometry in aqueous solution.[188] Analysis of the proton NMR data not only confirmed the presence of the guest counterion within the cavity but also confirmed the D_{3h}-symmetry necessary for a trigonal prism. In the absence of the specific guest, the self-assembly resulted in the formation of a considerable amount of oligomeric product, which disappeared upon addition of the guest under formation of the cage-like complex. Variations of the guest showed that bulky hydrophobic moieties such as 1-phenylethyl or adamantyl groups favor the formation of the product, whereas less hydrophobic substrates such as dicarboxylates or acetates showed hardly any effect.

In analogy to the formation of the above-mentioned trigonal prism, the construction of a rigid tetragonal prism from two preformed cavitands and four square-planar transition-metal bistriflates was reported by Dalcanale.[192] When the specifically designed tetracyano cavitand **162** reacted with Pd(II) and Pt(II) bistriflates **78a** and **78b** at room temperature, they produced the rigid dimeric assemblies **163a** and **163b** (Scheme 64). In addition to the D_{4h}-symmetrical nature of this compound, spectroscopic studies revealed that one triflate counterion was trapped within the rigid three-dimensional cavity. Unfortunately, no solid-state data were reported to support the observed inclusion of the counterion.

The self-assembly of multicomponent superstructures requires a design and a choice of components that must fulfill the three most important criteria: recognition, orientation, and termination. Therefore, a design of systems capable of spontaneously generating well-defined complexes from a larger set of components, comprising at least two different types of ligands and/or metals, is needed. One example of such a multiligand, multimetal self-assembly involv-

Scheme 64

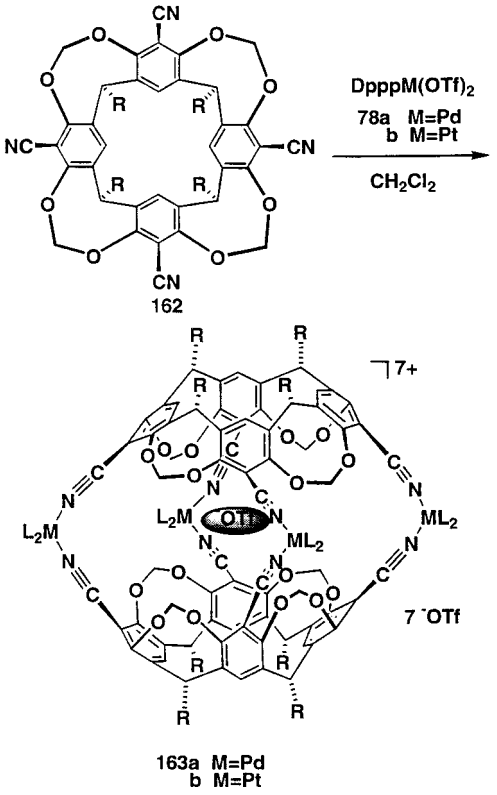

Scheme 65

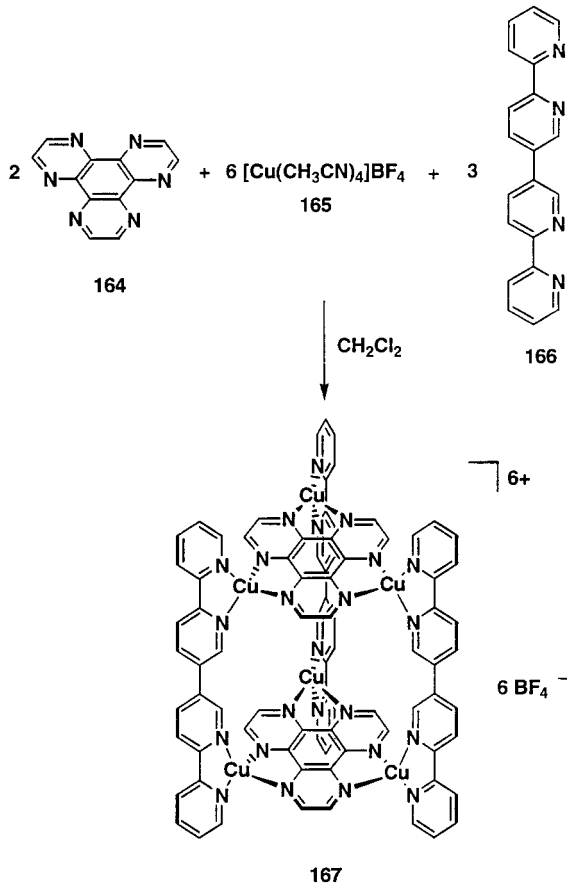

ing two types of ligands and several Cu^+ ions was demonstrated by Lehn and co-workers.[193] Slow addition of a solution of $[Cu(CH_3CN)_4]BF_4$, **165**, to a 2:3 mixture of hexaphenylhexaazatriphenylene, **164**, and

Scheme 66

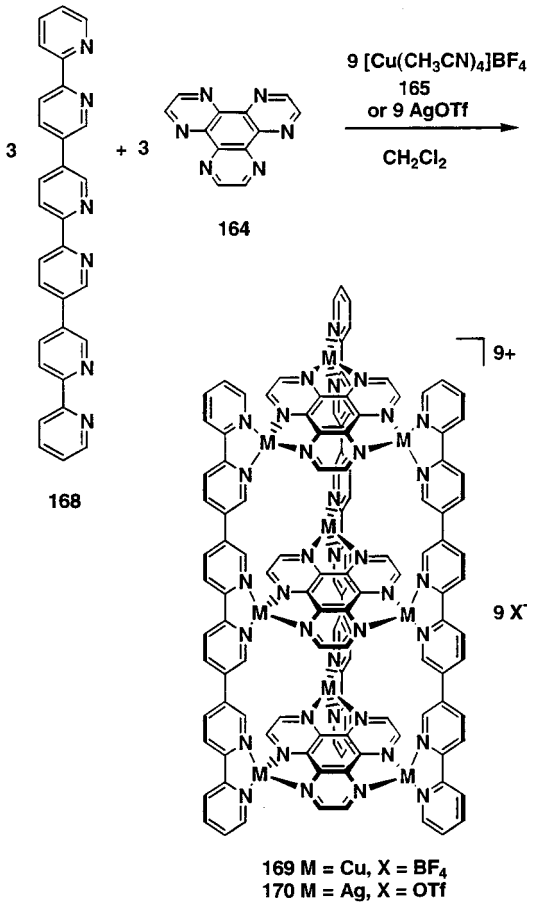

the tetrapyridine, **166**, furnished assembly **167** as a dark-purple, air-stable solid after 20 h (Scheme 65). The ^{1}H NMR spectrum, the FAB mass spectrum, and the elemental analysis were consistent with the formulation of this compound as a cylindrical cage-like structure with D_{3h} symmetry. X-ray analysis revealed a self-assembled cylindrical complex **167** formed by two flat circular hexaphenylhexaazatriphenylene ligands that form the top and bottom and three bridging tetrapyridine groups as well as six Cu^+ ions, which connect the organic components. Taking the van der Waals radii into account, the cylindrical interior, which does not show any guest inside, has a height of approximately 4 Å and a radius of 4 Å.[193] The overall twist of the structure results in a slightly triple-helical shape. Insertion of different spacer units such as acetylene, benzene, and 1,4-bis(ethynyl)benzene into the tetrapyridine ligands resulted in the formation of larger nanoscale cylinders showing increased heights of up to 33 Å.[27]

Extending this design of cylindrical macromolecules, Lehn and co-workers[28] were able to self-assemble multicomponent and multicompartmental cylindrical nanoarchitectures. Mixing the linear hexapyridine linker **168** with hexaphenylhexaazatriphenylene, **164**, and $[Cu(CH_3CN)_4]PF_6$, **165**, in a 1:1:3 stoichiometric ratio yielded complex **169** after 5 days (Scheme 66). Analogous reaction with silver triflate afforded a similar cylindrical complex **170**. Inspection of the ^{1}H NMR spectra (COSY and NOESY) suggested that the product possessed a multicellular cage-type structure. Confirmation of the proposed structure was obtained from the X-ray structure analysis of **169**. Two of the three platelike ligands **164** formed the top and bottom lid of a cylindrical cage, while the third unit was centered between the other two, dividing the cage into two compartments. Due to tilting of the outer lids promoted by distortion of the tetrahedral coordination polyhedron about the Cu centers, the cylindrical cage compound as a whole forms a helicate. Each of the slightly different compartments of **169** enclosed a cavity with a radius of approximately 5.4 Å and were each filled with two PF_6 guest ions.[28]

B. Platonic Solids

The number of ways in which more than three identical building blocks can be regularly arranged on the surface of a sphere is represented by the Platonic and Archimedean solids. Platonic solids embody a family of five convex uniform polyhedra that are made of the same regular polygons (equilateral triangle, square, and pentagon). As a result of the way in which identical regular polygons have to be adjoined in order to construct convex corners, there is a finite number of Platonic solids. Thus, triangles can be adjoined to give tetrahedra, octahedra, or icosahedra, whereas squares and pentagons can only be adjoined to give cubes and dodecahedra.[194] Since all five polyhedra are isometric and the corners along with the three coordinate directions are equivalent, they are ideal candidates for the construction of spherical molecular hosts via self-assembly. The regular polygons on the surface of these polyhedra serve as a blueprint for the construction of suitable building blocks giving the appropriate angles and bonding arrangements.

1. Tetrahedra

The shape of the simplest Platonic solid, the tetrahedron, can be obtained via the simultaneous combination of four angular tritopic building blocks with six linear ditopic building blocks according to the "molecular library" model (see Figure 4). According to the "symmetry interaction" model, formation of a tetrahedral M_4L_6 system can be achieved via self-assembly of six bischelating ligands that have an angle between the chelate vectors of 70.6°, with four octahedral metal ions (see Figure 2).

While covalently bonded systems of tetrahedral symmetry-like spherands[195,196] or spheriphanes[187] have been well-known for quite some time, Saalfrank and co-workers[197,198] were the first to introduce metal-based tetrahedral assemblies taking advantage of the "symmetry interaction" model. Reaction of 2,3-dihydroxy-1,3-butadiene-1,1,4,4-tetracarboxylate, formally obtained by template coupling of two malonate diesters **171** with oxalyl dichloride **172** and methyllithium, with magnesium, manganese, cobalt, or nickel dichloride in water gave the corresponding tetranuclear complexes **173a**−**d** in good yields (Scheme 67). Due to paramagnetism, the ^{1}H and ^{13}C NMR spectra of **173b**−**d** did not reveal much information about the structure of these complexes. However,

Scheme 67

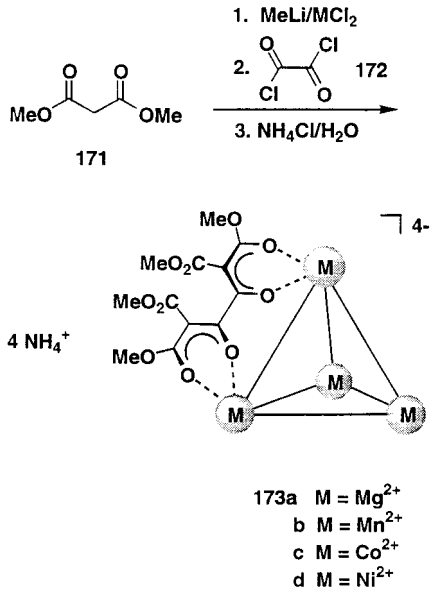

X-ray structure analyses revealed the 4-fold charged structure of the tetramanganate complex **173b** and the tetracobaltate complex **173c**. Both compounds were present as tetraammonium salts in the crystal. The core of **173c** showed a distorted tetrahedron composed of four cobalt(II) ions with a crystallographic C_2 symmetry. The cobalt ions were linked along each of the six edges of the tetrahedron by a doubly bidentate tetramethyl 2,3-dioxobutane-1,1,4,4-tetracarboxylato bridge, forming an octahedral coordination of six oxygen atoms around each metal center. Due to atropisomerism of the bridging ligand, complex **173c** showed chirality with all six chelate bridges twisted in the same sense resulting in an overall *T* symmetry. As a result of a bend in each of the six ligands, these M_4L_6 cage compounds have also been described as adamantanoids or adamantane-like structures.[197,198]

Utilizing the rich coordination chemistry of iron(II) salts, Saalfrank and co-workers were able to synthesize and characterize iron complexes similar to **173**.[199,200] For the first time a tetranuclear, mixed-valence iron complex was described which formed via self-assembly from reaction of dialkyl malonate, **171**, with methyllithium and $FeCl_2$ in tetrahydrofuran at low temperature (Scheme 68). Assembly **174** was capable of encapsulating ammonium ions, as confirmed by mass spectrometry and X-ray crystallographic studies. The mixed-valence character of this assembly was also established by studying their Mössbauer spectra and further proven by measurements of cyclic voltammograms.

To form larger tetrahedra, Saalfrank and co-workers doubly deprotonated the stable tetramethyl 2,2′-terephthaloyldimalonate, **175**, with sodium hydride to yield a bisbidentate chelate ligand, which reacted with iron(III) chloride to form compound **176**.[200] In analogy to **173** and **174**, complex **176** also showed a tetrahedral tetrairon core bridged by six chelate ligands. As a result of the phenyl spacer introduced into the bisbidentate chelate ligand, the tetrahedral iron complex **176** showed a substantially larger cavity compared to **173** and **174** (Scheme 68).

Scheme 68

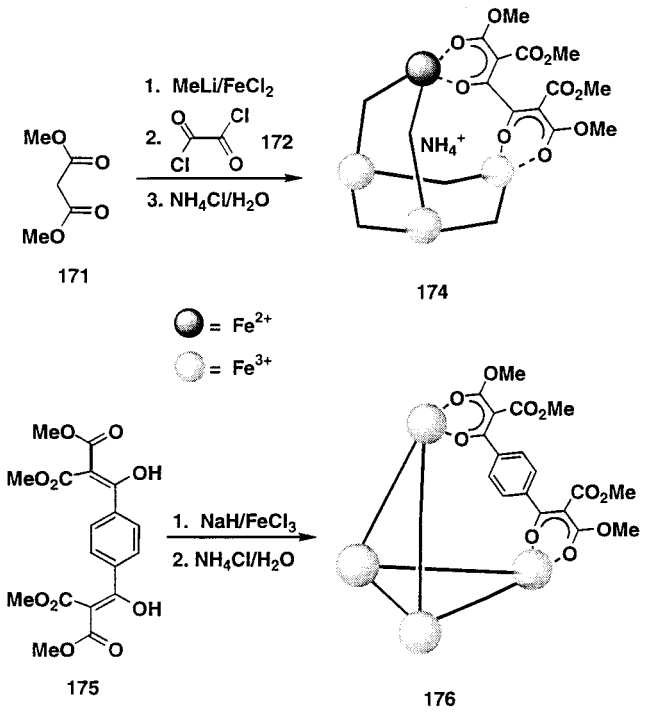

Following Saalfrank's design approach, Raymond and co-workers succeeded in isolating similar tetrahedral cage compounds. Furthermore, they were able to elaborate several design principles in order to predict and construct the formation of self-assembled systems, as discussed in section II.

As an example of a perfect theory−experiment match, isophthal-di-*N*-(4-methylphenyl)hydroxamic acid, **177**, was chosen as a ligand in combination with trivalent Fe and Ga complexes.[201] To synthesize a M_4L_6 tetrahedral cluster, the coordinate vectors within a given ligand must be oriented approximately 70° from each other according to the model. Since hydroxamate ligands form very stable but kinetically labile complexes with trivalent metals and ligand **177** has an angle between the coordinate vectors close to that predicted by theory, this allowed for the formation of the thermodynamically favored assembly over a wide range of other possible polymeric structures. Reaction of **177** with either $Fe(acac)_3$, **9**, or $Ga(acac)_3$, **10**, in acetone afforded the desired assemblies **178a,b** in high yields (Scheme 69). FAB mass spectra and NMR spectroscopic data were consistent with the formation of highly symmetrical tetrahedral assemblies. When the reaction was carried out with an excess of ligand and the gallium precursor, the formation of only a closed assembly was detected whereas the excess ligand remained intact in solution.[201] The solid-state structure of **178a** was studied by X-ray crystallography. The unit cell contained two crystallographically independent assemblies, each of them with the metals separated by an average of 9.0 Å. Both self-assembled molecules contained four DMF molecules that partially filled the rigid cavities.[201]

The versatility of this elegant synthetic design strategy was recently shown to be useful in the study

Scheme 69

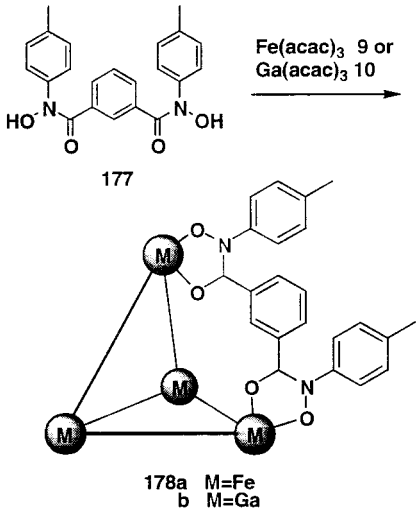

of dynamic guest exchange reactions.[202,203] To be able to synthesize a M_4L_6 cluster with tetrahedral symmetry requires a unique fixing of the bi and the tridentate ligands. Interaction of a C_2-symmetrical bisbidentate ligand with an octahedral metal complex could lead to the formation of a M_2L_3 helicate, if the angle between the 2-fold and the 3-fold axes is about 90°. To avoid the formation of the entropically favored helicate, the ligand used in a M_4L_6 system has to be rigid and of suitable geometry. Implementation of a naphthalene spacer between two pyrocatechol units suppresses the formation of a possible helicate due to unfavorable ligand conformation. Deprotonation of **179** with KOH in methanol followed by addition of Et_4NCl and $Fe(acac)_3$, **9**, led to precipitation of the product **180** (Scheme 70). X-ray structure analysis of this compound showed a racemic mixture of homochiral $[Fe_4L_6]^{12-}$ clusters with almost molecular

Scheme 70

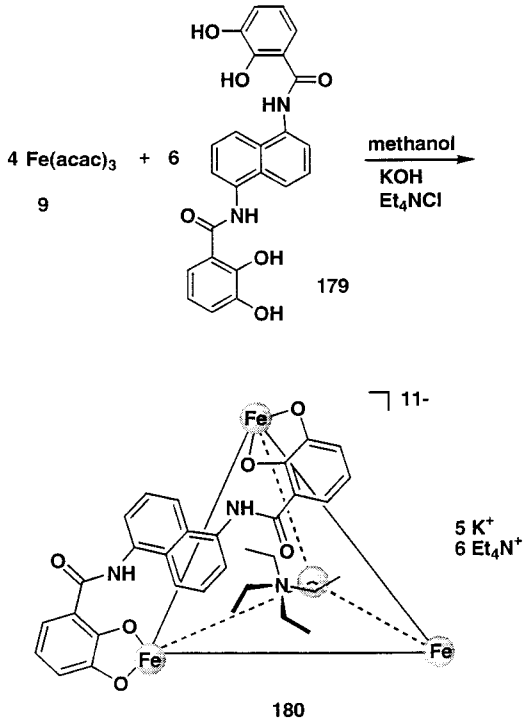

T-symmetry.[202] The iron complex showed average Fe−Fe distances of 12.8 Å. Embedded within the cavity of **180** was a Et_4N^+ ion. Interestingly, the methylene signals for the encapsulated Et_4N^+ ion showed a complex multiplet, which resulted from the nonequivalence of those two protons as a result of the chiral environment. Guest exchange reactions of the isostructural gallium complex gave equilibrium constants for Me_4N^+ and Pr_4N^+ 200 times smaller than that for Et_4N^+. Van't Hoff plots for the encapsulation of the guests revealed positive enthalpies and entropies, clearly showing an entropy-driven process.[203]

An anion-templated assembly of a supramolecular cage compound has recently been reported by McCleverty.[204] Using the flexible multidentate ligand **181**, which contains two bidentate pyrazolylpyridine binding sites separated by an *o*-xylyl spacer, the reaction with cobalt(II) bisacetate hydrate, **182**, in methanol and subsequent addition of $NaBF_4$ (Scheme 71) results in the formation of complex **183**.[204] The

Scheme 71

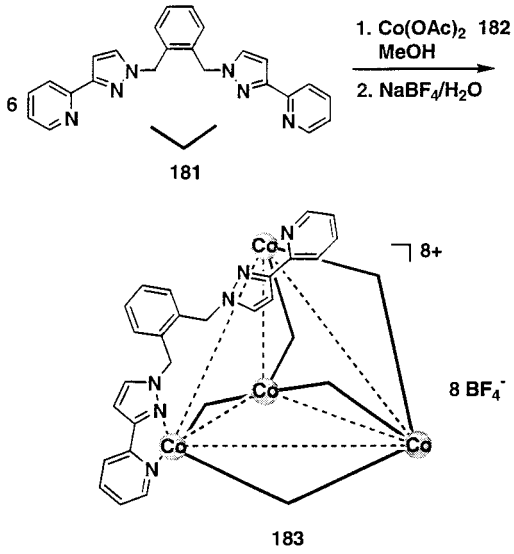

FAB-mass spectrum showed peaks for the Co_4L_6 species, associated with different numbers of BF_4^- anions. Crystal structure analysis revealed the tetrahedral nature of this complex in which each cobalt cation occupies the vertex of a tetrahedron and the ligands span over the edges of the tetrahedron. In addition, the X-ray structure uncovered multiple π-stacking interactions in the solid state between the aromatic rings of adjacent organic linkers. Analogous to the earlier mentioned compounds **173**, **174**, and **178**, complex **183** showed a similar adamantane-like topology due to the bent structure of the organic linker. One out of the eight BF_4^- anions was constrained inside the tetrahedral cavity but showed no interaction of the fluorine atoms with the cobalt atoms. On the contrary, the fluorine atoms of the trapped counterion were directed toward the center of the triangular tetrahedral faces. It was assumed that the association derives from a size match between the guest anion and the host cavity as well as favorable electrostatic effects.[204]

Scheme 72

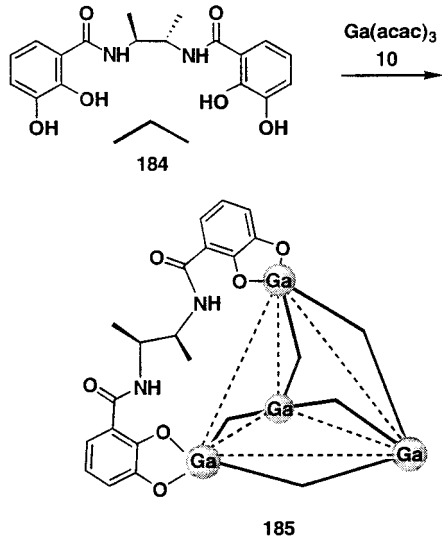

Stereospecificity and self-selectivity in the generation of a chiral molecular tetrahedron was demonstrated by Stack and Enemark in their route to metal-assisted self-assembly.[205] Reaction of the biscatecholamide **184** with $Ga(acac)_3$, **10**, in the presence of a base stereoselectively formed the tetrahedral compound **185** (Scheme 72). The use of the enantiomerically pure ligand gave rise to only one highly symmetrical complex with a Λ-configuration at each metal center, which showed a single set of resonances in the ^1H NMR spectrum.[205] The crystal structure analysis clearly showed a chiral tetrahedral complex with *T*-symmetry, with 3-fold axes passing through each metal center and 2-fold axes bisecting each ligand. Even more impressive was the fact that the use of a racemic mixture of the ligands produced only one enantiomeric pair of homochiral isomers in solution. The results were based on ^1H NMR spectral analysis which showed the stereospecificity of this reaction: only 2 out of 112 theoretically possible diastereomers were observed indicating a high degree of chiral induction.[205]

Huttner and co-workers[206] reported the formation and isolation of an iron(II)-containing self-assembled tetrahedron by employing the "molecular library" model. As the angular tridentate unit they used a six-coordinated iron(II) complex in which three facial coordination sites were blocked by a tridentate phosphine ligand, namely, $CH_3C(CH_2PPh_3)_3$ (tripod), **186**. The fact that the tripod−iron(II) complex binds quite strongly to three other ligands and that the resulting bonds are at right angles to one another allowed this complex to be used in the construction of a supramolecular tetrahedron. The preparation of assembly **189** was achieved by mixing **186**, the hexaaqua complex of $Fe(BF_4)_2$ **187**, and fumaronitrile **188** in a mixture of dichloromethane and ethanol (Scheme 73).[206] The isolated product **189** was characterized by NMR spectroscopy as well as X-ray crystallography. An interesting feature of the crystal structure is that it indicates an encapsulated tetrafluoroborate anion present within the tetrahedral cavity of the assembly. The B−F bonds of the guest are pointing toward the iron centers of the assembly. Since the symmetry of

Scheme 73

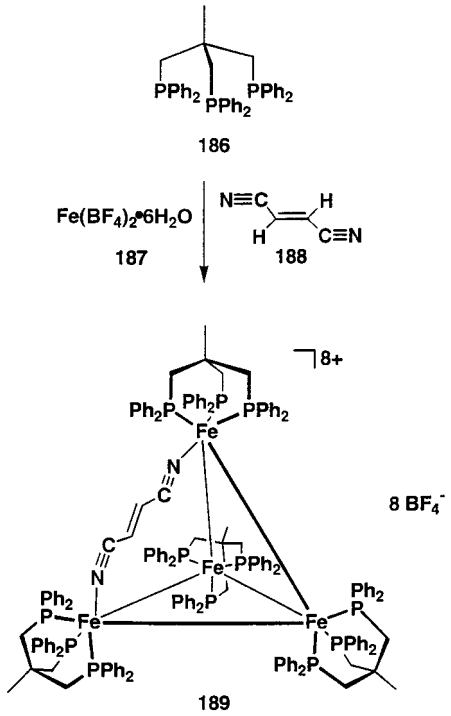

the guest molecule and the host anion are strikingly similar, the templating effect of the BF_4^- anion may ultimately be responsible for such a remarkable assembly of 15 components in solution to give the highly symmetrical host framework. This host inclusion was also detected in solution by low-temperature ^{19}F NMR. Another interesting fact is that the rigidity of the fumaronitrile unit is probably not responsible for the formation of this host: when a much more flexible succinonitrile was used, it led to the formation of the analogous macrocyclic tetrahedron whose salt crystallizes isotypic to the salt of **189**. The high positive charge of the product cluster forces the other three counterions to occupy the space above the centers of the four triangular faces of each tetrahedron. They are oriented in such a way that in each case three B−F bonds are directed toward the iron centers, which form the faces of each triangle.[206]

According to the "symmetry interaction" model, the construction of a tetrahedral M_4L_4 cluster can be achieved via usage of pseudo-octahedral metals as the corner units and trigonal trisbidentate ligands for the tetrahedral faces, relying on the same strategy as that for the synthesis of M_4L_6 clusters. An example of such a face-directed self-assembly of a tetrahedron was reported by Raymond and co-workers.[207] Reaction of the easily accessible C_3-symmetrical ligand **191** with $Ti(O^nBu)_4$ **190** in a mixture of methanol and Et_3N first resulted in the formation of a polymeric mixture. Refluxing the polymer in DMF for 12 h finally furnished the thermodynamically more stable tetrahedral cluster **192** (Scheme 74). Electrospray mass spectrometry and X-ray structure analysis confirmed the formation of a racemic mixture of *T*-symmetrical homochiral M_4L_4 clusters. A similar but rather unintended self-assembly of a ferromagnetically coupled manganese(II) M_4L_4 cluster was described by McCleverty and co-workers.[208]

Scheme 74

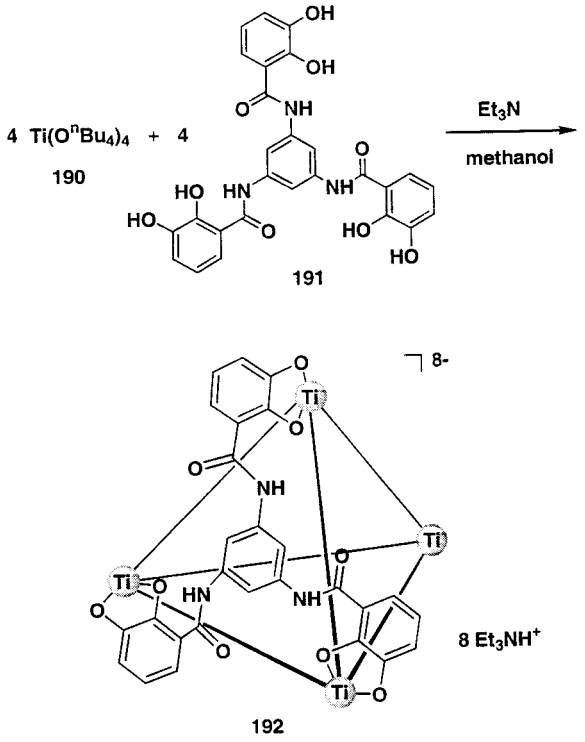

Scheme 75

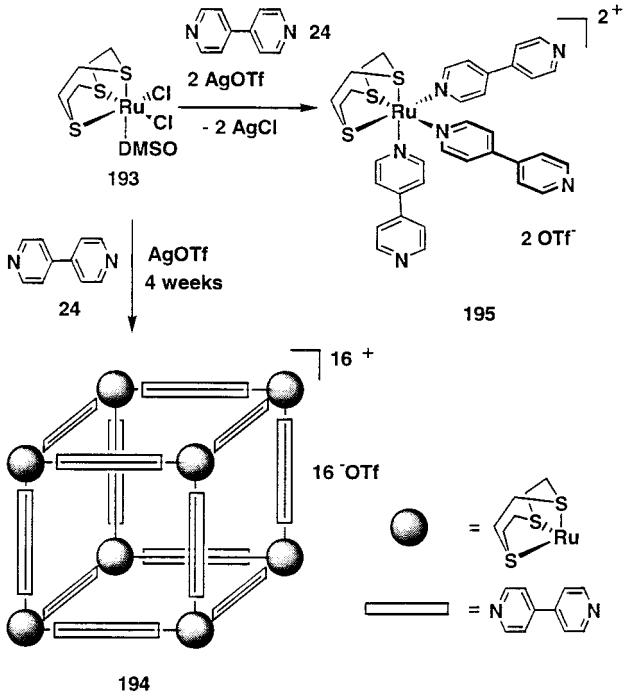

2. Cubic-Shaped Systems

A cubic system requires per definition eight corners that are all perpendicular to each other. Although only a few elements can provide three facial 90° angles, there are a surprisingly large number of cubic systems known. While the most interesting system of all, the parent hydrocarbon cubane,[178] was synthesized in 1964, many main-group-element-containing systems have been characterized.[209] Surprisingly, only a few metal-based self-assembled cubic systems have been reported to date.

A one-step self-assembly of a supramolecular cube from 8 octahedral metal corners and 12 linear linkers following the "molecular library" design strategy was recently reported by Thomas and co-workers.[210] Reaction of the ruthenium complex [([9]aneS$_3$)Ru(DMSO)Cl$_2$], **193**, and 4,4′-bipyridyl, **24**, in a 8:12 stoichiometry in the presence of silver triflate in nitromethane resulted in the cubelike complex **194** over a period of four weeks (Scheme 75). The structure of the cage compound was confirmed by NMR spectroscopy as well as ES-MS. In agreement with the assumed high symmetry of the complex, only one set of signals for the 4-pyridyl groups was found in the ^{1}H NMR spectrum.[210] Furthermore, the integral ratio of the bipyridine and the [9]aneS$_3$ corner protons as well as the elemental analysis of the compound suggested a 3:2 ratio of linear linkers and metal corners. Peaks in the ES-MS spectra for [cube(OTf)]$^{15+}$, [cube(OTf)$_3$]$^{13+}$, and [cube(OTf)$_6$]$^{10+}$ with correct isotopic pattern distributions support the proposed structure. Additional proof for the octahedral structure of the metal center was given by an X-ray structure analysis of the tris(bipyridyl) ruthenium complex **195**, derived from the reaction of [([9]aneS$_3$)Ru(DMSO)Cl$_2$] and an excess of bipyridine in the presence of AgPF$_6$. The structure unambiguously shows three bipyridine ligands oriented at mutually right angles.

The chemistry of cubic lattice polymers, such as Prussian Blue,[211] has been known for a long time. Prussian Blue and its analogous cyanometalate[212−214] exhibit ion-exchange properties, facilitated by the relatively large M$_4$(CN)$_4$ square face windows (∼25 Å^2), which makes them interesting as sequestering agents for Cs$^+$.[214,215] Compounds such as Fe$_4$[Fe(CN)$_6$]$_3$ are polymeric by virtue of the 6-fold bridging of the octahedral hexacyanometalate subunits. By replacing three of the cyano ligands with a cyclopentadienyl ligand, so that one face of the octahedral metal complex is blocked, polymerization can be prevented and the building blocks can be used for the formation of discrete structures. In a stepwise self-assembly process, Rauchfuss and co-workers successfully applied this approach to the design of novel organometallic cubelike structures.[216] The first step in this synthesis involves reaction of the tricyanometalate K[CpCo(CN)]$_3$, **196**, with the dimeric rhodium chloride complex [Cp*RhCl$_2$]$_2$, **197**, to form the molecular square **198**. The final assembly of cube **199** was achieved by removing the chloride ligand from the rhodium complex **198** with AgPF$_6$ in acetonitrile and dimerization of two molecular squares in a complementary orientation (Scheme 76). The high symmetry of the product is shown in the simplicity of the ^{1}H NMR spectrum, which consists of one signal each for Cp and Cp* in a ratio of 1:3.[216] The X-ray structure analysis of the ethyltetramethyl cyclopentadienyl derivative established the idealized T_d-symmetry of the cage. The 8 octahedral metal centers with alternating Co and Rh positions are bridged by 12 CN ligands, consistent with a facial assembly process. The regularity of the cubelike structure is indicated by the fact that all C−Co−C angles lie

Scheme 76

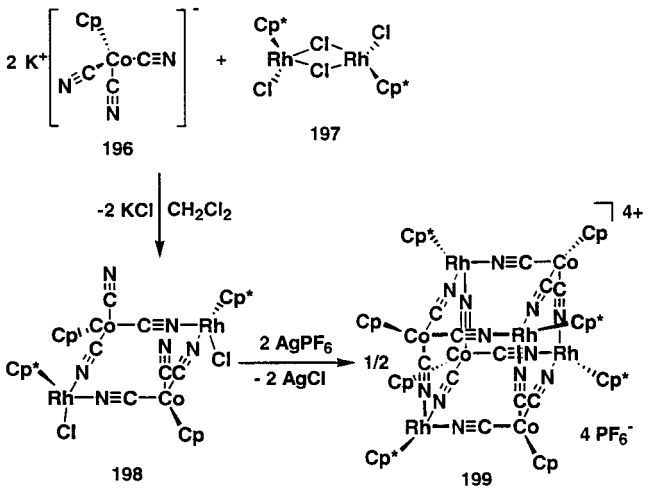

between 90° and 95° and all N−Rh−N angles are between 85° and 89°. Six additional noninteracting acetonitrile solvent molecules are located near the six faces of the box. The cavity itself is empty and encloses an idealized volume of approximately 132 Å^3.

In contrast, attempts to self-assemble a cubic system in a one-step reaction from appropriate precursors only afforded complex mixtures of different compounds. Given the considerable interior volume (~132 Å^3) as well as the large $M_4(CN)_4$ windows (~25 Å^2), the cubic $M_8(CN)_{12}$ cages have the potential to exhibit inclusion properties. Relying on a cationic template effect, Rauchfuss and co-workers[217] successfully assembled the cubic complexes **202a** and **202b** by mixing the anionic tricyano rhodium complex **200** with the neutral tricarbonyl molybdenum complex **201** in the presence of either potassium or cesium salts (Scheme 77). The products were isolated in good yields as crystalline compounds that proved to be

Scheme 77

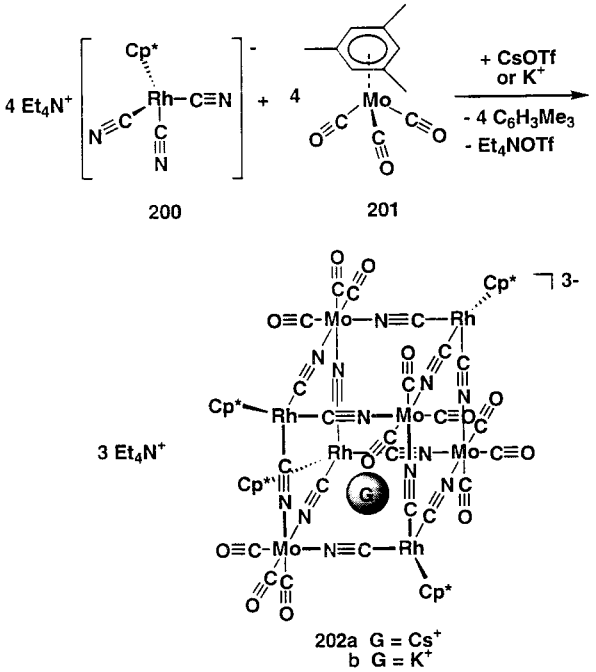

extremely sensitive to desolvation. Electrospray mass-spectrometric measurements demonstrated that the molecular cages are stable in solution, showing correct isotopic distributions for $\{(Et_4N)K[Cp^*Rh(CN)_3]_4[Mo(CO)_3]_4\}^{2-}$ and $\{Cs[Cp^*Rh(CN)_3]_4[Mo(CO)_3]_4\}^{3-}$. X-ray structure analysis of both compounds revealed two isostructural box-like cages (Figure 13). The Mo_4Rh_4 cores in **202a** and **202b** are

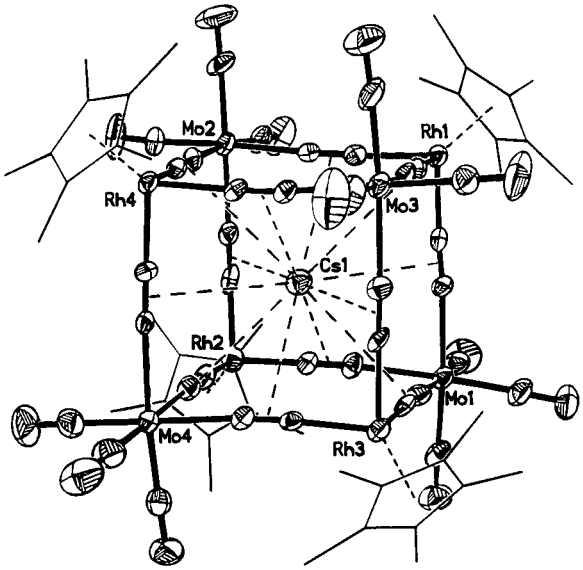

Figure 13. SHELXTL plot of the cubic complex $\{Cs[Cp^*Rh_9(\mu\text{-}CN)_3]_4[Mo(CO)_3]_4\}^{3-}$, **202a**.

virtually indistinguishable and highly symmetrical with Rh−Rh and Co−Co facial distances of 7.38 and 7.72 Å, respectively, and body diagonal distances of about 9.25 Å. While in **202b** the alkali-metal cation is situated in one of two off-center positions, with almost equal populations, the cesium cation in **202a** is located at the center of the cage, showing an idealized T_d symmetry. For the centric Cs^+ ion, the Cs−C and Cs−N distances range from 3.6 to 3.85 Å, averaging a distance of 3.71 Å for both interactions. Competition experiments revealed that the cubic cage compound has a higher affinity for Cs^+ than K^+, showing a poorer fit for K^+ as indicated by the fact that it is disordered over two sites.[217]

Taking advantage of the same strategy and using the tridentate ligand 1,4,7-triazacyclononane (tacn) to block three facial coordination sites of the transition-metal complex to prevent growth of the three-dimensional framework, Long and co-workers constructed a similar Prussian Blue analogue.[218] Reaction of $[Co(H_2O)_3(tacn)][OTs]_3$, **203**, and $[Co(CN)_3(tacn)]$, **204**, in boiling water furnished the cubic complex **205**, which was isolated from a methanol solution as a yellow solid in 86% yield (Scheme 78). The cubic $[Co_8(CN)_{12}]$ core structure was confirmed by X-ray structure analysis, showing edge to edge distances of 4.94 Å which are slightly smaller than those in similar Prussian Blue complexes. On the basis of the van der Waals radii, the minimum width of the square openings is about 1.7 Å and the minimum diameter of the internal cavity is about 3.7 Å.

Scheme 78

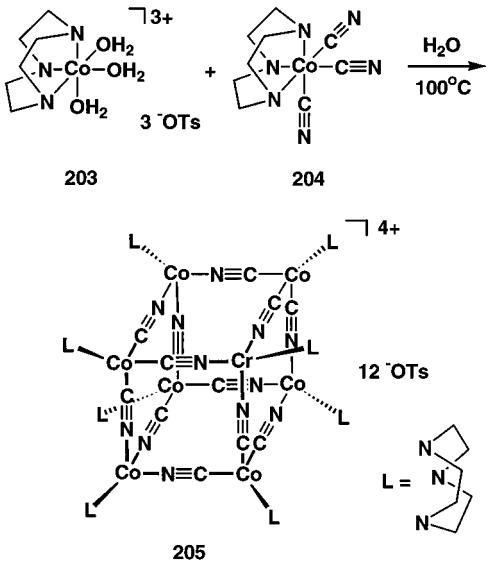

C. Archimedean Solids

In addition to the Platonic solids, there exists a family of Archimedean solids consisting of 13 convex uniform polyhedra that are made of at least two different regular polygons (Figure 14). They can be derived from at least one Platonic solid through truncation of corners or twisting of faces (which also includes C_{60}, Buckminster fullerene, a truncated icosahedron). Though all the vertexes of an Archimedean solid are identical, the whole family possesses a larger variety of polygons compared to the family of Platonic solids. Since the Archimedean solids compliment the Platonic solids, they are also ideal models for the design of spherical molecular hosts.

1. Truncated Tetrahedra

The shape of an truncated tetrahedron, the smallest member of the Archimedean solids, can be derived by capping all four corners of a tetrahedron (Figure 15). Each of the identical vertices is part of two

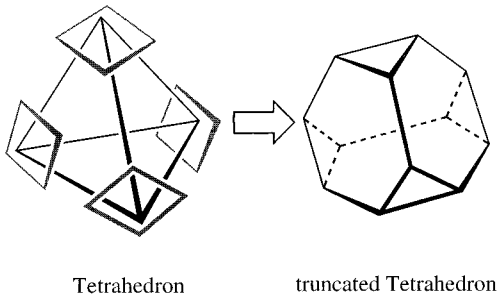

Figure 15. Archimedean truncated tetrahedron derived by capping four corners of a platonic tetrahedron.

hexagons and one equilateral triangle. Therefore, construction of such a system can be achieved via self-assembly of a flat tritopic building block in combination with an approximately 70° angular linking unit.

In work reported by Steel and co-workers, the coordination chemistry of 1,3,5-tris(pyrazol-1-ylmethyl)-2,4,6-triethylbenzene, **206**, along with the square-planar Pd(II) ions were utilized to assemble the 10-component, three-dimensional cage **207** (Scheme 79).[219] The highly symmetrical nature of **207** was apparent from the NMR data, showing only one set of signals for the organic linkers. Single crystals of this compound were analyzed by X-ray crystallography, confirming the truncated tetrahedral structure of this metallacycle with idealized T_d-symmetry. The diagonally opposite palladium atoms are separated by 13−15 Å, indicating that the cavity size in this assembly is sufficient to encapsulate relatively large guests.

Similar nanoscopic three-dimensional molecules with the shape of a truncated tetrahedra were self-assembled earlier by Fujita and co-workers[220] utilizing ethylenediamine Pd(II) dinitrate, **13**, in combi-

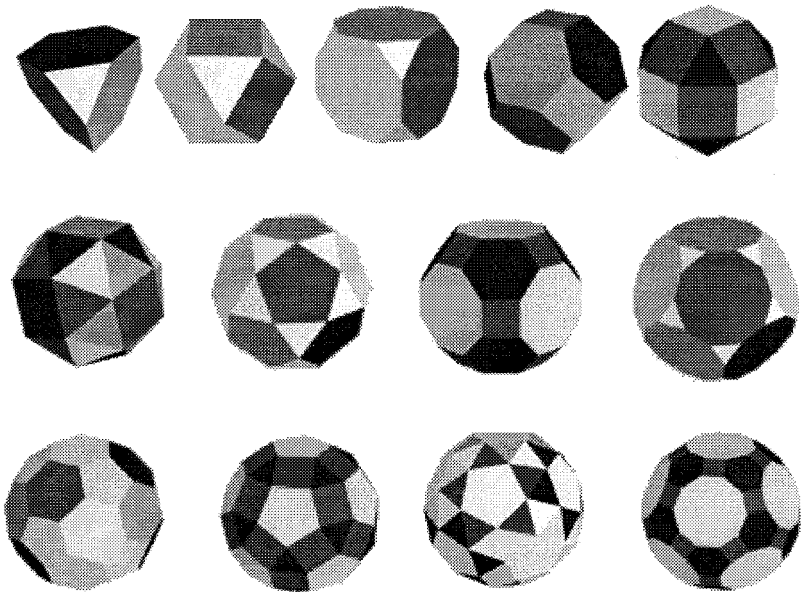

Figure 14. Representation of the 13 Archimedean solids in order of increasing numbers of vertices (left to right, top to bottom): truncated tetrahedron, cuboctahedron, truncated cube, truncated octahedron, rhombicuboctahedron, snub cube, icosidodecahedron, rhombitruncated cuboctahedron, truncated dodecahedron, truncated icosahedron, rhombicosidodecahedron, snub dodecahedron, rhombitruncated icosidodecahedron.

Scheme 79

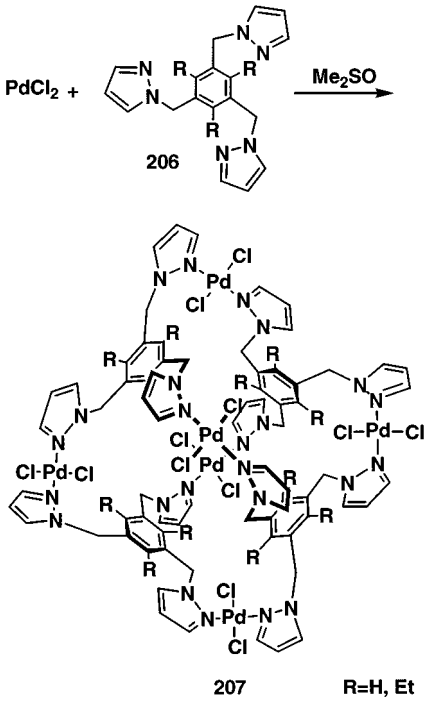

nation with the tritopic aromatic ligands **208a**−**c** (Scheme 80). The yields of assemblies **209** were near-quantitative and the products were shown to be very stable, since they formed even in the presence of an excess of the transition-metal-containing subunit.[220] These molecules were soluble in water and capable of encapsulating up to four guests, such as adamantane carboxylate. The thermodynamic stability of the final products is remarkable: when the transition-metal complex **13** and the ligand **208** were mixed in a 2:1 ratio, only the assembly with a 3:2 stoichiometry

Scheme 80

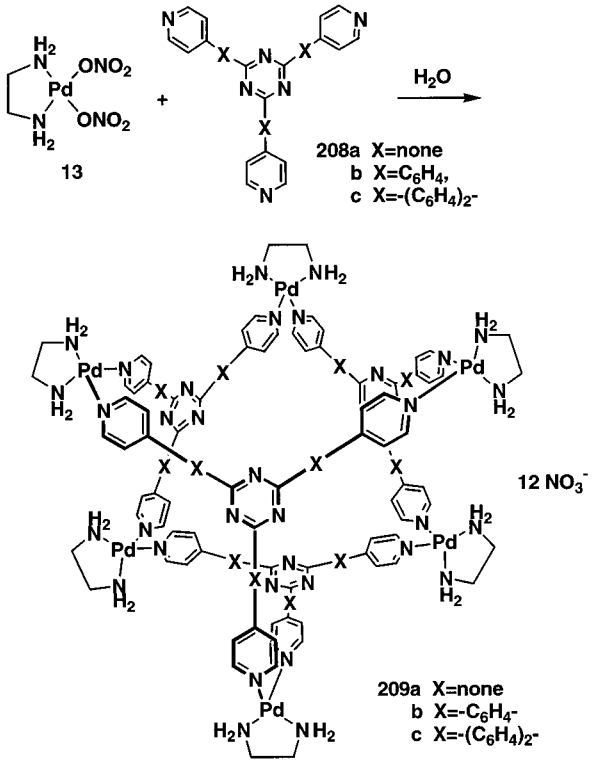

Scheme 81

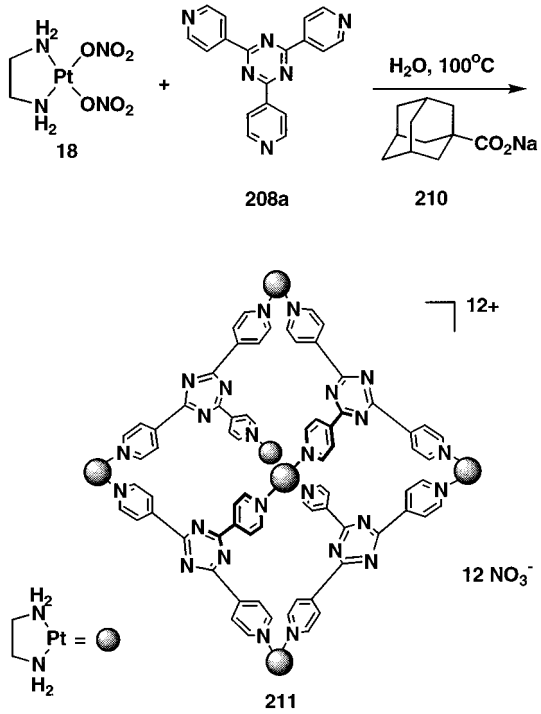

was observed while the excess free transition-metal complex remained intact. These molecules were studied by NMR spectroscopy in aqueous solution. The inclusion complex of assembly **209a** with adamantyl carboxylate was also studied in the solid state by X-ray crystallography.[220] Both methods as well as the titration studies confirmed the structure of the assembly and the aggregates formed with this guest. Thus, assembly **209a** formed a host−guest complex with four molecules of adamantyl carboxylate with no intermediate inclusion complexes with one, two, or three guest molecules being observed. This is likely due to allosteric effects: the hydrophobicity of the cavity increases and the complexation between **209a** and the guest becomes more effective with an increasing number of guests in the cavity.

These three-dimensional assemblies belong to the category of nanoparticles, and hence, their size could be explored by volume-weighted distribution analysis of the particle sizes employing a laser light scattering method. The assemblies **209a** and **209b** were shown to have respective mean diameters of 1.5 and 4.6 nm.

While the formation of the Pd complexes **209a**−**c** proceed under mild reaction conditions, the homologous Pt complex **211** (Scheme 81) is only formed in the presence of a templating guest under harsh conditions.[221] The high-yield formation of **211** was achieved by stirring the platinum dinitrate, **18**, and the organic linker **208a** in boiling water for 24 h in the presence of sodium adamantyl carboxylate **210**. Without such a templating guest, only traces of the cage compound **211** were formed. This reaction provides an example for induced fit since the guest induced the organization of its own receptor. As a result of the stronger Pt−pyridine bond, the cage compound **211** showed remarkable kinetic stability.

In contrast to the palladium counterpart **209**, this truncated tetrahedron is stable under highly acidic and basic conditions, and is not destroyed by strong nucleophiles. As a result, compound **211** was used to design a pH-responsive host−guest system. Under basic conditions, *N*,*N*-dimethylaniline was effectively bound in the hydrophobic cavity in a 1:4 (host:guest) ratio, whereas under acidic conditions, the guests were immediately liberated due to decreased hydrophobic interaction as well as cationic repulsion between the host and the protonated *N*,*N*-dimethylaniline.[221]

Besides the inclusion of charged molecules, Fujita was also able to encapsulate large neutral molecules into the approximately 2-nm-wide cavity.[222,223] By mixing a hexane solution of *o*-carborane with a water solution of **209a**, 4 equiv of the o-carborane were transferred into the aqueous phase and encapsulated into **209a**. The 1:4 stoichiometry was confirmed by integration of the host and guest signals in the proton NMR spectrum. Inclusion of 1- and 2-adamantanol showed that the interior of the cage has highly hydrophobic characteristics, which resulted in the outward pointing of the hydroxyl groups of the adamantanol. For molecules that were slightly larger than the portal of **209a**, encapsulation of just one guest molecule was very slow as a result of thermally induced slippage. Once inside the cavity, the guest did not escape even when treated with organic solvents.[222]

A chiral example for an Archimedean solid was prepared by using the chiral transition-metal complexes *R*-(+)-BINAP Pd (II) bistriflate, **43a**, and its platinum homologue **43b** as shape-defining angular units.[224] Additionally, the BINAP ligand provides a significant degree of conformational rigidity, which is quite important since the loss of conformational entropy is minimized upon binding of the connecting unit. As a suitable planar tritopic building block, tris-1,3,5-(4′-pyridyl)ethynylbenzene, **212**, was prepared from tris-1,3,5-triethynylbenzene and 4-bromopyridine via cross-coupling. Addition of **212** to a dichloromethane solution of the transition-metal bistriflates **43a** and **43b** resulted in the formation of the single highly symmetrical entities **213a** and **213b** with the stoichiometry of the reactants being 3:2 (Scheme 82), as observed by NMR. The stoichiometry of chiral assembly **213a** was firmly established by mass spectrometry. The ESI−FTICR mass spectrum of **213a** obtained from a dichloromethane solution resolved the peak centered at $m/z = 1768.19$ with an m/z peak spacing of 1/4 corresponding to the $[M - 4^{-}OTf]^{4+}$ ion with the 4^{+} charge state. The observed molecular weight and close match of the calculated and observed isotopic distribution patterns of the 4+ charge state (7092.76 Da) are in agreement with the theoretical MW of 7092.89, corresponding to the cyclic assembly with loss of four triflate counterions.[224] Spectroscopic data as well as force field simulations have further established the expected structure of the final products **213a** and **213b** as spherical *T*-symmetrical, chiral, truncated tetrahedron.

Scheme 82

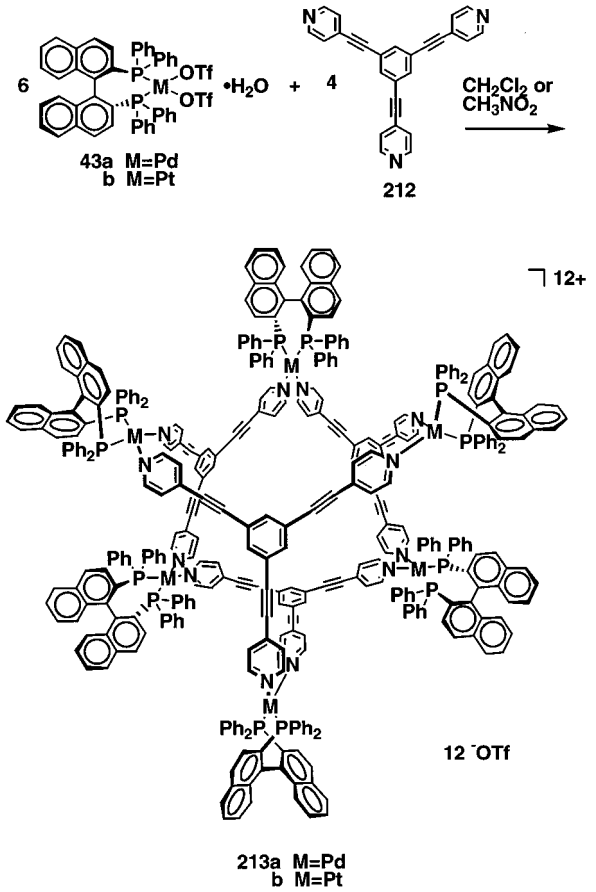

2. Cuboctahedra

Although to date very little is known about unnatural assemblies of *I* and *O* symmetries, there are numerous examples of noncovalently bound assemblies in nature showing such high symmetries. These macromolecules are much larger and significantly more complex than any of the man-made nanoscopic assemblies. The structure of the protein apoferritin consists of 24 individual subunits that are arranged in such a way that they form a highly symmetrical cluster with the *O* symmetry group. Its spherical cavity holds over 4000 iron atoms.[225] Other examples of noncovalently linked highly symmetrical nanostructures include proteins that form viral coats, for instance the human rhinovirus. Its protein cluster consists of 60 subunits that assemble into a hollow, roughly spherical 60-mer of *I* symmetry.[226] An interesting feature of both these proteins is that once disassembled into their constituents, they tend to spontaneously reassemble back to their highly symmetrical forms.

The cuboctahedron, the second smallest member of the Archimedean family of truncated polyhedra, combines square and triangular faces in a regular fashion and is difficult to make by conventional organic synthesis. Fortunately, the shape of a cuboctahedron can be achieved via coordination-driven, face-directed self-assembly, combining 8 planar tritopic ligands and 12 ditopic angular subunits with an angle close to 108°.[227] Slow addition of a dichloromethane solution of bispyridyl acetal **214** to a

Scheme 83

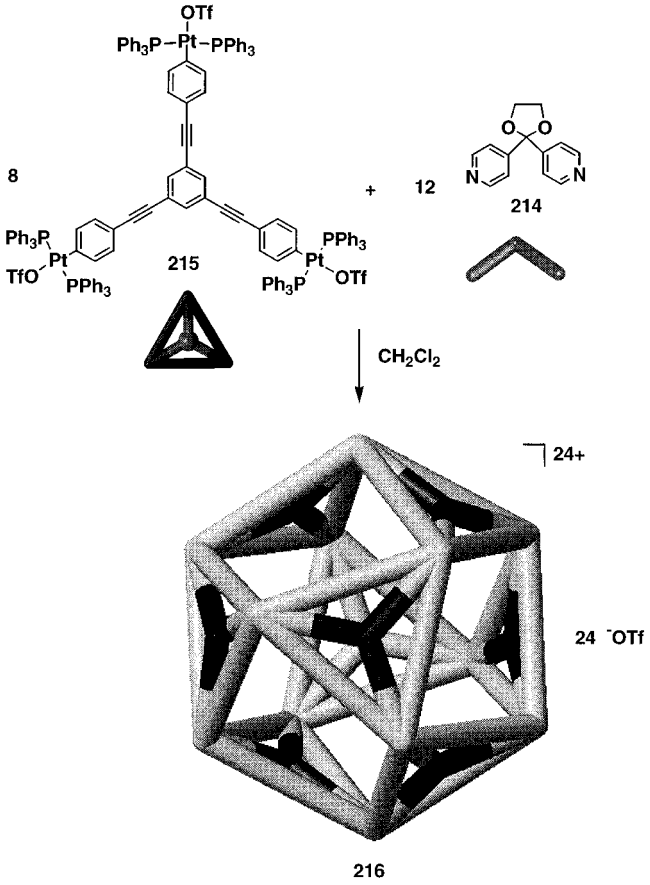

Scheme 84

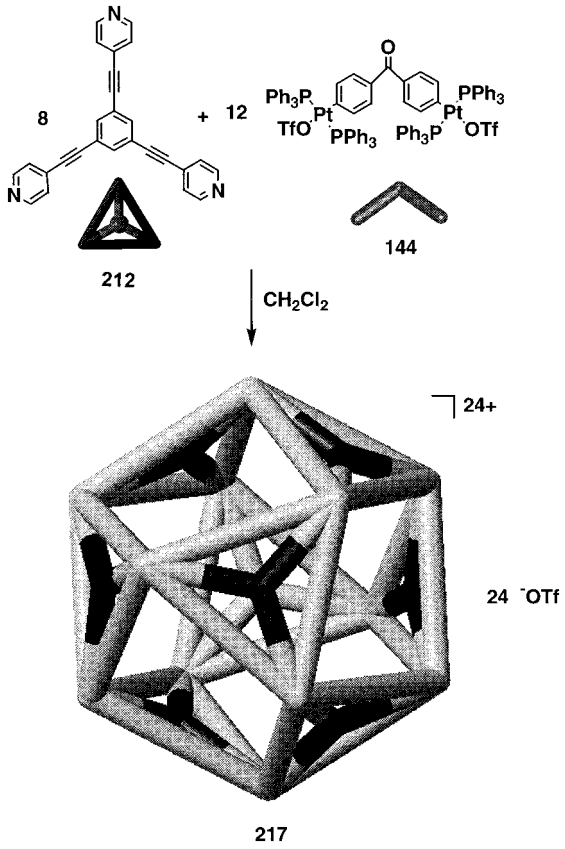

solution of the platinum tris(triflate), **215**, in a 3:2 stoichiometry resulted in a single highly symmetrical entity (Scheme 83). Despite its large molecular weight (26 592.2 Da) and high charge (+24), compound **216** is remarkably soluble in organic solvents, which allowed identification of its composition by electrospray mass spectrometry. Upon gentle ionization of **216**, multiply charged species were observed, resulting from the loss of the appropriate number of triflate counterions. Formation of a second cuboctahedron was observed via a different route using complementary building blocks. Reaction of 2 equivs of tritopic donor component 1,3,5-tris(4-pyridylethynyl)benzene, **212**, with 3 equivs of the ditopic angular unit **144** furnished cuboctahedron **217** in quantitative yield (Scheme 84). The ^{1}H and ^{31}P NMR spectra once again indicated the clean formation of a single, highly symmetrical compound. In addition to standard characterization methods, the experimental size of cuboctahedron **217** was assessed by measuring its self-diffusion coefficient using the pulsed gradient spin−echo (PGSE) NMR technique.[228] The experimental hydrodynamic diameter for **217** of 5.0 nm, derived from the self-diffusion coefficient,[229] was in agreement with predictions based on force field simulations (Figure 16). Both face-directed self-assembled cuboctahedra **216** and **217** belong to a unique class of artificial synthetic assemblies of *O* symmetry. Despite the different analytic and spectroscopic results in favor of the proposed cuboctahedral structure, to date no unambiguous solid-state structure has been reported.

While the truncated tetrahedral complexes **207**, **209** and **213** as well as the cuboctahedral complexes **216** and **217** were constructed taking advantage of the "molecular library" model, the first example for the construction of an Archimedean polyhedron via the "symmetry interaction" design strategy was recently reported by Robson and co-workers.[230] Reaction of the deprotonated trianion **218** (tapp^{3-}), derived from 2,4,6-triazophenyl-1,3,5-trihydroxybenzene and tetramethylammonium hydroxide, with $Cu(NO_3)_2$ in a 2:3 molar ratio in DMF gave dark brown crystals of $Cu_{12}(tapp)_8$ (**219**) (Scheme 85). Single-crystal X-ray diffraction of **219** showed that each of the eight 2,4,6-triazophenyl-1,3,5-trihydroxybenzene subunits is attached to three Cu(II) centers via a bidentate N,O-chelating system. Each Cu(II) center on the other hand is chelated by two ligands acquiring a somewhat distorted trans N_2O_2 square-planar coordination environment. While the benzene cores of the ligands are located very close to the corners of a cube, the 12 Cu centers are located at the corners of an idealized cuboctahedron, giving rise to an almost spherical shell. The volume of the enclosed cavity was estimated to be 816 Å^3, sufficient to accommodate about six DMF molecules. Though no DMF molecules could be refined within the cavity of **219** itself, there was enough electron density left to make up for five to six solvent molecules.[230] As a result of the azophenyl groups all pointing either clockwise or counterclockwise, the cell consists of a racemic mixture of independent chiral cuboctahedra (Figure 17). To date, this self-assembled cuboctahedron **219**, built from 8 tribidentate chelators and 12

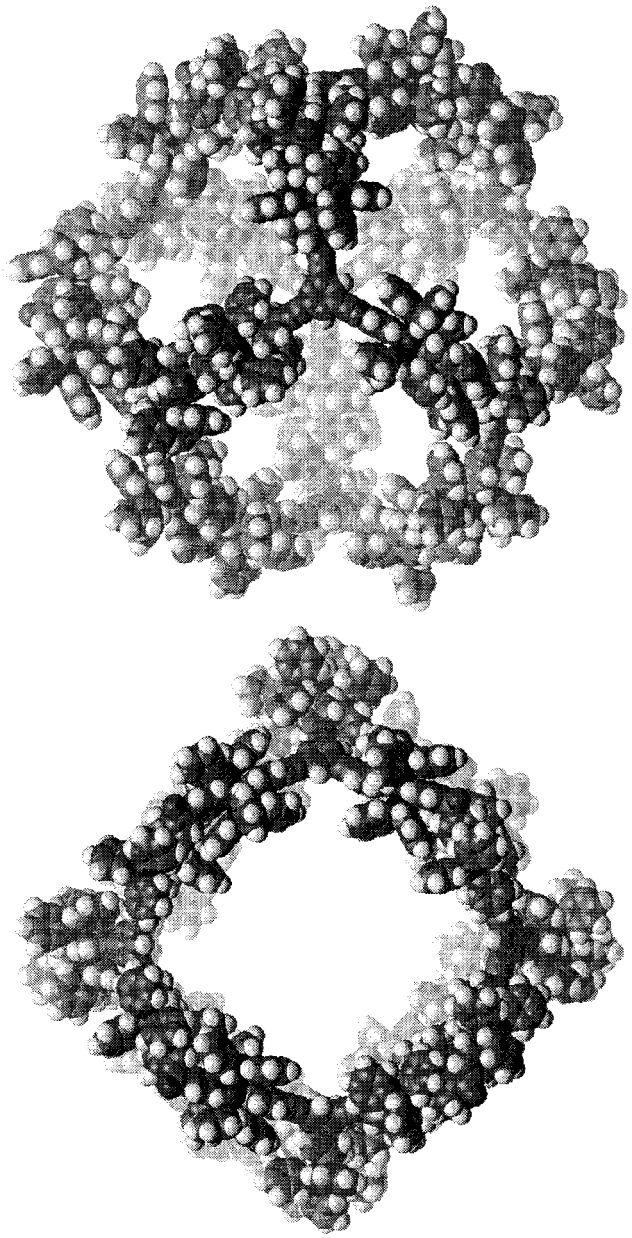

Figure 16. Space-Filling model of cuboctahedron **217** based on forcefield calculations; (a) view along the C_3-axis, (b) view along the C_4-axis.

copper ions, is the largest discrete coordinative cage compound that has been fully characterized.

D. Irregular Polygons and Nanocages

Besides the three classes of convex uniform polyhedra, the prisms, the Platonic solids, and the Archimedean solids, which form spherical or pseudospherical molecular hosts, there exists a number of cage compounds that are Archimedean duals, irregular polygons, or systems of low symmetry.[23]

The formation of an unusual macrotricyclic cage complex was reported by Fujita and co-workers.[231] Reaction of ethylenediamine palladium dinitrate, **13**, and tripyridylmethyl acetate, **220**, resulted in the spontaneous formation of the D_{2h}-symmetrical macrotricycle **221** (Scheme 86). The lower symmetry of this assembly becomes obvious in the ^{1}H NMR spectrum where two nonequivalent sets of pyridine

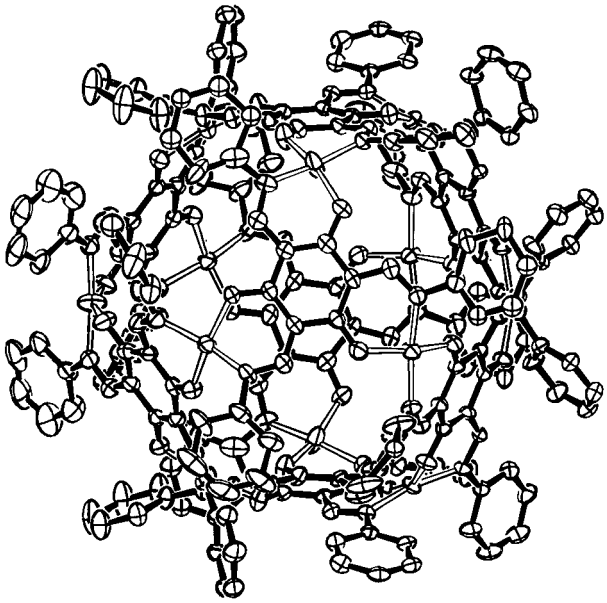

Figure 17. View along the three-fold axis of cuboctahedron **219**.

Scheme 85

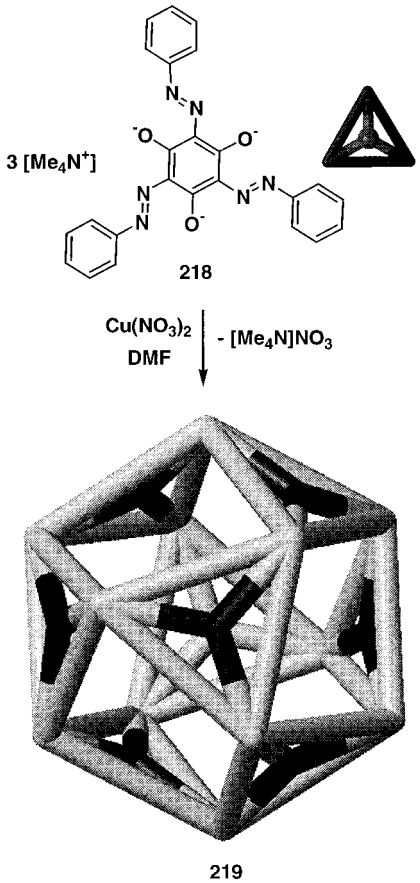

signals as well as two signals for the ethylenediamine palladium emerge in a 2:1 ratio, respectively. The macrotricyclic structure was proven by X-ray structure analysis, which revealed a large elliptical cavity of about 14 Å in diameter despite the small size of the building blocks. Surprisingly, the same type of macrotricycle was formed in the reaction of ethylenediamine palladium dinitrate, **13**, and the tris(3-pyridyl)-1,3,5-triazene, **222**, (Scheme 87). The X-ray

Scheme 86

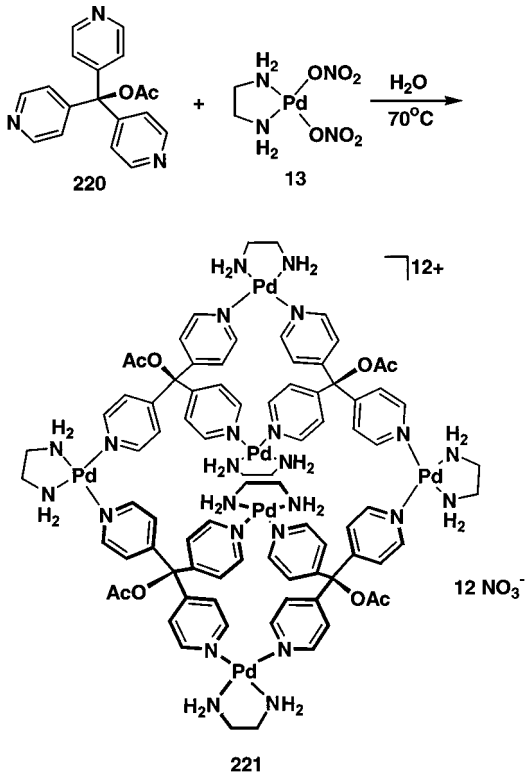

Scheme 87

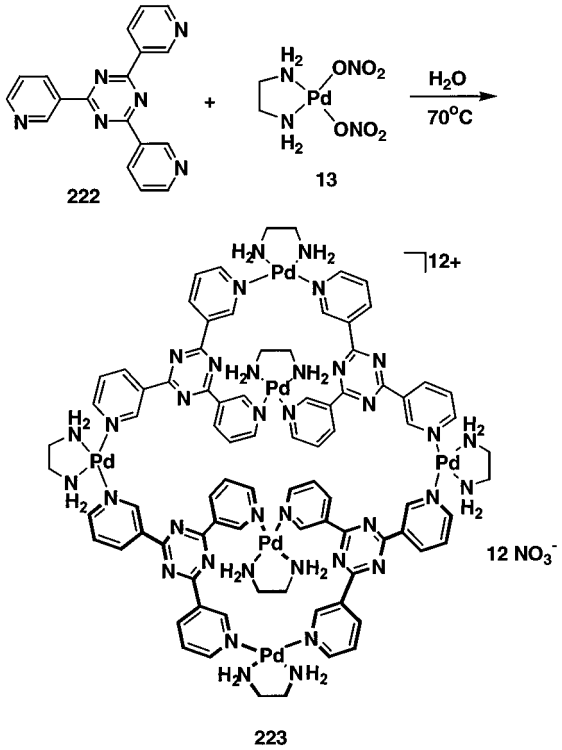

structure analysis of the 3-D assembly **223** shows a slightly different, bowl-type structure compared to **221**.[231] The formation of both complexes via self-assembly occurs in two steps: first two pyridyl groups of either ligand are involved in the formation of a dinuclear macrocycle and the third pyridyl group stays unbound. A compound similar to the postulated intermediate was characterized by X-ray analysis

Scheme 88

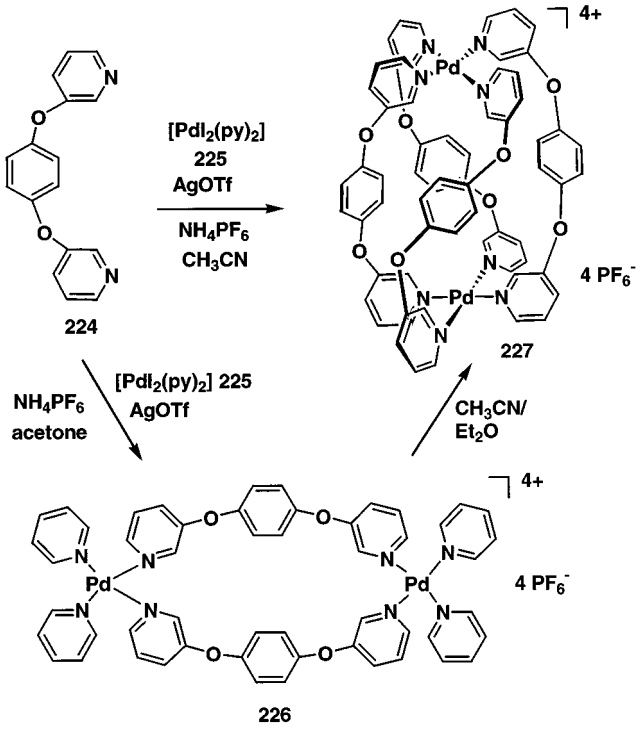

from the reaction of 2,2′-bipyridine palladium dinitrate and tris(3-pyridyl)-1,3,5-triazene. In a second step, the free pyridyl groups of the two macrocycles are connected via ethylenediamine palladium to form the final tricyclic M_6L_4 structure.

It was also shown that the two macrotricyclic structures **221** and **223** are capable of incorporating dicarboxylate anions such as sodium terephthalate and 1,4-benzodicarboxylate. The host−guest interaction is explained by electrostatic interaction of the positively charged cage and the negatively charged dicarboxylate. From the fact that the structure of these M_6L_4 complexes differ so much from those of octahedral M_6L_4 complexes,[219−224] the authors concluded that the shape of the three-dimensional cage not only depends on the rigid shape of the building blocks but also on a subtle thermodynamic equilibrium.[231]

Steel and McMorran[232] achieved formation of hitherto unknown coordinatively saturated quadruple helicates via combination of square-planar metals and oligomonodentate bridging ligands (Scheme 88). Reaction of 1,4-bis(3-pyridyloxy)benzene, **224**, with 1 equiv of $[PdI_2(py)_2]$, **225**, in the presence of silver triflate furnished the dimeric complex **226**. Diffusion of diethyl ether into a solution of **226** and NH_4PF_6 in acetonitrile led to the reorganization of **226**, forming the M_2L_4 complex **227**, which precipitated as the tetrakis(hexafluorophosphate) salt. By using the appropriate ligand to metal stoichiometry (2:1), complex **227** was isolated in about 70% yield in a one-step reaction. The X-ray structure analysis of the quadruple helicate **227** revealed two square-planar palladium atoms, each coordinated to one pyridine group of four bridging ligands. One of the four PF_6 anions is located within the cavity and shows two weak Pd−F interactions. It has been shown that

these supramolecular compounds are capable of hosting neutral,[201] cationic,[233] and anionic guest molecules.[192] Providing the first example of a helical inclusion of a multiatom anion, this X-ray structure analysis is also a rare example for the structural proof of PF_6^- inclusion in a three-dimensional assembly.[234] Even more interesting is the fact that the inclusion phenomenon exists in solution, which was indicated by the observation of two ^{19}F NMR signals. Therefore, it was assumed that on the NMR time scale the anion stays inside the cavity, although it rotates freely.

In an attempt to construct a molecular polyhedron, Fujita and co-workers designed a hexatopic ligand, 1,3,5-tris(3,5-pyrimidyl)benzene (**228**), as a triangular assembly unit.[235] By coordinating the almost coplanar triangle **228** to the *cis*-palladium(II) complex **13**, they expected to be able to construct either a tetrahedron or an octahedron. Reaction of 1,3,5-tris(3,5-pyrimidyl)benzene (**228**) with **13** in a 1:3 molar ratio gave a single product (Scheme 89). However, interpretation of the NMR spectra revealed that the final product **229** was of lower symmetry than expected for a Platonic solid. Seven singlet-like signals in an integral ratio of 2:2:2:2:2:1:1 in the ^1H NMR spectrum confirmed a σ_2-symmetrical environment with only one symmetry axis passing through the organic ligands, suggesting a trigonal-bipyramidal structure for **229**. X-ray crystallographic analysis provided final evidence for the proposed structure, clearly showing a truncated trigonal bipyramid with dimensions of 3 × 2.5 × 2.5 nm. In the so-called hexahedron,[235] each equatorial corner is made up by the assembly of a tetranuclear [Pd(II)−pyrimidyl]$_4$ cyclic framework while each apical corner is made up by the assembly of a trinuclear [Pd(II)−pyrimidyl]$_3$ cyclic framework. The openings at the equatorial corners are small (2 × 2 Å) and may only allow small molecules such as water and molecular oxygen to pass. The internal cavity on the other hand has a large volume of about 900 Å^3, making complex **229** an ideal host for larger molecules such as fullerene. A possible mechanism for the self-assembly of **229** was derived from the characterization of intermediates formed under different molar ratios. At a 1:1 molar ratio, a single complex was isolated and identified as a dimeric dinuclear complex, while addition of more palladium(II) lead to the formation of a trimeric hexanuclear complex (Figure 18). Although the individual coordination bonds are weak due to cationic repulsion between adjacent Pd(II) ions and the electron-withdrawing effects of adjacent Pd(II)−pyrimidyl bonds, the strong positive cooperative effect of 36 coordinative bonds contribute to the thermodynamic stability of **229**. Thus, reaction of **13** with pyrimidine only resulted in the formation of oligomers rather than the possible macrocycles.[235]

Scheme 89

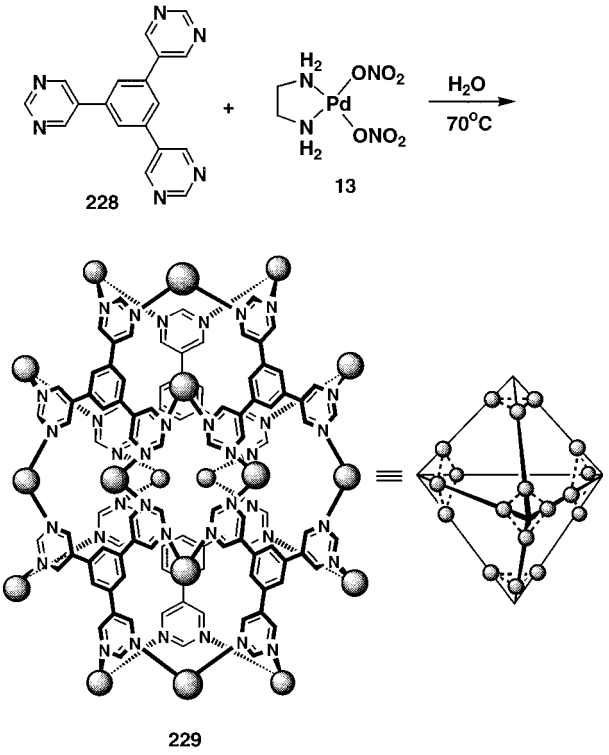

Mingos and co-workers described the formation of an anion-templated inorganic "super adamantanoid" by simply mixing triphos, **230**, with the silver salt of a weakly coordinated oxo anion, such as triflate (Scheme 90).[236] The X-ray structure analysis of complex **231** showed an approximately *T*-symmetrical entity, where the four faces of the cage corresponded to fused 18-membered rings each having local C_3-symmetry. The triflate counterions were centered above each facial trio of silver atoms and coordinated via their oxygen atoms. Surprisingly, the methyl groups of the triphos ligands pointed toward the center of the cage, resulting in an unusual "endo-methyl" conformation. As a consequence, the cavity inside the adamantanoid structure became very small, only about 2.4 Å in diameter, and at the same time formed a hydrophobic interior. Changing the counterion to BF_4^- or SbF_6^- resulted in the

Scheme 90

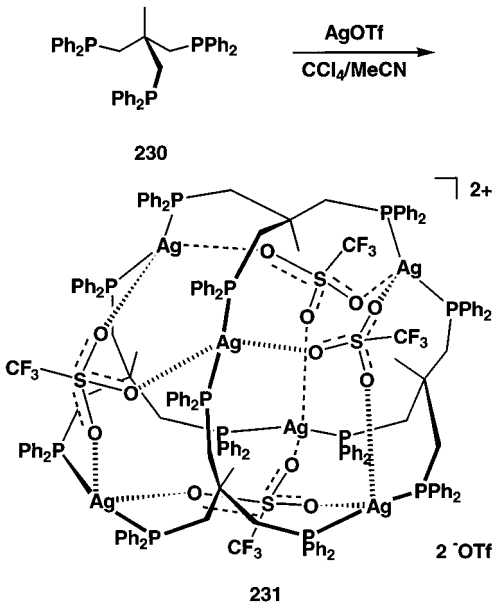

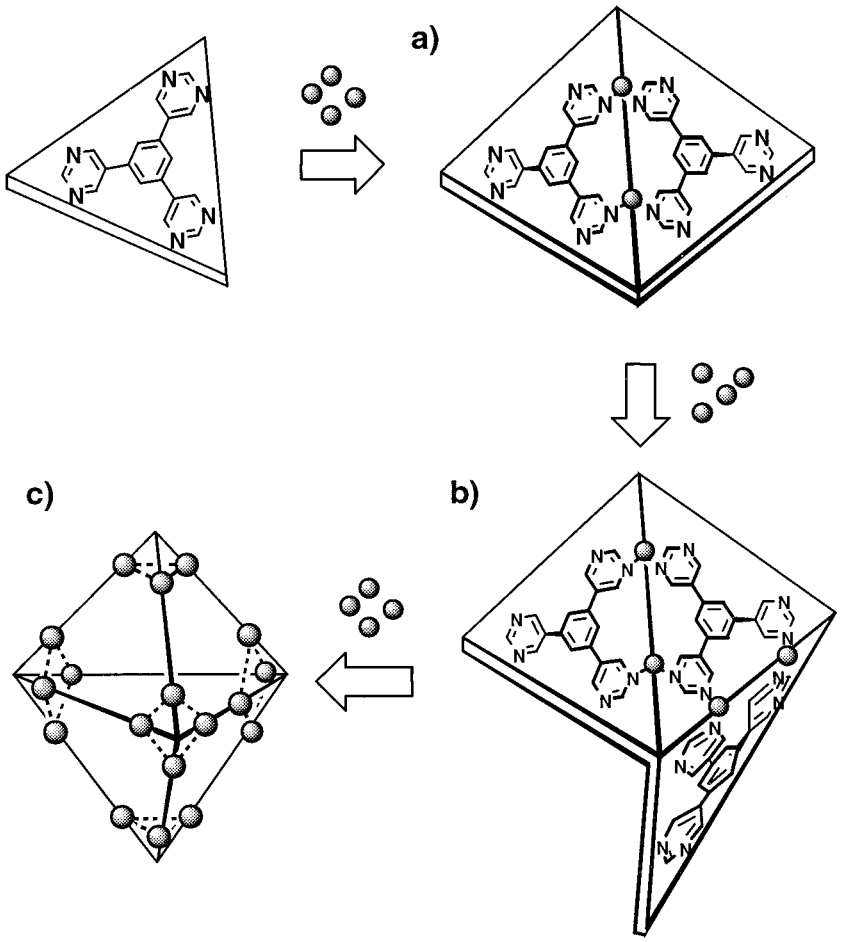

Figure 18. Stepwise self-assembly of **228** and **13**. (a) Formation of a dinuclear dimeric complex. (b) Trimeric complex made up of dinuclear units. (c) Final assembly of a stable hexahedron.

dissociation of the cage and suggested an anion-specific behavior, which may be related to the μ_3-face-capping coordination of the anions.[236] The term "super-adamantanoid" was suggested because every tetrahedral face was composed of 18-membered rather than 6-membered rings and the bridgehead atoms were replaced by tridentate triphos ligands.

Interpenetrating ring systems or catenanes have long intrigued chemists and material scientists because of their unique chemical and physical properties.[237] The field of self-assembly provides an ideal methodology for the synthesis of catenanes since it allows chemists to construct and obtain such interpenetrating systems in near quantitative yields without much synthetic effort. Some of these systems, taking advantage of coordinative metal interactions, have been discussed earlier in this review,[39−41,175] while a wide variety of catenanes were synthesized using other noncovalent interactions.[237,238] Fujita and co-workers recently managed to take this synthetic methodology one step further, reporting the self-assembly of two interlocked molecular cage compounds.[239] The framework of each of the two interpenetrating cages is assembled by interaction of three *cis*-palladium corner units with two different tritopic organic linkers (Scheme 91). While reaction of 3 equivs of **18** with 1 equiv of 2,4,6-tris(4-pyridyl)-triazine (**208a**) and 1 equiv of the benzyl extended linker **232** gave a kinetically distributed oligomeric mixture, heating at 100 °C for 3 days gradually turned the mixture into the thermodynamically stable product **233a**. The slow conversion of the product was due to a strong Pt(II)−pyridyl coordinate bond which becomes labile at higher temperatures. The interlocked cage structure of **233a** was confirmed by ES-MS and X-ray analysis. An interesting feature revealed in the solid state is the stacking of the four core triazine rings, making the interlocked structure the most stable of any possible structures due to efficient $\pi-\pi$ interactions.[240] Furthermore, intermolecular stacking of the triazine π-systems in the solid state leads to an infinite one-dimensional strand.[239]

The extreme thermodynamic stability of the interlocked cage compounds **233** was shown in an unique NMR experiment. Reorganization of a 2:1 mixture of the two cage compounds **234** and **211** lead to the sole formation of the three-dimensionally interlocked complex **233a** (Scheme 92). While the conversion occurred gradually at room temperature along with decomposition of the unstable cage compound **234**, the reorganization was significantly accelerated at higher temperatures as shown by ^{1}H NMR. This example among others[41,193] showed that molecular self-assembly via coordinative interactions cannot only be used to construct highly symmetrical entities, but that application of the same methodology can also be used in multicomponent self-assembly reac-

Scheme 91

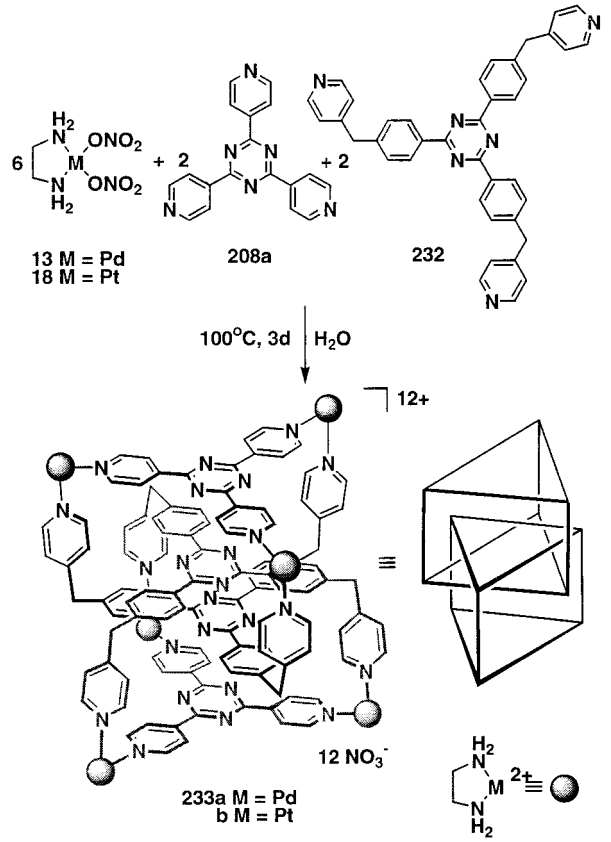

Scheme 92

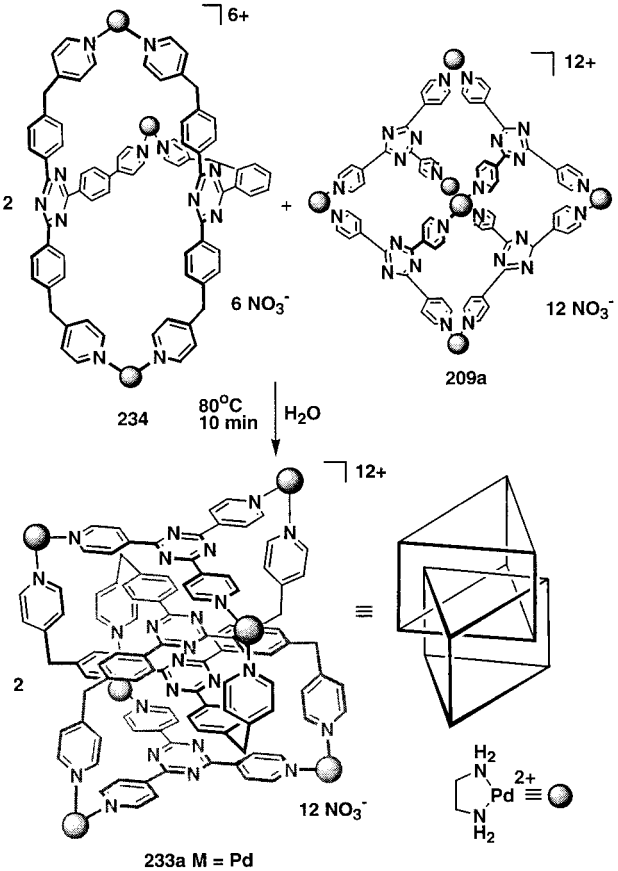

tions to form complex and highly sophisticated structures.

V. Challenges in the Characterization of Large Supramolecules

In the field of supramolecular chemistry, the greatest challenge posed is the characterization of the supramolecules themselves, in particular the characterization of discrete, highly symmetrical large self-assembled entities. While multinuclear NMR spectroscopy provides a first insight, it quite often lacks the ability to provide adequate unique data due to magnetically equivalent nuclei as a result of the high symmetry of the molecules. Nevertheless, NMR techniques are useful to monitor the formation of the final products via observation of characteristic shifts due to metal−ligand interaction.

Deduction of the molecular weight and subsequent confirmation of the empirical formula by mass spectrometry has become an important tool. The method of choice here is electrospray mass spectrometry (ES-MS) since EI-, CI-, and FABMS require harsher conditions and have limited mass ranges. Soft ionization of the metal-based assemblies lead to highly charged systems that allow for the determination of the *m*/*z* ratio along with isotopic distribution patterns. Moreover, the high dilution conditions generally required to run ES-MS can often influence dynamic equilibrium processes, favored by the labile nature of the coordination bonds, resulting in the additional formation of entropically favored smaller assemblies. Thus, identification and characterization of the thermodynamically favored product may not always be definitive.

The most unambiguous method for the characterization of solid-state structures is single-crystal structure analysis. Unfortunately, the larger the self-assembled structures get, the more difficult it is to grow suitable crystals. This observation can be partially attributed to crystal packing effects, which in the case of larger high-symmetry spherical-like entities can result in disorder. Furthermore, the cavities within the molecules as well as the void space between the molecules are often filled with volatile solvent molecules and/or counterions, making the crystals highly solvent dependent and therefore quite difficult to handle. In addition, the quality of the structure refinement decreases as a result of disordered or nonlocated solvent molecules and counterions, often making it impossible to fully refine the collected data. Furthermore, some of the larger assemblies have molecular weights comparable to proteins and hence just the large number of atoms and sheer size pose a challenge to the refinement and solution of the exact structure. Moreover, there is always the risk of the solid-state structure being different from the structure in solution.

Other methods, such as molecular weight determinations by colligative properties (boiling and freezing point depression) suffer from problems of solubility, high charges, and precision of measurement. Pulse gradient spin−echo NMR techniques provide for measurements of self-diffusion coefficients that can be related to hydrodynamic volume and ultimately the size of the macromolecule.[241] Unfortunately, hydration effects and counterion coordination can contribute to larger values compared to the

actual size. Likewise, microscopic techniques such as scanning tunneling microscopy (STM) and transmission electron microscopy (TEM) have become useful tools in providing macroscopic as well as microscopic characteristics of suitable deposited monolayers, thereby providing valuable information on the size and shape of the ensembles.

It is evident that the intrinsic properties along with their size and high symmetry make the characterization of self-assembled metallacycles and supramolecules in general rather different and more challenging from that of classical organic and inorganic compounds and rather akin to the problems of larger biomolecules. Therefore, the best approach to the proper and full characterization of these unique species lies in a combination of as many as possible of the aforementioned techniques.

VI. Potential Applications for Metal-Based Polygons and Polyhedra

It is evident that self-assembly strategies offer advantages over classical, linear covalent synthesis in the formation of complex supramolecular entities and hence for nanotechnology are likely to be the methodology of choice.[242] Present applications involve molecular recognition, host−guest chemistry, chiral recognition, and catalysis, while long-term goals are focused on the design of new materials with desirable properties and the manufacturing of nanoscale devices and molecular machinery.[5,17]

One of the earliest reports on the inclusion properties and host−guest behavior of transition-metal-based supramolecules was given by Maverick and co-workers.[31] Exploiting the Lewis-acidic properties of Cu^{2+} centers in β-diketonate-coordinated metallamacrocycles, they were able to selectively bind nitrogen heterocycles inside the macrocyclic cavity. While the *m*-xylylene bridged system was too small to incorporate a guest molecule within the cavity, the 2,7-naphthylidenediylbis(methylene) bridged complex **1** showed a significantly larger cavity. Addition of Lewis bases resulted in equilibrium constants for binding of pyridine ($K = 0.5$ L/mol), pyrazine ($K = 5$ L/mol), and quinuclidine ($K = 7$ L/mol) to complex **1** comparable to those in the literature for binding to $Cu(acac)_2$.[243] While these results did not speak for an internal bridging, the much larger equilibrium constants for diazabicyclo[2,2,2]octane ($K = 220$ L/mol) showed selective internal binding. X-ray structure analysis of **1** confirmed the findings. Molecular mechanics calculations on compound **1** using van der Waals interactions gave a rotation barrier of ca. 20 kJ/mol which was very similar to the experimental thermodynamic data ($\Delta H = -30$ kJ/mol and $\Delta S = -50$ kJ/mol).[31]

Host−guest inclusion complexes become significantly more stable when the host is a water-soluble molecule with a hydrophobic cavity. This is due to the strengthening of the hydrophobic interactions between the encapsulated guest and the host cavity surrounded by the shell of the polar hydrophilic medium. These forces are far stronger than the interactions between lipophilic hosts and guests in organic solvents. In all cases, however, the complementarity of the shape and the electronic effects also play an important role. Thus, macrocyclic assembly **14** was shown to bind electron-rich aromatic guests in water with strikingly high affinity.[37,244] Since it contains an electron-deficient perfluorinated benzene unit, it was capable of binding 1,3,5-trimethoxybenzene, *p*-dimethoxybenzene, *m*-dimethoxybenzene, and *o*-dimethoxybenzene with association constants of $K = 2500$, 2680, 1560, and 1300 L/mol, respectively. For the larger *N*-(2-naphthyl)acetamide, only weak host−guest interaction was observed ($K = 15$ L/mol). In contrast, the binding constants for electron-deficient guests, such as *p*-dinitrobenzene and *p*-dicyanobenzene, were in the range of 30−80 L/mol and no complexation was observed with the nonaromatic 1,4-dimethoxycyclohexane. When analogous experiments with electron-rich guest molecules and the larger molecular square assembly **77a** were carried out, different results were obtained. While the smaller molecules 1,3,5-trimethoxybenzene, *p*-dimethoxybenzene, *m*-dimethoxybenzene, or *o*-dimethoxybenzene gave smaller equilibrium constants ($K = 750$, 330, 580, and 30 L/mol, respectively), the larger guest, *N*-(2-naphthyl)acetamide, showed a large binding constant of 1800 L/mol.[71] Similar findings were reported by Bilyk and Harding[35] for the inclusion of 1,4-dimethoxybenzene and 1,2-dimethoxybenzene into the electron-deficient cavity of the dinuclear zinc complex **5b**. X-ray structure analysis of the corresponding complexes definitely established guest inclusion.[35]

Three-dimensional assemblies also have great potential to become artificial hosts due to their cage-like structure and cavities, which are capable of interacting with guests more strongly than the typical two-dimensional polygons. While moving from two-dimensional assemblies to three-dimensional assemblies, the actual size of the guest molecules compared to the size of the host becomes much smaller although the actual size of the cavity is much bigger. This effect is mainly due to the smaller window size that the three-dimensional ensembles offer for guest transport in and out of the cavity. As shown by Raymond and co-workers, the adamantanoid-type M_4L_6 complex **180** was able to incorporate a tetramethylammonium ion into the cavity. Guest exchange reactions with tetraethyl- and tetrapropylammonium salts revealed guest selectivity. Tetraethylammonium ions showed a 200 times higher binding constant than the other two cations, suggesting an optimal interaction of host and guest. Encapsulation itself seems to be an entropy-driven process. The entropy gained from desolvation of the guest cation as well as from liberation of solvent molecules trapped inside the cavity makes up for the entropy lost by encapsulation of the cation, resulting in an overall positive entropy.[202,203]

The octahedral complexes described by Fujita and co-workers give an example for the inclusion of larger molecules. Indeed, assembly **211** is capable of forming an inclusion complex with four molecules of adamantane carboxylate.[220] X-ray structure analysis revealed an interesting inclusion geometry of **211**. While the hydrophobic adamantyl groups are located inside the

cavity, the hydrophilic carboxylate groups point outward. The bulky adamantyl groups apparently stabilize the complex in the solid state, which otherwise would contain large amounts of disordered solvent.[220] The encapsulation of four guest molecules by assembly **211** was also observed in aqueous solution and studied by NMR-monitored titration. This experiment also permitted the observation of a slow exchange between the free and complexed guest in solution. Another interesting effect was found: when different host-to-guest ratios were used, only two types of host frameworks were observed, a free assembly and a host−guest complex with a host-to-guest ratio of 1:4. The absence of intermediary complexes with lesser number of guests is quite remarkable, and it may be explained by the increased hydrophobicity of the cavity with each successively bound guest. The ability to encapsulate otherwise unstable species or conformations was shown by selective enclathration of two molecules of *cis*-azobenzene or *cis*-stilbene derivatives into the cavity of **211**.[231] The guest molecules were encapsulated through the "ship in a bottle" formation of a hydrophobically interacted dimer showing a topology similar to Rebek's hydrogen-bonded "tennis ball".[182a,245] No isomerization of the cis-conformation of the guest in the cavity was observed even after a few weeks under visible light at room temperature. The effect was attributed to the formation of a hydrophobic dimer within the cavity.

An example for extended functionality of molecular assemblies was provided by Hupp and co-workers by using photoluminescent rhenium corners.[129] The self-assembled molecular squares **90** were photoluminescent as a result of the metal to ligand charge transfer within the *fac*-[$Re(CO)_3Cl(4,4'$-bipyridine$)_2$] chromophore. The effect of the palladium corner was seen in a decrease of the MLCT exited state energy by stabilizing the π^*-acceptor orbital of the 4,4′-bipyridine ligand, resulting in a substantial red shift in the electronic absorption spectrum. An analogous red shift was also observed in the emission spectrum from the triplet MLCT exited state, while the emission intensity decreased by ca. 25-fold. This intensity loss was attributed mainly to an attenuation of the exited state lifetime (τ(corner) = 645 ns; τ(square) = 17 ns) caused by quenching of the Pd(II) fragments. Addition of tetraethylammonium perchlorate increased the emission intensity, presumably as a result of guest binding in the tetraionic host cavity, thus altering the quenching energetics.[129]

An interesting application of the neutral molecular squares **90** as nanocrystalline and/or amorphous thin films for size-selective guest transport was reported by Hupp and co-workers.[246] The advantage of these systems as microporous materials is due to the extended one-dimensional channel formations, observed in X-ray structural studies, as well as in the absence of channel-blocking counterions. While the compounds were readily dissolved in organic solvents, the thin films were strongly adherent and resisted dissolution under aqueous conditions. Electrochemical transportation experiments with $Ru(NH_3)_6^{3+}$ ($d \approx 5.5$ Å) and $Co(phen)_3^{2+}$ ($d \approx 13$ Å) revealed that for small molecules the materials were exceptionally porous while larger molecules were blocked. Furthermore, these sieving phenomena were characterized by sharp molecular size cutoffs predictable by model-determined cavity diameters and adjustable on the basis of simple synthetic variations. This makes these systems an alternative for organic[247] and metallopolymers[248] since the later systems depend on cross-linking and the nature of the counterions incorporated into the thin films.

VII. Summary and Outlook

During the past decade, the intense activity in the preparation of molecular polygons and polyhedra, whether by rational design or by mimicking natural structures, was initiated in many cases by purely aesthetic motivations. Today, the wealth of potential applications of self-assembled metallacyclic macromolecules has surpassed the strictly academic interest and is gradually becoming a new driving force in the field. The degrees of spatial and dimensional control of the encoded structural and electronic information as well as solubility, polarity, and charge distribution are well-established and have lead to new active fields of research in material science, inorganic clusters, transition-metal chemistry, and chemical topology. In this context, the development of fully functional molecular devices with desired optical, electronic, and magnetic properties is still a big challenge. Despite the fact that the synthetically viable path to the rational design of these macromolecules is still largely unknown, the attempts to prepare self-assembled structures that contain chemically functionalized sites, capable of performing useful tasks, such as guest encapsulation, catalysis, and others, are well underway.

In light of the remarkable reliance of complex biological machinery on self-assembled structures, it is tempting to conclude that, at least in the future, transition-metal-based self-organized nanostructures will prove to be capable of performing catalytic reactions, receptor and transportation functions on a molecular level, operations such as binary logic and memory storage, and building micro machines. To reach this ambitious goal, we must demonstrate even greater and better ability to rationally design nanoscopic structures of predefined and predictable shapes and sizes. Even after more than a decade of research, the synthetic challenges are still enormous and the preparation and unambiguous characterization of three-dimensional metallacyclic assemblies is still a significant challenge.

It was 1959 when Richard Feynman pointed out "I can hardly doubt that when we have some *control* of the arrangement of things on a small scale we will get an enormously greater range of possible properties that substances can have".[249] In these last days of the 20th century, we can only say that it will most likely be viewed as the time when science and engineering achieved synthetic and technical control over small molecules. The new century is poised to extend this control to the assemblies of nanoscopic and microscopic dimensions. This will provide chemists with an entirely new universe of synthetic

macromolecules that will not only profoundly influence science, life, and society but will be both intellectually fulfilling and exciting.

VIII. Acknowledgments

We thank the National Science Foundation and the National Institute of Health for support of our own work described in this review and the Alexander von Humboldt Foundation for a Feodor Lynen Postdoctoral Fellowship to Stefan Leininger and a University of Utah Graduate Fellowship to Bogdan Olenyuk.

IX. References

(1) Ball, P. *Designing the Molecular World Chemistry at the Frontier*; Princeton University: Princeton, NJ, 1994.
(2) Lehn, J.-M. *Supramolecular Chemistry: Concepts and Perspectives*; VCH: Weinheim, 1995.
(3) *Supramolecular Chemistry*; Balzani, V., DeCola, L., Eds.; Kluwer Academic: The Netherlands, 1992.
(4) *Frontiers in Supramolecular Chemistry*; Schneider, H., Dürr, H., Eds.; VCH: Weinheim, Germany, 1991.
(5) *Monographs in Supramolecular Chemistry*; Stoddard, J. F., Ed.; Royal Society of Chemistry: Cambridge, UK, **1989**, 1991, 1994−1996; Vols. 1−6.
(6) *Comprehensive Supramolecular Chemistry*; Lehn, J.-M., Chair Ed.; Atwood, J. L., Davis, J. E. D., MacNicol, D. D., Vögtle, F., Exec. Eds.; Pergamon: Oxford, UK, 1987−1996; Vols. 1−11.
(7) Robson, R.; Abrahams, B. F.; Batten, S. R.; Gable, R. W.; Hoskins, B. F.; Liu, J. *Supramolecular Architecture;* Bein, T., Ed.; In ACS Symposium Series 499; American Chemical Society: Washington, DC, 1992; Chapter 19. See also: Chambron, J.-C.; Dietrich-Buchecker, C.; Sauvage, J.-P. Transition Metals as Assembling and Templating Species. In *Comprehensive Supramolecular Chemistry;* Lehn, J.-M., Chair Ed.; Atwood, J. L., Davis, J. E. D.; MacNicol, D. D., Vögtle, F., Exec. Eds.; Pergamon Press: Oxford, 1996; Vol. 9, Chapter 2, p 43. Baxter, P. N. W. Metal Ion Directed Assembly of Complex Molecular Architectures and Nanostructures. *IBID.;* Vol. 9, Chapter 5, p 165.
(8) Constable, E. C. Polynuclear Transition Metal Helicates. In *Comprehensive Supramolecular Chemistry;* Lehn, J.-M., Chair Ed.; Atwood, J. L., Davis, J. E. D., MacNicol, D. D., Vögtle, F., Exec. Eds.; Pergamon Press: Oxford, 1996; Vol. 9, Chapter 6, p 213.
(9) Horne, R. W. *Virus Structure;* Academic Press: New York, 1974. Cann, A. J. *Principles of Molecular Virology*, 2nd ed.; Academic Press: New York, 1997.
(10) (a) Haeckel, E. *Challenger Monograph;* Georg Reimer: Berlin, 1887. (b) Haeckel, E. *Zoology* **1887**, *18*, 1803.
(11) Ercolani, G. *J. Phys. Chem. B* **1998**, *102*, 5699.
(12) Whitesides, G. M.; Mathias J. P.; Seto, C. T. *Science* **1991**, *254*, 1312.
(13) Tecilla, P.; Dixon, R. P.; Slobodkin, G.; Alavi, D. S.; Waldeck, D. H.; Hamilton, A. D. *J. Am. Chem. Soc.* **1990**, *112*, 9408.
(14) Stang, P. J.; Olenyuk, B. *Acc. Chem. Res.* **1997**, *30*, 502.
(15) Olenyuk, B.; Fechtenkötter, A.; Stang, P. J. *J. Chem. Soc., Dalton. Trans.* **1998**, 1707.
(16) (a) Fujita, M.; Ogura, K. *Coord. Chem. Rev.* **1996**, *148*, 249. (b) Fujita, M. *Chem Soc. Rev.* **1998**, *27*, 417.
(17) (a) Amabilino, D. B.; Stoddart, J. F. *Chem. Rev.* **1995**, *95*, 2725. (b) Amabilino, D. B.; Asakawa, M.; Ashton, P. R.; Ballardini, R.; Balzani, V.; Belohradský, M.; Credi, A.; Higuchi, M.; Raymo, F. M.; Shimizu, T.; Stoddart, J. F.; Venturi, M.; Yase, K. *New J. Chem.* **1998**, *22*, 959.
(18) Albrecht, M. *Chem. Soc. Rev.* **1998**, *27*, 281.
(19) Piguet, C.; Bernardinelli, G.; Hopfgartner, G. *Chem. Rev.* **1997**, *97*, 2005.
(20) Jones, C. J. *Chem. Soc. Rev.* **1998**, *27*, 289.
(21) Linton, B.; Hamilton, A. D. *Chem. Rev.* **1997**, *97*, 1669.
(22) (a) Caulder, D. L.; Raymond, K. N. *J. Chem. Soc., Dalton Trans.* **1999**, 1185. (b) Caulder, D. L.; Raymond, K. N. *Acc. Chem. Res.* **1999**, *32*, 975.
(23) MacGillivray, L. R.; Atwood, J. L. *Angew. Chem., Int Ed.* **1999**, *38*, 1018.
(24) Navarro, J. A. R.; Lippert, B. *Coord. Chem. Rev.* **1999**, *186*, 653.
(25) Saalfrank, R. W.; Bernt, I.; Uller, E.; Hampel, F. *Angew. Chem., Int. Ed. Engl.* **1997**, *36*, 2482.
(26) Saalfrank, R. W.; Burak, R.; Reihs, S.; Low, N.; Hampel, F.; Stachel, H. D.; Lentmaier, J.; Peters, K.; Peters, E. M.; von Schnering, H. G. *Angew. Chem., Int. Ed. Engl.* **1995**, *34*, 993.
(27) Baxter, P. N. W.; Lehn, J.-M.; Baum, G.; Fenske, D. *Chem. Eur. J.* **1999**, *5*, 102.
(28) Baxter, P. N. W.; Lehn, J.-M.; Kneisel, B. O.; Baum, G.; Fenske, D. *Chem. Eur. J.* **1999**, *5*, 113.
(29) Cotton, F. A.; Wilkinson, G. *Advanced Inorganic Chemistry*, 5th ed.; John Wiley and Sons: New York, 1988.
(30) Stricklen, P. M.; Volcko, E. J.; Verkade, J. G. *J. Am. Chem. Soc.* **1983**, *105*, 2494.
(31) (a) Maverick, A. W.; Buckingham, S. C.; Yao, Q.; Bradbury, J. R.; Stanley, G. G. *J. Am. Chem. Soc.* **1986**, *108*, 7430. (b) Maverick, A. W.; Klavetter, F. E. *Inorg. Chem.* **1984**, *23*, 4129.
(32) Hartshorn, C. M.; Steel, P. J. *Inorg. Chem.* **1996**, *35*, 6902.
(33) Duhme, A.-K.; Davies, S. C.; Hughes, D. L. *Inorg. Chem.* **1998**, *37*, 5380.
(34) Hannon, M. J.; Painting, C. L.; Errington, W. *J. Chem. Soc., Chem. Commun.* **1997**, 307.
(35) (a) Bilyk, A.; Harding, M. M. *J. Chem. Soc., Dalton. Trans.* **1994**, 77. (b) Houghton, M. A.; Bilyk, A.; Harding, M. M.; Turner, P.; Hambley, T. W. *J. Chem. Soc., Dalton. Trans.* **1997**, 2725.
(36) Caulder, D. L.; Raymond, K. N. *Angew. Chem., Int. Ed. Engl.* **1997**, *36*, 1440.
(37) (a) Fujita, M.; Nagao, S.; Iida, M.; Ogata, K.; Ogura, K. *J. Am. Chem. Soc.* **1993**, *115*, 1574. (b) Fujita, M.; Yazaki, J.; Kuramochi, T. Ogura, K. *Bull. Chem. Soc. Jpn.* **1993**, *66*, 1837.
(38) Fujita, M.; Yazaki, J.; Ogura, K. *J. Am. Chem. Soc.* **1990**, *112*, 5645.
(39) (a) Fujita, M.; Ibukuro, F.; Hagihara, H. Ogura, K. *Nature* **1994**, *367*, 720. (b) Fujita, M. *Acc. Chem. Res.* **1999**, *32*, 53.
(40) Fujita, M.; Ibukuro, F.; Seki, H.; Kamo, O.; Imanari, M.; Ogura, K. *J. Am. Chem. Soc.* **1996**, *118*, 899.
(41) (a) Fujita, M.; Ibukuro, F.; Yamaguchi, K.; Ogura, K. *J. Am. Chem. Soc.* **1995**, *117*, 4175. (b) Fujita, M.; Aoyagi, M.; Ibukuro, F.; Ogura, K.; Yamaguchi, K. *J. Am. Chem. Soc.* **1998**, *120*, 611.
(42) Fujita, M. *J. Synth. Org. Chem. Jpn.* **1996**, *54*, 953.
(43) Schneider, R.; Hosseini, M. W.; Planeix, J.-M.; De Cian, A. D.; Fischer, J. *J. Chem. Soc., Chem. Commun.* **1998**, 1625.
(44) Jeong, K.-S.; Cho, Y. L.; Song, J. U.; Chang, H.-Y.; Choi, M.-G. *J. Am. Chem. Soc.* **1998**, *120*, 10982.
(45) Constable, E. C.; Schofield, E. *J. Chem. Soc., Chem. Commun.* **1998**, 403.
(46) Philp, D.; Stoddart, J. F. *Angew. Chem., Int. Ed. Engl.* **1996**, *35*, 1154.
(47) Lagunas, M.-C.; Gossage, R. A.; Smeets, W. J. J.; Spek, A. L.; van Koten, G. *Eur. J. Inorg. Chem.* **1998**, 163.
(48) Bondi, A. *J. Phys. Chem.* **1964**, *68*, 441
(49) Constable, A.; McDonald, W. S.; Shaw, B. L. *J. Chem. Soc., Dalton. Trans.* **1979**, 496.
(50) Constable, A.; McDonald, W. S.; Shaw, B. L. *J. Chem. Soc., Dalton. Trans.* **1979**, 1109.
(51) Fujita, M.; Aoyagi, M.; Ogura, K. *Inorg. Chim. Acta* **1996**, *246*, 53.
(52) Habicher, T.; Nierengarten, J.-F.; Gramlich, V.; Diederich, F. *Angew. Chem., Int. Ed. Engl.* **1998**, *37*, 1916.
(53) Constable, A.; McDonald, W. S.; Shaw, B. L. *J. Chem. Soc., Dalton Trans.* **1979**, 496.
(54) (a) Varvoglis, A. *The Organic Chemistry of Polycoordinated Iodine*; VCH: Weinheim, Germany, 1992. (b) Varvoglis, A. *Hypervalent Iodine in Organic Synthesis*; Academic: New York, 1997. (c) Varvoglis, A. *Tetrahedron* **1997**, *53*, 1179.
(55) Stang, P. J.; Zhdankin, V. V. *Chem. Rev.* **1996**, *96*, 1123.
(56) Stang, P. J.; Olenyuk, B.; Chen, K. *Synthesis* **1995**, 937.
(57) Stang, P. J.; Chen, K. *J. Am. Chem. Soc.* **1995**, *117*, 1667.
(58) Stang, P. J.; Chen, K.; Arif, A. M. *J. Am. Chem. Soc.* **1995**, *117*, 8793.
(59) Olenyuk, B.; Whiteford, J. A.; Stang, P. J. *J. Am. Chem. Soc.* **1996**, *118*, 8221.
(60) Hall, J.; Loeb, S. J.; Shimizu, G. K. H.; Yap, G. P. A. *Angew. Chem., Int. Ed. Engl.* **1998**, *37*, 121.
(61) Fujita, M.; Sasaki, O.; Mitsuhashi, T.; Fujita, T.; Yazaki, J.; Yamaguchi, K.; Ogura, K. *J. Chem. Soc., Chem. Commun.* **1996**, 1535.
(62) Lee, S. B.; Hwang, S. G.; Chung, D. S.; Yun, H.; Hong, J.-I. *Tetrahedron Lett.* **1998**, *39*, 873.
(63) Schnebeck, R.-D.; Randaccio, L.; Zangrando, E.; Lippert, B. *Angew. Chem., Int. Ed. Engl.* **1998**, *37*, 119.
(64) Schnebeck, R.-D.; Freisinger, E.; Lippert, B. *Angew. Chem., Int. Ed.* **1999**, *38*, 168.
(65) Lai, S.-W.; Chan, M. C.-W.; Peng, S.-M.; Che, C.-M. *Angew. Chem., Int. Ed.* **1999**, *38*, 669.
(66) Baker, A. T.; Crass, J. K.; Maniska, M.; Craig, D. C. *Inorg. Chim. Acta* **1995**, *230*, 225.
(67) Romero, F. M.; Ziessel, R.; Dupont-Gervais, A.; van Dorsselaer, A. *J. Chem. Soc., Chem. Commun.* **1996**, 551.
(68) Leize, E.; van Dorsselaer, A.; Krämer, R.; Lehn, J.-M. *J. Chem. Soc., Chem. Commun.* **1993**, 990.
(69) Hopfgartner, G.; Piquet, C.; Henion, J. D. *J. Am. Soc. Mass Spectrom.* **1994**, *5*, 748.
(70) Cotton, F. A.; Daniels, L. M.; Lin, C.; Murillo, C. A. *J. Am. Chem. Soc.* **1999**, *121*, 4538.
(71) Fujita, M.; Yazaki, J.; Ogura, K. *Tetrahedron Lett.* **1991**, *32*, 5589.

(72) Stang, P. J.; Cao, D. H. *J. Am. Chem. Soc.* **1994**, *116*, 4981.
(73) Stang, P. J.; Cao, D. H.; Saito, S.; Arif, A. M. *J. Am. Chem. Soc.* **1995**, *117*, 6273.
(74) Stang, P. J.; Olenyuk, B. *Angew. Chem., Int. Ed. Engl.* **1996**, *35*, 732.
(75) Brown, J. M.; Perez-Torrente, J. J.; Alcock, N. W. *Organometallics* **1995**, *14*, 1195.
(76) Lippert, B. *Inorg. Chem.* **1981**, *20*, 4326.
(77) (a) Rauter, H.; Hillgeris, E. C.; Lippert, B. *J. Chem. Soc., Chem. Commun.* **1992**, 1385. (b) Rauter, H.; Hillgeris, E. C.; Erxleben, A.; Lippert, B. *J. Am. Chem. Soc.* **1994**, *116*, 616. (c) Navarro, J. A. R.; Janik, M. B. L.; Freisinger, E.; Lippert, B. *Inorg. Chem.* **1999**, *38*, 426.
(78) Slone, R. V.; Hupp, J. T.; Stern, C. L.; Albrecht-Schmitt, T. E. *Inorg. Chem.* **1996**, *35*, 4096.
(79) Slone, R. V.; Benkstein, K. D.; Bélanger, S.; Hupp, J. T.; Guzei, I. A.; Rheingold, A. L. *Coord. Chem. Rev.* **1998**, *171*, 221.
(80) Yan, H.; Süss-Fink, G.; Neels, A.; Stoeckli-Evans, H. *J. Chem. Soc., Dalton Trans.* **1997**, 4345.
(81) Benkstein, K. D.; Hupp, J. T.; Stern, C. L. *Inorg. Chem.* **1998**, *37*, 5404.
(82) Woessner, S. M.; Helms, J. B.; Shen, Y.; Sullivan, B. P. *Inorg. Chem.* **1998**, *37*, 5406.
(83) Benkstein, K. D.; Hupp, J. T.; Stern, C. L. *J. Am. Chem. Soc.* **1998**, *120*, 12982.
(84) Vogler, A.; Kisslinger, J. *Inorg. Chim. Acta* **1986**, *115*, 193.
(85) Youinou, M.-T.; Rahmouri, N.; Fischer, J.; Osborn, J. A. *Angew. Chem., Int. Ed. Engl.* **1992**, *31*, 733.
(86) Kajiwara, T.; Ito, T. *J. Chem. Soc., Chem. Commun.* **1994**, 1773.
(87) Stang, P. J.; Olenyuk, B.; Fan, J.; Arif, A. M. *Organometallics* **1996**, *15*, 904.
(88) Pedersen, C. J. *J. Am. Chem. Soc.* **1967**, *89*, 7017.
(89) Pedersen, C. J. *J. Am. Chem. Soc.* **1970**, *92*, 391.
(90) Pedersen, C. J.; Frensdorff, K. K. *Angew. Chem., Int. Ed. Engl.* **1972**, *11*, 16.
(91) *Crown Ethers and Analogues;* Patai, S.; Rappoport, Z., Eds, Wiley: New York, 1989.
(92) *Progress in Macrocyclic Chemistry*; Izatt, R. M.; Christensen, J. J., Eds, Wiley-Interscience: New York, 1979; 1981, 1987.
(93) *Crown Compounds*; Hiraoka, M., Ed.; Elsevier: Amsterdam, 1982.
(94) *Calixarenes: A Versatile Class of Macrocyclic Compounds*; Vicens, J., Bohmer, V., Eds.; Kluwer Academic: The Netherlands, 1990.
(95) Gutsche, C. D. *Calixarenes;* The Royal Society of Chemistry: London, 1989.
(96) Cram, D. J.; Cram, J. M. *Container Molecules and Their Guests*; The Royal Society of Chemistry: Cambridge, 1994.
(97) *Inclusion Phenomena and Molecular Recognition*; Atwood, J. L., Ed.; Plenum: New York, 1990.
(98) *Host−Guest Complex Chemistry: Synthesis, Structure, Applications*; Vögtle, F., Weber, E., Eds.; Springer-Verlag: Berlin, 1985.
(99) Powell, J.; Lough, A.; Wang, F. *Organometallics* **1992**, *11*, 2289.
(100) Powell, J.; Gregg, M. R.; Meindl, P. E. *Organometallics* **1989**, *8*, 2942.
(101) Powell, J.; Kuksis, A.; May, C. J.; Meindl, P. E.; Smith, S. J. *Organometallics* **1989**, *8*, 2933.
(102) Powell, J.; Gregg, M. R.; Kuksis, A.; May, C. J.; Smith, S. J. *Organometallics* **1989**, *8*, 2918.
(103) Powell, J.; Gregg, M. R.; Kuksis, A.; Meindl, P. E. *J. Am. Chem. Soc.* **1983**, *105*, 1064.
(104) Cameron, B. R.; van Veggel, F. C. J. M.; Reinhoudt, D. N. *J. Org. Chem.* **1995**, *60*, 2802.
(105) Gray, G. M. *Comments Inorg. Chem.* **1995**, *17*, 95.
(106) Gray, G. M.; Duffey, C. H. *Organometallics* **1995**, *14*, 245.
(107) Gray, G. M.; Varshney, A.; Duffey, C. H. *Organometallics* **1995**, *14*, 238.
(108) Gray, G. M.; Duffey, C. H. *Organometallics* **1994**, *13*, 1542.
(109) Varshney, A.; Gray, G. M. *Inorg. Chem.* **1991**, *30*, 1748.
(110) Varshney, A.; Webster, M. L.; Gray, G. M. *Inorg. Chem.* **1992**, *31*, 2580.
(111) Stang, P. J.; Cao, D. H.; Chen, K.; Gray, G. M.; Muddiman, D. C.; Smith, R. D. *J. Am. Chem. Soc.* **1997**, *119*, 5163.
(112) Cheng, X. H.; Gao, Q. Y.; Smith, R. D.; Simanek, E. E.; Mammen, M.; Whitesides, G. M. *Rapid Commun. Mass Spectrom.* **1995**, *9*, 312.
(113) Alcock, N. W.; Brown, J. M.; Jeffery, J. C. *J. Chem. Soc., Dalton Trans.* **1976**, 583.
(114) Alcock, N. W.; Brown, J. M.; Jeffery, J. C. *J. Chem. Soc., Chem. Commun.* **1974,** 829.
(115) Stang, P. J.; Whiteford, J. A. *Organometallics* **1994**, *13*, 3776.
(116) Whiteford, J. A.; Lu, C. V.; Stang, P. J. *J. Am. Chem. Soc.* **1997**, *119*, 2524.
(117) Whiteford, J. A.; Rachlin, E. M.; Stang, P. J. *Angew. Chem., Int. Ed. Engl.* **1996**, *35*, 2524.
(118) Back, S.; Pritzkow, H.; Lang, H. *Organometallics* **1998**, *17*, 41.
(119) Kohler, K.; Silverio, S. J.; Hyla-Kryspin, I.; Gleiter, R.; Zsolnai, L.; Driess, A.; Huttner, G. Lang, H. *Organometallics* **1997**, *16*, 4970.
(120) Janssen, M. D.; Herres, M.; Zsolnai, L.; Spek, A. L.; Grove, D. M.; Lang, H.; van Koten, G. *Inorg. Chem.* **1996**, *35*, 2476.
(121) (a) Lang, H.; Weinmann, M. *Synlett* **1996**, 1. (b) Lang, H.; Blau, S.; Pritzkow, H.; Zsolnai, L. *Organometallics* **1995**, *14*, 1850.
(122) Whiteford, J. A.; Stang, P. J.; Huang, S. D. *Inorg. Chem.* **1998**, *37*, 5595.
(123) Manna, J.; John, K. D.; Hopkins, M. D. *Adv. Organomet. Chem.* **1995**, *38*, 79 and references therein.
(124) Berenguer, J. R.; Forniés, J.; Lalinde, E.; Martínez, F. *J. Organomet. Chem.* **1994**, *470*, C15.
(125) Wisner, J. M.; Bartczak, T. J.; Ibers, J. A.; Low, J. J.; Goddard, W. A., III *J. Am. Chem. Soc.* **1986**, *108*, 347.
(126) Müller, C.; Whiteford, J. A.; Stang, P. J. *J. Am. Chem. Soc.* **1998**, *120*, 9827.
(127) Dixit, S. C.; Sharan, R.; Kapoor, R. N. *Inorg. Chim. Acta* **1989**, *158*, 109.
(128) Stang, P. J.; Persky, N. E. *J. Chem. Soc., Chem. Commun.* **1997**, 77.
(129) Slone, R. V.; Yoon, D. I.; Calhoun, R. M.; Hupp, J. T. *J. Am. Chem. Soc.* **1995**, *117*, 11813.
(130) Manna, J.; Whiteford, J. A.; Stang, P. J.; Muddiman, D. C.; Smith, R. D. *J. Am. Chem. Soc.* **1996**, *118*, 8731.
(131) Manna, J.; Kuehl, C. J.; Whiteford, J. A.; Stang, P. J. *Organometallics* **1997**, *16*, 1897.
(132) Manna, J.; Kuehl, C. J.; Whiteford, J. A.; Stang, P. J.; Muddiman, D. C.; Hofstadler, S. A.; Smith, R. D. *J. Am. Chem. Soc.* **1997**, *119*, 11611.
(133) Chi, X.; Guerin, A. J.; Haykock, R. A.; Hunter, C. A.; Sarson, L. D. *J. Chem. Soc., Chem. Commun.* **1995**, 2563.
(134) Dinur, U.; Hagler, A. T. Approaches to Empirical Force Fields. In *Review of Computational Chemistry*; Lipkowitz, K. B., Boyd, D. B., Eds.; VCH: New York, 1991; Vol. 2, Chapter 4.
(135) Maple, J. R.; Thacher, T. S.; Dinur, U.; Hagler, A. T. *Chem. Des. Autom. News* **1990**, *5*, 5.
(136) Ermer, O. *Struct. Bonding* **1976**, *27*, 161.
(137) Vorm, O.; Roepstorff, P.; Mann, M. *Anal. Chem.* **1994**, *66*, 3281.
(138) Deisenhofer, J.; Epp, O.; Miki, K.; Huber, R.; Michel, H. *J. Mol. Biol.* **1984**, *180*, 385.
(139) Zuber, H.; Brunisholz, R. A. In *Chlorophylls*; Scheer, H., Ed.; CRC Press: Boca Raton, FL, 1991.
(140) Webber, S. E. *Chem. Rev.* **1990**, *90*, 1469.
(141) Wasielewski, M. R. *Chem. Rev.* **1992**, *92*, 435.
(142) Gosztola, D.; Niemczyk, M. P.; Wasielewski, M. R. *J. Am. Chem. Soc.* **1998**, *120*, 5118.
(143) Wagner, R. W.; Lindsey, J. S.; Seth, J.; Palaniappan, V.; Bocian, D. F. *J. Am. Chem. Soc.* **1996**, *118*, 3996.
(144) (a) Van Patten, P. G.; Shreve, A. P.; Lindsey, J. S.; Donohoe, R. J. *J. Phys. Chem. B* **1998**, *102*, 4209. (b) Gust, D.; Moore, T. A.; Moore, A. L. *Acc. Chem. Res.* **1993**, *26*, 198. (c) Harriman, A.; Sauvage, J.-P. *Chem. Soc. Rev.* **1996**, *25*, 41.
(145) De Silva, A. P.; Gunaratne, H. Q. N.; Gunnlaugsson, T.; Huxley, A. J. M.; McCoy, C. P.; Rademacher, J. T.; Rice, T. E. *Chem. Rev.* **1997**, *97*, 1515.
(146) Wagner, R. W.; Lindsey, J. S. *J. Am. Chem. Soc.* **1994**, *116*, 9759.
(147) (a) Sousa, C.; Maziere, C.; Melo, T. S. E.; Vincent-Fiquet, O.; Rogez, J. C.; Santus, R.; Maziere, J. C. *Cancer Lett.* **1998**, *128*, 177. (b) deVree, W. J. A.; Essers, M. C.; Sluiter, W. *Cancer Res.* **1997**, *57*, 2555. (c) Jasat, A.; Dolphin, D. *Chem. Rev.* **1997**, *97*, 2267.
(148) (a) Taylor, P. N.; Wylie, A. P.; Huuskonen, J.; Anderson, H. L. *Angew. Chem., Int. Ed. Engl.* **1998**, *37*, 986. (b) Nishino, N.; Wagner, R. W.; Lindsey, J. S. *J. Org. Chem.* **1996**, *61*, 7534. (c) Wagner, R. W.; Johnson, T. E.; Lindsey, J. S. *J. Am. Chem. Soc.* **1996**, *118*, 11166. (d) Osuka, A.; Tanabe, N.; Zhang, R. P.; Maruyama, K. *Chem. Lett.* **1993**, 1505. (e) Hammel, D.; Erk, P.; Schuler, B.; Heinze, J.; Müllen, K. *Adv. Mater.* **1992**, *4*, 737.
(149) (a) Vidal-Ferran, A.; Clyde-Watson, Z.; Bampos, N.; Sanders, J. K. M. *J. Org. Chem.* **1997**, *62*, 240. (b) Anderson, S.; Anderson, H. L.; Sanders, J. K. M. *J. Chem. Soc., Perkin Trans. 1* **1995**, 2255.
(150) (a) Drain, C. M.; Lehn, J. M. *J. Chem. Soc., Chem. Commun.* **1994**, 2313. (b) Wagner, R. W.; Seth J.; Yang, S. I.; Kim, D.; Bocian, D. F.; Holten, D.; Lindsey, J. S. *J. Org. Chem.* **1998**, *63*, 5042. (c) Slone, R. V.; Hupp, J. T. *Inorg. Chem.* **1997**, *36*, 5422.
(151) Xu, Z.; Moore, J. S. *Acta Polym.* **1994**, *45*, 83.
(152) Drain, C. M.; Nifiatis, F.; Vasenko, A.; Batteas, J. D. *Angew. Chem., Int. Ed. Engl.* **1998**, *37*, 2344.
(153) Yuan, H.; Thomas, L.; Woo, L. K. *Inorg. Chem.* **1996**, *35*, 2808.
(154) Drain, C. M.; Russell, K. C.; Lehn, J.-M. *J. Chem. Soc., Chem. Commun.* **1996**, 337.
(155) Harriman, A.; Odobel, F.; Sauvage, J.-P. *J. Am. Chem. Soc.* **1995**, *117*, 9461.
(156) Gouterman, M. In *The Porphyrins;* Dolphin, D., Ed.; Academic: New York, 1978; Vol. 3 (Physical Chemistry, Part A).
(157) Drain, C. M.; Russel, K. C.; Lehn, J.-M. *Chem. Commun.* **1996**, 337.
(158) Hunter, C. A.; Hyde, R. K. *Angew. Chem., Int. Ed. Engl.* **1996**, *35*, 1936.
(159) Fleischer, E. B.; Shachter, A. M. *Inorg. Chem.* **1991**, *30*, 3763.

(160) Stang, P. J.; Fan, J.; Olenyuk, B. *J. Chem. Soc., Chem. Commun.* **1997**, 1453.
(161) Fan, J.; Whiteford, J. A.; Olenyuk, B.; Levin, M. D.; Stang, P. J.; Fleischer, E. B. *J. Am. Chem. Soc.* **1999**, *121*, 2741.
(162) Fuss, M.; Siehl, H.-U.; Olenyuk, B.; Stang, P. *Organometallics* **1999**, *18*, 758.
(163) Hasenknopf, B.; Lehn, J.-M.; Baum, G.; Kneisel, B. O.; Fenske, D. *Angew. Chem., Int. Ed. Engl.* **1996**, *35*, 1838.
(164) Hasenknopf, B.; Lehn, J.-M.; Boumediene, N.; Dupont-Gervais, A.; van Dorsselaer, A.; Kneisel, B.; Fenske, D. *J. Am. Chem. Soc.* **1997**, *119*, 10956
(165) Stang, P. J.; Persky, N.; Manna, J. *J. Am. Chem. Soc.* **1997**, *119*, 4777.
(166) Leininger, S.; Schmitz, M.; Persky, N. E.; Fan, J. Unpublished results.
(167) Tzeng, B. C.; Lo, W. C.; Che, C. M.; Peng, S. M. *J. Chem. Soc., Chem. Commun.* **1996**, 181.
(168) Lai, S. W.; Cheung, K. K.; Chan, M. C.; Che, C. M. *Angew. Chem., Int. Ed. Engl.* **1998**, *37*, 182.
(169) Mamula, O.; von Zelewsky, A.; Bernardinelli, G. *Angew. Chem., Int. Ed. Engl.* **1998**, *37*, 289.
(170) Piquet, C.; Bernardinelli, G.; Hopfgartner, G. *Chem. Rev.* **1997**, *97*, 2005.
(171) (a) Libman, J.; Tor, Y.; Shanzer, A. *J. Am. Chem. Soc.* **1987**, *109*, 5880. (b) Albrecht, M. *Synlett* **1996**, 565. (c) Woods, C. R.; Benaglia, M.; Cozzi, F.; Siegel, J. S. *Angew. Chem., Int. Ed. Engl.* **1996**, *35*, 1830.
(172) (a) Hayoz, P.; Von Zelewsky, A.; Stoeckli-Evans, H. *J. Am. Chem. Soc.* **1993**, *115*, 5111. (b) Muerner, H.; Belser, P.; Zelewsky, A. *J. Am. Chem. Soc.* **1996**, *118*, 7989.
(173) Matsumoto, N.; Motoda, Y.; Matsuo, T.; Nakashima, T.; Re, N.; Dahan, F.; Tuchagues, J.-P. *Inorg. Chem.* **1999**, *38*, 1165.
(174) See, for example: Kepert, D. L. *Comprehensive Inorganic Chemistry*; Pergamon Press: Oxford, 1973; Vol. 4, pp 607−620.
(175) Mingos, D. M. P.; Yau, J.; Menzer, S.; Williams, D. J. *Angew. Chem., Int. Ed. Engl.* **1995**, *34*, 1894.
(176) Grossmann, B.; Heinze, J.; Herdtweck, E.; Köhler, F. H.; Nöth, H.; Schwenk, H.; Spiegler, M.; Wachter, W.; Weber, B. *Angew. Chem., Int. Ed. Engl.* **1997**, *36*, 387.
(177) Jones, P. L.; Byrom, K. J.; Jeffery, J. C.; McCleverty, J. A. Ward, M. D. *J. Chem. Soc., Chem. Commun.* **1997**, 1361.
(178) (a) Eaton, P. E.; Cole, F. W. *J. Am. Chem. Soc.* **1964**, *86*, 3157. Fleischer, E. B. *J. Am. Chem. Soc.* **1964**, *86*, 3889.
(179) (a) Prelog, V.; Seiwerth, R. *Chem. Ber.* **1941**, *74*, 1769. (b) Stetter, H.; Bänder, O.-E.; Neumann, W. *Chem. Ber.* **1956**, *89*, 1922. (c) Fort, R.; Schleyer, P. v. R. *Chem. Rev.* **1964**, *64*, 277.
(180) (a) Paquette, L. A.; Ternansky, R. J.; Balogh, D. W. *J. Am. Chem. Soc.* **1982**, *104*, 4502. (b) Ternansky, R. J.; Balogh, D. W.; Paquette, L. A. *J. Am. Chem. Soc.* **1982**, *104*, 4503.
(181) (a) Kroto, H. W.; Heath, J. R.; O'Brien, S. C. *Nature* **1985**, *318*, 162. (b) Krätschmer, W.; Lamb, L. O.; Fostiropoulos, K.; Huffman, D. R. *Nature* **1990**, *347*, 354. (c) Curl, R. F.; Smalley, R. E. *Sci. Am.* **1991**, *265*, 54. (d) Hirsch, A.; Lamparth, I.; Karfunkel, H. R. *Recent Advances in the Chemistry and Physics of Fullerene and Related Materials*; Kadish, K. M., Ruoff, R. S., Eds.; The Electrochemical Society; Pennington, NJ, 1994; Vol. 1, p 734. (e) Lamparth, I.; Herzog, A.; Hirsch, A. *Tetrahedron* **1996**, *52*, 5065.
(182) (a) Rebek, J., Jr. *Chem. Soc. Rev.* **1996**, *25*, 255. (b) Rebek, J., Jr. *Pure Appl. Chem.* **1996**, *68*, 1261. (c) Conn, M. M.; Rebek, J., Jr. *Chem. Rev.* **1997**, *97*, 1647.
(183) For bacterial cell surface assemblies, see: Sleyter, U. B.; Sára, M. *Tibtech.* **1997**, *15*, 20 and references therein.
(184) For virus capside assemblies, see: Klug, A. *Angew. Chem., Int. Ed. Engl.* **1983**, *22*, 565.
(185) Dietrich, B.; Lehn, J.-M.; Sauvage, J. P. *Tetrahedron Lett.* **1969**, *34*, 2885, 2889.
(186) Cram, D. J.; Truesdale, E. A. *J. Am. Chem. Soc.* **1973**, *95*, 5825.
(187) Vögtle, F.; Seel, S.; Windscheif, P.-M. In *Comprehensive Supramolecular Chemistry*; Atwood, J. L., Davies, J. E. D., MacNicol, D. D., Vögtle, F., Eds.; Elesevier: New York, 1996; Vol. 2, Cyclophane Hosts: Endoacidic, Endobasic, and Endolipophilic Large Cavities; pp 211−265.
(188) Fujita, M.; Ogura, K.; Nagao, S. *J. Am. Chem. Soc.* **1995**, *117*, 1649.
(189) Anderson, S.; Anderson, H. L.; Sanders, J. K. M. *Acc. Chem. Res.* **1993**, *26*, 469.
(190) (a) Rebek, J., Jr.; Askew, B.; Killoran, M.; Nemeth, D.; Lin, F.-T. *J. Am. Chem. Soc.* **1987**, *109*, 2426. (b) Sijbesma, R. P.; Nolte, R. J. M. *J. Am. Chem. Soc.* **1991**, *113*, 6695. (c) Conn, M. M.; Deslongchamps, G.; De Mendoza, J.; Rebek, J., Jr. *J. Am. Chem. Soc.* **1993**, *115*, 3548.
(191) (a) Hamilton, A. D.; Van Engen, D. *J. Am. Chem. Soc.* **1987**, *109*, 5035. (b) Güther, R.; Nieger, M.; Vögtle, F. *Angew. Chem., Int. Ed. Engl.* **1993**, *32*, 601.
(192) Jacopozzi, P.; Dalcanale, E. *Angew. Chem., Int. Ed. Engl.* **1997**, *36*, 613.
(193) Baxter, P. N. W.; Lehn, J.-M.; DeCian, A.; Fischer, J. *Angew. Chem., Int. Ed. Engl.* **1993**, *32*, 69.
(194) Holden, A. *Shapes, Space, and Symmetry;* Columbia University Press: New York, 1971.
(195) Schmidtchen, F. P.; Müller, G. *J. Chem. Soc., Chem. Commun.* **1984**, 1115.
(196) Graf, E.; Lehn, J.-M. *J. Am. Chem. Soc.* **1975**, *97*, 5022.
(197) Saalfrank, R. W.; Stark, A.; Peters, K.; von Schnering, H. G. *Angew. Chem., Int. Ed. Engl.* **1988**, *27*, 851.
(198) Saalfrank, R. W.; Stark, A.; Bremer, M.; Hummel, H.-U. *Angew. Chem., Int. Ed. Engl.* **1990**, *29*, 311.
(199) Saalfrank, R. W.; Burak, R.; Breit, A.; Stalke, D.; Herbst-Irmer, R.; Daub, J.; Porsch, M.; Bill, E.; Müther, M.; Trautwein. A. X. *Angew. Chem., Int. Ed. Engl.* **1994**, *33*, 1621.
(200) Saalfrank, R. W.; Hörner, B.; Stalke, D.; Salbeck, J. *Angew. Chem., Int. Ed. Engl.* **1993**, *32*, 1179.
(201) (a) Beissel, T.; Powers, R. E.; Raymond, K. N. *Angew. Chem., Int. Ed. Engl.* **1996**, *35*, 1084. (b) Beissel, T.; Powers, R. E.; Parac, T. N.; Raymond, K. N. *J. Am. Chem. Soc.* **1999**, *121*, 4200.
(202) Caulder, D. L.; Powers, R. E.; Parac, T. N.; Raymond, K. N. *Angew. Chem., Int. Ed. Engl.* **1998**, *37*, 1840.
(203) Parac, T. N.; Caulder, D. L.; Raymond, K. N. *J. Am. Chem. Soc.* **1998**, *120*, 8003.
(204) Fleming, J. S.; Mann, K. L. V.; Carrez, C.-A.; Psillakis, E.; Jeffrey, J. C.; McCleverty, J. A.; Ward, M. D. *Angew. Chem., Int. Ed. Engl.* **1998**, *37*, 1279.
(205) Enemark, E. J.; Stack, T. D. P. *Angew. Chem., Int. Ed. Engl.* **1998**, *37*, 932.
(206) Mann, S.; Huttner, G.; Zsolnai, L.; Heinze, K. *Angew. Chem., Int. Ed. Engl.* **1996**, *35*, 2808.
(207) Bruckner, C.; Powers, R. E.; Raymond, K. N. *Angew. Chem., Int. Ed. Engl.* **1998**, *37*, 1837.
(208) Amoroso, A. J.; Jeffery, J. C.; Jones, P. L.; McCleverty, J. A.; Thornton, P.; Ward, M. D. *Angew. Chem., Int. Ed. Engl.* **1995**, *34*, 1443.
(209) (a) Murakami, Y.; Kikuchi, J.; Hirayama, T. *Chem. Lett.* **1987**, 161. (b) Wettling, T.; Schneider, J.; Wagner, O.; Kreiter, G.; Regitz, M. *Angew. Chem., Int. Ed. Engl.* **1989**, *28*, 1013. (c) Barron, A. R. *Chem. Soc. Rev.* **1993**, 93.
(210) Roche, S.; Haslam, C.; Adams, H.; Heath, S. L.; Thomas, J. A. *J. Chem. Soc., Chem. Commun.* **1998**, 1681.
(211) Herren, F.; Fischer, P.; Ludi, A.; Halg, W. *Inorg. Chem.* **1980**, *19*, 956.
(212) Sharpe, A. G. *The Chemistry of Cyano Complexes of the Transition Metals*; Academic Press: London, 1976.
(213) Fehlhammer, W. P.; Fritz, M. *Chem. Rev.* **1993**, *93*, 1243.
(214) Dunbar, K. R.; Heitz, R. A. *Prog. Inorg. Chem.* **1997**, *45*, 283.
(215) Davis, J. T.; Tirumala, S. K.; Marlow, A. L. *J. Am. Chem. Soc.* **1997**, *119*, 5271.
(216) (a) Klausmeyer, K. K.; Rauchfuss, T. B.; Wilson, S. R. *Angew. Chem., Int. Ed. Engl.* **1998**, *37*, 1694. (b) Contakes, S. M.; Klausmeyer, K. K.; Milberg, R. M.; Wilson, S. R.; Rauchfuss, T. B. *Organometallics* **1998**, *17*, 3633.
(217) Klausmeyer, K. K.; Wilson, S. R.; Rauchfuss, T. B. *J. Am. Chem. Soc.* **1999**, *121*, 2705.
(218) Heinrich, J. L.; Berseth, P. A.; Long, J. R. *J. Chem. Soc., Chem. Commun.* **1998**, 1231.
(219) Hartshorn, C. M.; Steel, P. J. *J. Chem. Soc., Chem. Commun.* **1997**, 541.
(220) Fujita, M.; Oguro, D.; Miyazawa, M.; Oka, H.; Yamaguchi, K.; Ogura, K. *Nature* **1995**, *378*, 469.
(221) Ibukuro, F.; Kusukawa, T.; Fujita, M. *J. Am. Chem. Soc.* **1998**, *120*, 8561.
(222) Kusukawa, T.; Fujita, M. *Angew. Chem., Int. Ed. Engl.* **1998**, *37*, 3142.
(223) Kusukawa, T.; Fujita, M. *J. Am. Chem. Soc.* **1999**, *121*, 1397.
(224) Stang, P. J.; Olenyuk, B.; Muddiman, D. C.; Smith, R. D. *Organometallics* **1997**, *16*, 3094.
(225) Trikha, J.; Theil, E.; Alleweil, N. M. *J. Mol. Biol.* **1995**, *248*, 949.
(226) Arnold, E.; Rossmann, M. G. *Acta Crystallogr., Sect. A* **1988**, *44*, 270.
(227) Olenyuk, B.; Whiteford, J. A.; Fechtenkötter, A.; Stang, P. J. *Nature*, **1999**, *398*, 796.
(228) Stejskal, E. O., Tanner, J. E. *J. Chem. Phys.* **1965**, *42*, 288.
(229) Hansen, J. P., McDonald, I. R. *Theory of Simple Liquids*; Academic Press: London, 1976.
(230) Abrahams, B. F.; Egan, S. J.; Robson, R. *J. Am. Chem. Soc.* **1999**, *121*, 3535.
(231) Fujita, M.; Yu, S.-Y.; Kusukawa, T.; Funaki, H.; Ogura, K.; Yamaguchi, K. *Angew. Chem., Int. Ed. Engl.* **1998**, *37*, 2082.
(232) McMorran, D. A.; Steel, P. J. *Angew. Chem., Int. Ed. Engl.* **1998**, *37*, 3295.
(233) Saalfrank, R. W.; Dresel, A.; Seitz, V.; Trummer, S.; Hampel, F.; Teichert, M.; Stalke, D.; Stadler, C.; Daub, J.; Schunemann, V.; Trautwein A. X. *Chem. Eur. J.* **1997**, *3*, 2058.
(234) Fyfe, M. C. T.; Glink, P. T.; Menzer, S.; Stoddart, J. F.; White, A. J. P.; Williams D. J. *Angew. Chem., Int. Ed. Engl.* **1997**, *36*, 2068.
(235) Takeda, N.; Umemoto, K.; Yamaguchi, K.; Fujita, M. *Nature* **1999**, *398*, 794.

(236) James, S. L.; Mingos, D. M. P.; White, A. J. P., Williams, D. J. *J. Chem. Soc., Chem. Commun.* **1998**, *2323*.
(237) (a) Amabilino, D. B.; Stoddart, J. F. *Chem. Rev.* **1995**, *95*, 2725. (b) Vögtle, F.; Dunnwald, T.; Schmidt, T. *Acc. Chem. Res.* **1996**, *29*, 451. (c) Stoddart, J. F.; Raymo, F.; Amabilino, D. B. In *Comprehensive Supramolecular Chemistry;* Lehn, J.-M., Chair Ed.; Atwood, J. L., Davis, J. E. D., MacNicol, D. D., Vögtle, F., Exec. Eds.; Pergamon Press: Oxford, 1996; Chapter 3. (d) Raymo, F. M.; Stoddart, J. F. *Chem. Rev.* **1999**, *99*, 1643.
(238) (a) Vögtle, F.; Meier, S.; Hoss, R. *Angew. Chem., Int. Ed. Engl.* **1992**, *31*, 1619. (b) Dietrich-Buchecker, C. O.; Sauvage, J.-P.; Kintzinger, J.-P. *Tetrahedron Lett.* **1983**, *24*, 5095. (c) Hunter, C. A. *J. Am. Chem. Soc.* **1992**, *114*, 5303.
(239) Fujita, M.; Fujita, N.; Ogura, K.; Yamaguchi, K. *Nature* **1999**, *400*, 52.
(240) (a) Hunter, C. A.; Sanders, L. K. M. *J. Am. Chem. Soc.* **1990**, *112*, 5525. (b) Jorgensen, W. L.; Severance, D. L. *J. Am. Chem. Soc.* **1990**, *112*, 4768.
(241) (a) Stejskal, E. O.; Tanner, J. E. *J. Chem. Phys.* **1965**, *42*, 288. (b) Tanner, J. E. *J. Chem. Phys.* **1970**, *52*, 2523. (c) Mayzel, O.; Cohen, Y. *J. Chem. Soc., Chem. Commun.* **1994**, 1901. (d) Kriwacki, R. W.; Blake-Hill, R.; Flanagan, J. M.; Carradona, J. P.; Prestegard, J. H. *J. Am. Chem. Soc.* **1993**, *115*, 8907.
(242) Lehn, J.-M. *Angew. Chem., Int. Ed. Engl.* **1990**, *29*, 1304.
(243) Graddon, D. P. *Coord. Chem. Rev.* **1969**, *4*, 1.
(244) Fujita, M.; Ogura, K. *Bull. Chem. Soc. Jpn.* **1996**, *69*, 1471.
(245) Wyler, R.; de Mendoza, J.; Rebek, J., Jr. *Angew. Chem., Int. Ed. Engl.* **1993**, *32*, 1699.
(246) Bélanger, S.; Hupp, J. T.; Stern, C. L.; Slone, R. V.; Watson, D. F.; Carrell, T. G. *J. Am. Chem. Soc.* **1999**, *121*, 557.
(247) (a) Ohsaka, T.; Hirokawa, T.; Miyamoto, H.; Oyama, N. *Anal. Chem.* **1987**, *59*, 1758. (b) Ohnuki, Y.; Matsuda, H.; Ohsaka, T.; Oyama, N. *J. Electroanal. Chem.* **1983**, *158*, 55. (c) McCarley, R. L.; Irene, E. A.; Murray, R. W. *J. Phys. Chem.* **1991**, *95*, 2492.
(248) (a) Could, S.; Strouse, G. F.; Meyer, T. J.; Sullivan, B. P. *Inorg. Chem.* **1991**, *30*, 2942. (b) Gould, S.; Meyer, T. J. *J. Am. Chem. Soc.* **1991**, *113*, 7442.
(249) "There's Plenty of Room at the Bottom," a talk by Richard Feynman at the annual meeting of the American Physical Society given on December 29, 1959. Reprinted in Caltech's Engineering and Science, February 1960; pp 22−36.

CR9601324